INSTITUTO POTOSINO DE INVESTIGACIÓN CIENTÍFICA Y TECNOLÓGICA, A.C.

POSGRADO EN CIENCIAS APLICADAS

Immobilization of humic substances on metal-oxides (nano)particles and their impact in redox processes

Tesis que presenta

Luis Humberto Alvarez Valencia

Para obtener el grado de

Doctor en Ciencias Aplicadas

En la opción de

Ciencias Ambientales

Director de la Tesis:

Dr. Francisco Javier Cervantes Carrillo

San Luis Potosí, S.L.P. México, Junio de 2012

This dissertation entitled "**Immobilization of humic substances on metal oxides (nano)particles and their impact in redox processes**" presented to obtain the degree of **Doctor in Applied Sciences** in the option of **Environmental Sciences**, was prepared by **Luis Humberto Alvarez Valencia** and approved on June 4th, 2012 by the undersigned, designated by the College of Professors of Environmental Sciences Division of Instituto Potosino de Investigación Científica y Tecnológica, A.C.

_____

Dr. Francisco Javier Cervantes Carrillo
Director of Dissertation

_____

Dr. José René Rangel Méndez
Member of Dissertation Committee

_____

Dr. José Luis Rodriguez López
Member of Dissertation Committee

_____

Dr. María Catalina Alfaro de la Torre
Member of Dissertation Committee

INSTITUTIONAL CREDITS

This Dissertation was developed in the laboratories of Environmental Sciences Division of Instituto Potosino de Investigación Científica y Tecnológica, A.C., under supervision of Dr. Francisco J. Cervantes Carrillo.

The author received an academic scholarship from the Consejo Nacional de Ciencia y Tecnología (Grant # 090337), and from Instituto Potosino de Investigación Científica y Tecnológica, A. C.

This study was financially supported by the projects SEP-CONACYT–55045, SEP-CONACYT-155656, and Lettinga Award 2007, granted by Lettinga Associates Foundation.

The author also received economic support from Environmental Sciences Division of Instituto Potosino de Investigación Científica y Tecnológica, A. C. to present the results generated in this study in four specialized conferences.

IPICYT

Instituto Potosino de Investigación Científica y Tecnológica, A.C.

Acta de Examen de Grado

El Secretario Académico del Instituto Potosino de Investigación Científica y Tecnológica, A.C., certifica que en el Acta 015 del Libro Primero de Actas de Exámenes de Grado del Programa de Doctorado en Ciencias Aplicadas en la opción de Ciencias Ambientales está asentado lo siguiente:

En la ciudad de San Luis Potosí a los 4 días del mes de junio del año 2012, se reunió a las 10:00 horas en las instalaciones del Instituto Potosino de Investigación Científica y Tecnológica, A.C., el Jurado integrado por:

Dra. Ma. Catalina Alfaro de la Torre	**Presidente**	**UASLP**
Dr. José Luis Rodríguez López	**Secretario**	**IPICYT**
Dr. Francisco Javier Cervantes Carrillo	**Sinodal**	**IPICYT**

a fin de efectuar el examen, que para obtener el Grado de:

DOCTOR EN CIENCIAS APLICADAS
EN LA OPCION DE CIENCIAS AMBIENTALES

sustentó el C.

Luis Humberto Alvarez Valencia

sobre la Tesis intitulada:

Immobilization of humic substances on metal-oxides (nano)particles and their impact on redox processes

que se desarrolló bajo la dirección de

Dr. Francisco Javier Cervantes Carrillo

El Jurado, después de deliberar, determinó

APROBARLO

Dándose por terminado el acto a las 13:05 horas, procediendo a la firma del Acta los integrantes del Jurado. Dando fe el Secretario Académico del Instituto.

A petición del interesado y para los fines que al mismo convengan, se extiende el presente documento en la ciudad de San Luis Potosí, S.L.P., México, a los 4 días del mes de junio de 2012.

Dr. Marcial Bonilla Marín
Secretario Académico

Mtra. Ivonne Lizette Cuevas Vélez
Jefa del Departamento del Posgrado

INSTITUTO POTOSINO DE INVESTIGACIÓN CIENTÍFICA Y TECNOLÓGICA, A.C.
IPICYT
SECRETARIA ACADEMICA

A Faby, mi compañera idónea, y a mis amados hijos: Luis Jarom, Clarissa y Diego Elías, por ser la fuente de inspiración, de entrega y de amor a mi trabajo.

A Papá y Mamá, y a mis amados Hermanos, por los grandes ejemplos que me dan.

AGRADECIMIENTOS

El valor de este trabajo va más allá de su contenido científico y tecnológico, simboliza los esfuerzos y sacrificios no solamente míos, sino de mi toda mi familia. Al voltear mi mirada hacia atrás, siento satisfacción y un gran gozo por las experiencias vividas en tierras Potosinas, y puedo ver que el fruto cosechado ha sido bueno.

Deseo primeramente agradecer a mi Padre Celestial por su gran amor incondicional y por siempre estar ahí, con las ventanas de los cielos abiertas para derramar su infinita bondad y grandes bendiciones. Gracias también por las pláticas especiales que me has permitido tener contigo, sin duda sé que Tú me condujiste hasta SLP.

Hace poco más de tres años (08/2009) y después de haber insistido varias ocasiones, acepté venir a trabajar con el Dr. Francisco J. Cervantes. Paco, a pesar de que me llamaste la atención (bueno, me regañaste) algunas veces en la clase de bioquímica microbiana, siempre hubo algo en que me invitaba a desear trabajar contigo. A lo largo de los años he descubierto que ese algo es: la disciplina, la entrega, la tenacidad, la visión, la capacidad para la buena crítica, y bueno creo que también algo de paciencia has ganado (creo que ya no te has molestado conmigo); pero sobretodo, valoro la gran persona que eres. Sin duda estas cualidades no adquieren fácilmente. Gracias Paco por ser un gran amigo y por enseñarme mis primeras lecciones en la investigación científica. Agradezco también a Liz y a los gemelos (Román y Alfonso) por la confianza y ayuda que siempre nos brindaron a mi familia y a mí.

Deseo agradecer también a todos con los que conviví en el IPICYT. Al Dr. José R. Rangel y al Dr. José L. Rodríguez por sus buenas críticas al trabajo. Así como a la Dra. Caty Alfaro por aceptar colaborar en mi comité tutoral. No puedo olvidarme del Cervantes TEAM: Jorge G., Ana M., Emilia R. y Claudia M., gracias por su amistad y colaboración. Es muy importante para mí agradecer a la Dra. Mariana, Dra. Vicky (Victoria), la “Srita.” Laura J. y Laura M., por ser parte fundamental del trabajo experimental. Así mismo, agradezco el apoyo técnico de Gladys Labrada, Dulce Partida, Carmen Rocha, Guillermo Vídriales y Juan Pablo Rodas, técnicos académicos del IPICYT. Por último, pero no menos

importante, un especial agradecimiento a mi buen amigo Bernardo, jamás olvidaré ese gran apoyo al inicio de mi llegada a tierras Potosinas, gracias Berny por tu confianza. Extiendo el agradecimiento a Alcione y sobretodo al Bernardito por prestarme su cama durante casi seis meses.

Un agradecimiento especial para mis suegros, Cuquita y Ramón. Ustedes han sido una pieza clave en este logro, sus palabras de ánimo y otras grandes ayudas han servido en gran manera para nosotros. También para ti Arturo, siempre he valorado la amistad que hemos tenido.

Nunca dejaré de agradecer a mis Padres, Rosa y Manuel, por ser grandes ejemplos de lucha y entrega. Siempre tengo presente los bellos momentos que pase a su lado en mi niñez y juventud, y también ahora que soy un poco más “grande”, estamos escribiendo otros momentos igual de bellos. Lo mismo agradezco a mis Hermanos: Chayito, Meño, Carlos y Naye; y a sus familias (mis cuñados y mis sobrinos), por cuidar de mis Hermanos y por ser parte de los Alvarez Valencia. No olvido a mis hermanitos que partieron muy pronto, casi al nacer, sé que por ahora están en un lugar muy especial y que en algún momento nos reuniremos nuevamente.

Estas últimas palabras de agradecimiento serán para Faby y nuestros amados hijitos. Gracias Faby por estar siempre a mi lado apoyándome y aconsejándome a fin de que yo busque aquello que me edifique. Sé que éste tiempo no ha sido fácil para tí, tampoco lo ha sido para mí; pero al mismo tiempo hemos disfrutado juntos grandes momentos que seguramente jamás olvidaremos. Gracias por la hermosa bendición de este lindo bebe Diego Elías, tal como lo planeamos al inicio, recuerdas?. Jarom y Clarissa, ustedes aún son pequeños y lo eran aún mas cuando llegamos a SLP, sé que tal vez no recordarán muchos detalles de este largo viaje que hemos realizado, Mamá y Yo nos encargaremos de revivir en ustedes los maravillosos momentos que hemos vivido juntos. Me siento agradecido con ustedes por su gran amor y ejemplo al aceptar de buena gana acompañarme en esta aventura.

CONTENTS

ABBREVIATIONS*

AC	Activated carbon
AQDS	Anthraquinone-2,6-disulfonate
ATR	Attenuated total reflectance
CAW	Compost of agave wastes
CBM	Carbon-based materials
CCO	Commercial compost
CF	Chloroform
CFA	Coniferous forest of Aguascalientes
CFSLP	Coniferous forest of San Luis Potosi
CGW	Compost of gardening wastes
COD	Chemical oxygen demand
CT	Carbon tetrachloride
DCM	Dichloromethane
DFSLP	Deciduous forest of San Luis Potosi
DNT	Dinitrotoluene
DTFA	Deciduous tropical forest of Aguascalientes
EAC	Electron accepting contaminant
ECC	Electron carrying capacity
EDX	Energy dispersive X-ray
EGSB	Expanded granular sludge bed
EPA	Environmental Protection Agency
ETC	Electron transferring capacity
FA	Fulvic acids
FTIR	Fourier transform infrared spectroscopy
HA	Humic acids
HRA	Humus reducing activity
HRM	Humus reducing microorganisms
HS	Humic substances
IHSS	International Humic Substance Society
kd	First-order rate constant
MLE	Leonardite from a carbon mine
MONP	Metal-oxide nanoparticles
NP	Nanoparticle
NP-RM	Nanoparticles covered with redox mediators

NQ	Non-quinone
NT	Nanotechnology
Q_{max}	Maximum adsorption capacity
RM	Redox mediator
RR2	Reactive red 2
SAVO	Soil from avocado plantation
SCOC	Soil from cocoa plantation
SCOF	Soil from coffee plantation
SEM	Scanning electron microscopy
SMA	Specific methanogenic activity
SVM	Soil with volcanic matter (Popocatepetl volcano)
TEA	Terminal electron accepting
TOC	Total organic carbon
UASB	Upflow anaerobic sludge blanket
VSS	Volatile suspended solids

* This list includes only the main abbreviations used.

ABSTRACT

Alvarez, L.H. (2012) *Immobilization of humic substances on metal-oxides (nano)particles and their impact in redox processes.* PhD Thesis. IPICYT

During the last two decades, evidence has been accumulated indicating that humic substances (HS) and quinoid analogues can act as redox mediators (RM), accelerating the reduction rates of different electron accepting contaminants (EAC) such as azo dyes, nitroaromatics compounds, halogenated solvents, and metalloids. Nevertheless, it is necessary to develop suitable strategies to immobilize RM in order to eliminate the prerequisite of their continuous addition in anaerobic wastewater treatments systems. In this dissertation HS extracted from soils and composts from different parts of Mexico were identified and characterized, in order to select those effective sources, considering their electron transferring capacity (ETC). Metal-oxides (MO) particles at nano- and micrometric scale were used to immobilize those HS selected from the study of characterization. Once immobilized, the catalytic effect of HS was tested during the anaerobic biotransformation of EAC, acting as solid-phase RM. Finally, relevant processes such as methanogenesis and humus reduction were considered in order to evaluate the toxicological effects of MO nanoparticles (NP), covered with HS, on an anaerobic consortium. This study provides with essential information required for the co-immobilization of RM and humus reducing microorganisms through the granulation process.

The results presented in chapter 3 indicate that suitable sources of RM can be found in natural environments to be used in wastewater treatment systems. ETC values depended of the origin of the HS sample, which ranging between 112–392 μmol g^{-1} by chemical method. In addition, it was demonstrated that non-quinone functional groups accounted for an important fraction of ETC of different HS samples and that the humus-reducing microorganism *Geobacter sulfurreducens*, is able to reduce both quinone and non-quinone redox functional groups in HS. From this characterization study, two HS samples were selected to be immobilized on MO particles at micrometric (chapter 4) and nanometric scale (chapter 6). In chapter 4, the impact of immobilized HS on alumina microparticles during the reductive dehalogenation of carbon tetrachloride by anaerobic sludge was studied. Immobilized HS preserved their catalytic properties, which was evidenced by an increase up to 10.4-fold in the rate of reduction of carbon tetrachloride compared to the control lacking HS, achieving a dehalogenation efficiency >90%. Chapter 5 presents the capacity of different NP to immobilize the model quinone anthraquinone-2,6-disulfonate (AQDS). Among all NP tested, $Al(OH)_3$ was the most appropriated material for immobilization of AQDS. For instance, an adsorption capacity of 0.105 mmol of AQDS g^{-1} was achieved, representing a capacity of 67-times higher respect to other NP tested. Immobilized AQDS on $Al(OH)_3$ NP was used as a solid-phase RM during decolorization of Reactive Red 2 using an anaerobic sludge. Immobilized RM increased up to 7.5-fold the

rate of decolorization of the pollutant respect to the control without RM, during an incubation period of 12 h. In the chapter 6 the toxicological effects of γ-Al_2O_3 NP on a humus-reducing consortium were evaluated. For this study, relevant processes such as methanogenesis and humus reduction were considered. Results presented in chapter 6 indicate that toxicological effects were mitigated using NP covered with HS as compared with uncoated NP, which was evidenced by an increment on methane production. Likewise, it was demonstrated that immobilized HS on γ-Al_2O_3 NP can act as effective terminal electron acceptor during microbial respiration. It was documented that methanogenesis out-competed microbial humus reduction regardless if HS are immobilized or suspended. In addition, this study also provides a significant basis for the feasibility of the co-immobilization of HS (adsorbed on NP) and humus-reducing microorganisms trough the anaerobic granulation process, which can improve the efficiency of wastewater treatments systems during the treatment of industrial effluents containing EAC.

RESUMEN

Alvarez, L.H. (2012) *Inmovilización de sustancias húmicas sobre (nano)partículas de óxidos metálicos y su aplicación en procesos redox.* Tesis Doctoral. IPICYT

Durante las dos últimas décadas se ha demostrado que el uso de sustancias húmicas (SH) y sus análogos (quinonas) pueden servir como mediadores redox (MR), acelerando la velocidad de reducción de diferentes contaminantes electrofílicos (CE) como colorantes azo, compuestos nitroaromáticos, compuestos polihalogenados y metaloides. Sin embargo, es necesario desarrollar estrategias apropiadas para lograr la inmovilización de MR a fin de erradicar el requisito de adicionarlos de manera continua en sistemas anaerobios de tratamientos de aguas residuales. En esta tesis se identifican y caracterizan SH extraídas de suelos y compostas de distintos sitios de México, a fin de seleccionar aquellas con apropiada capacidad de transferencia de electrones (CTE). Se utilizan partículas de óxidos metálicos (OM), a escala nanométrica y micrométrica, para inmovilizar las distintas SH seleccionadas a partir del proceso de caracterización. También se evalúa el impacto catalítico de las SH inmovilizadas durante la biotransformación de distintos CE, actuando como MR. Por último, se muestran los efectos toxicológicos de nanopartículas (NP) de óxidos metálicos cubiertas con SH sobre un consorcio anaerobio, considerando procesos relevantes como la metanogénesis y la reducción del humus; esto permitirá establecer las bases para la co-inmovilización de MR y microorganismos reductores del humus por medio del proceso de granulación.

Los resultados mostrados en el capítulo 3 indican que existen fuentes apropiadas de SH para ser utilizadas como MR en sistemas de tratamiento de aguas residuales, de acuerdo a los valores de CTE observados en las muestras, lo cual depende de su origen. De igual forma se demostró que existen grupos funcionales presentes en las SH, distintos a los grupos quinona, que son capaces de participar en la transferencia microbiológica de electrones utilizando *Geobacter sulfurreducens*, lo que sólo había sido demostrado anteriormente por métodos químicos. A partir de este estudio de caracterización se seleccionaron dos muestras de SH que se utilizaron para ser inmovilizadas sobre partículas de OM a escala micrométrica (capítulo 4) y nanométrica (capítulo 6). En el capítulo 4 se estudia el impacto de SH, previamente inmovilizadas en micropartículas de alúmina, durante la deshalogenación reductiva de tetracloruro de carbono por un consorcio anaerobio. Las SH inmovilizadas preservaron sus propiedades catalíticas, lo cual fue evidenciado por un aumento de hasta 10.4 veces en la velocidad de reducción de tetracloruro de carbono en comparación con el control sin SH, con una eficiencia de reducción >90%. En el capítulo 5 se presenta la capacidad de diferentes NP de OM para inmovilizar la quinona modelo antraquinona 2,6-disulfonato (AQDS). Las NP de $Al(OH)_3$ fue el material que presentó una mejor capacidad de adsorción de AQDS, con un valor de hasta 67 veces mayor respecto a otras NP. La AQDS inmovilizada en NP de $Al(OH)_3$ se

utilizó durante la decoloración de Rojo Reactivo 2 utilizando un lodo anaerobio; incrementándose hasta 7.5 veces la velocidad de decoloración del contaminante en comparación al control sin MR, durante un periodo de incubación de 12 h. En el capítulo 6 se evalúan los efectos toxicológicos de NP de γ-Al_2O_3 sobre la actividad metanogénica y reductora de humus de un consorcio anaerobio, que contiene bacterias capaces de utilizar el humus como un aceptor de electrones. Los resultados descritos en este capítulo indican que el efecto toxicológico de las NP se mitiga cuando éstas previamente adsorben SH, lo cual es evidenciado por una mayor producción de metano. Así mismo, se demuestra que las SH inmovilizadas en NP de γ-Al_2O_3 sirven como aceptores finales de electrones durante la respiración microbiana. Con esto se documenta por primera vez que la metanogénesis compite con la reducción del humus, sin importar si las SH se encuentran suspendidas o inmovilizadas. Estos resultados sientas las bases y demuestran que es factible la co-inmovilzación de MR (adsorbidos en NP) y microorganismos reductores del humus durante la formación de gránulos, lo cual puede permitir el mejoramiento de los sistemas de tratamiento de efluentes industriales que contengan CE.

1

Introduction

The chemical and petrochemical industry produces worldwide thousands of compounds each year and is still in expansion [1]. Unfortunately, linked to the greats benefits obtained from these industries, large volumes of wastewaters containing many different toxic and recalcitrant priority pollutants are also generated [2]. Among the contaminants discharged are electron-accepting contaminants (EAC), such as azo dyes, nitroaromatics, chlorinated aliphatic and aromatic compounds, and metalloids. These contaminants remain unaffected during convectional aerobic wastewater treatment. However, under anaerobic conditions, these pollutants are susceptible to redox biotransformations [3] using anaerobic bioreactors, such as UASB and EGSB systems. Nevertheless, the biotransformation of many different recalcitrant compounds proceeds very slowly due to electron transfer limitations and to toxicity effects leading to poor performance or even collapse of anaerobic bioreactors [4, 5].

During the last two decades, evidence has been accumulated indicating that humic substances (HS) and quinoid analogues can act as redox mediators (RM) during the reductive biotransformation of EAC [6, 7, 8], accelerating redox reactions in several orders of magnitude, and in some cases they are essential for reactions to take place [9]. One of

the main limitations for applying RM in wastewater treatment systems is that continuous addition of HS or quinones should be supplied to increase conversion rates, which is economically and environmentally unviable. Nevertheless, quinoid RM not necessarily have to be supplied abundantly in bioremediation processes to accelerate the redox transformation of different contaminants, as they are being recycled during the transfer of electron from an electron donor to the terminal electron acceptor. An approach to eradicate the requisite of continuous supply of RM in anaerobic bioreactors is to create a niche for their immobilization [10].

The immobilization of RM could be the solution for the application of these catalysts in wastewater treatment systems treating EAC. Few reports have documented the use of different materials to immobilize model RM; among these, we find activated carbon [11], polymeric matrixes [12], polypyrrole [13], ion exchange resins [14], and polyurethane foam [15]. In addition, Cervantes et al. [16] and Lian et al. [17] documented the use of immobilized RM in continuous bioreactors. These authors reported the immobilization of quinones on activated carbon and telyrene fibers, respectively. However, all these previous reports have been conducted with synthetic model RM. Recently, Cervantes et al. [18], reported the use of non-synthetic RM, namely HS extracted from different natural environments, immobilized in an ion exchange resins, for their use as a solid-phase RM. Metal-oxides particles at micro and nanometric scale have never been used as a supporting material for the immobilization of RM. This thesis is focused on the use of different metal-oxides (nano and micro) particles for the immobilization of HS, and their use as a solid-phase RM during the anaerobic reduction of EAC.

Research objectives

1. Characterize different samples of HS and select the most effective source to be used as RM, according to their electron-transferring capacity (ETC).
2. Identify the most adequate metal-oxides (nano)particles to be used as immobilizing material of HS with suitable ETC, by physisoprtion experiments.

3. Elucidate the impact of immobilized HS on metal-oxides (nano)particles, during the redox biotransformation of EAC in batch incubations, in order to identify if the RM maintain their catalytic properties.
4. Study the toxicity effects of metal-oxides nanoparticles (NP) on an anaerobic consortium in order to elucidate the feasibility for the co-immobilization HS (adsorbed on nanoparticles) and humus reducing microorganisms through the anaerobic granulation process.

Thesis outline

Chapter 2 of this thesis presents a literature review about the advances of the use of RM during reductive biotransformations, especially those focused on immobilization process. In addition, chapter 2 presents the impact of nanotechnology in wastewater treatment process. Chapter 3 describes the characterization of twelve HS samples extracted from many soils and composts obtained from different regions of Mexico. At this stage, were identified some suitable sources of HS to be used as RM in wastewater treatment systems, according to their chemical and microbial ETC. The microbial ETC (by *Geobacter sulfurreducens*) of some HS samples associated to non-quinoid redox functional groups, which had never been documented, is also presented in chapter 3. Chapter 4 presents the capacity of HS extracted from a temperate pine forest soil, previously immobilized on microparticles of alumina, to serve as a solid-phase RM during the reductive dechlorination of carbon tetrachloride by an anaerobic sludge. The capacity of different metal-oxides NP to immobilize anthraquinone-2,6-disulfonate (AQDS) is presented in chapter 5. Chapter 5 also describes the potential of using immobilized AQDS on metal-oxides NP as a solid phase RM during the reductive decolorization of Reactive Red 2 by anaerobic sludge. Chapter 6 presents the impact of γ-Al_2O_3 NP on specific methanogenic activity and humus reducing activity in an anaerobic consortium. The study provides a clear demonstration that HS immobilized on NP are effective terminal electron acceptor for microbial respiration and suggests that HS could mitigate the toxicological effects of metal-oxides NP on anaerobic microorganisms. In addition, this study also provides a significant base for the feasibility of co-immobilization of HS (adsorbed on NP) and humus reducing microorganisms, through the anaerobic

granulation process. Finally, chapter 7 presents the final remarks and future prospects of this thesis.

References

1. Storck W.J., Tullo A.H., Short P.L., Tremblay J.F. (2005) World chemical outlook. *Chem Eng News* 83:15–29.

2. Razo-Flores E., Macarie H., Morier F. (2006) Application of biological treatment systems for chemical and petrochemical wastewaters. In: Cervantes F.J., Pavlostathis S.G., Van Haandel A.C., editors. Advanced biological treatment processes for industrial wastewaters: principles & applications. London, UK: IWA Publishing; 2006. p. 267–297.

3. Field JA., Stams A.J.M., Kato M., Schraa G. (1995) Enhanced biodegradation of aromatic pollutants in cocultures of anaerobic and aerobic bacterial consortia. *Anton Leeuw Int J G* 67:47–77.

4. Rodgers J.D., Bunce N.J. (2001) Treatment methods for the remediation of nitroaromatic explosives. *Water Res* 35:2101–2111.

5. Van der Zee F.P., Bouwman R.H.M., Strik D.P.B.T.B., Lettinga G., Field J.A. (2001) Application of redox mediators to accelerate the transformation of reactive azo dyes in anaerobic bioreactors. *Biotechnol Bioeng* 75:691–701.

6. Barkovskii A.L., Adriaens P. (1998) Impact of humic constituents on microbial dechlorination of polychlorinated dioxins. *Environ Toxicol Chem* 17:1013–1020.

7. Borch T., Inskeep W.P., Harwood J.A., Gerlach R. (2005) Impact of ferrihydrite and anthraquinone-2,6-disulfonate on the reductive transformation of 2,4,6-trinitrotoluene by a Grampositive fermenting bacterium. *Environ Sci Technol* 39:7126–7133.

8. Guo J., Zhou J., Wang D., Tian C., Wang P., Salah Uddin M. (2007) Biocalalyst effects of immobilized anthraquinone on the anaerobic reduction of azo dyes by the salttolerant bacteria. *Water Res* 41:426–32.

9. Cervantes F.J. (2002) Quinones as electron acceptors and redox mediators for the anaerobic biotransformation of priority pollutants. Ph.D. Thesis Wageningen University, Wageningen, The Netherlands.

10. Van der Zee F.P., Cervantes F.J. (2009) Impact and application of electron shuttles on the redox (bio)transformation of contaminants: A review. *Biotechnol Adv* 27:256–277.

11. Van der Zee F.P., Bisschops I.A.E., Lettinga G., Field J.A. (2003) Activated carbon as an electron acceptor and redox mediator during the anaerobic biotransformation of azo dyes. *Environ Sci Technol* 37:402–408.

12. Guo J., Zhou J., Wang D., Tian C., Wang P., Salah Uddin M. (2007) Biocalalyst effects of immobilized anthraquinone on the anaerobic reduction of azo dyes by the salttolerant bacteria. *Water Res* 41:426–32.

13. Li L.,Wang J., Zhou J., Yang F., Jin C., Qu Y. (2008) Enhancement of nitroaromatic compounds anaerobic biotransformation using a novel immobilized redox mediator prepared by electropolymerization. *Biores Technol* 99:6908–6916.

14. Cervantes F.J., Garcia-Espinosa A., Moreno-Reynosa M.A., Rangel-Mendez J.R. (2010) Immobilized redox mediators on anion exchange resins and their role on the reductive decolorization of azo dyes. *Environ Sci Technol* 44:1747–1753.

15. Lu H., Zhou J., Wang J., Si W., Teng H., Liu G. (2010) Enhanced biodecolorization of azo dyes by anthraquinone-2-sulfonate immobilized covalently in polyurethane foam. *Biores Technol* 101:7185–7188.

16. Cervantes F.J., Ceballos K.M., Alatorre H.A., Sánchez F., Razo-Flores E. (2011) Inmovilización de un mediador redox en carbón activado y su aplicación en la reducción biológica de colorantes azo. *Ac Quím Mexicana* 3:62-70.

17. Lian J., Guo J., Feng G., Liu G., Yang J., Liu Chun., Li Z., Yue L., Zhao L. (2011) Development of bioreactor systems with functional bio-carrier modified by disperse turquoise blue S-GL for disperse scarlet S-BWFL decolorization. *Biores Technol* 102:11239–11243.

18. Cervantes F.J., Gonzalez-Estrella J., Márquez A., Alvarez L.H., Arriaga S. (2011) Immobilized humic substances on an anion exchange resin and their role on the redox biotransformation of contaminants. *Biores Technol* 102:2097-2100.

2

Application of redox mediators and (bio)nanotechnologies in wastewater treatment processes

Abstract

During the last two decades, evidence has been accumulated indicating that humic substances (HS) and quinoid analogues can play important role acting as redox mediator (RM) during the redox biotransformation of different priority pollutants such as azo dyes, nitroaromatic compounds, metalloids, and polyhalogenated solvents. Immobilization of RM is a current task focused to eliminate the prerequisite of continuous addition of RM in bioreactors. For this reason, different materials have been used to immobilize RM. On the other hand, many of the current wastewater treatment processes are now changing because of the introduction of nanotechnology (NT), improving the efficiency of the current processes. In spite of the application of nanomaterials offers significant advantages compared with their bulk forms, NT is yet an emerging area, and important aspects should firstly be addressed in order to apply these technologies. The aim of this chapter is summarize the advances related with the immobilization of quinones and HS, and their use as a solid-phase RM. In addition, the application of NT in the wastewater treatment processes is also presented.

A modified version of this chapter has partly been published as: Alvarez LH, Cervantes FJ (2011) *Journal of Chemical Technology and Biotechnology* 86:1354-1363.

2.1 Introduction

Humic substances (HS) represent the most abundant fraction of organic matter accumulated in aquatic and terrestrial environments. HS are polymeric compounds with amorphous structures and high molecular weight resulting from decomposition of litter, and contain a large number of aromatics rings and others aliphatic structures (Figure 2.1). The highly condensed aromatic structures are very recalcitrant to biodegradation as is evident from the mean residence time of humus in soil, which can vary from 250 to 1900 years [80]. Nevertheless HS are not inert by the fact they are involved in chemical, biological, and physical processes, due to the characteristics that confer their functional groups (e.g. ketone, carboxylic, amine, and quinone). For instance, HS can act as electron donors and terminal electron acceptors during respiration of anaerobic microorganisms; also HS can act as electron shuttles or redox mediators (RM) in both chemical and microbiological reactions. These roles of HS represent a promissory potential for applying them in wastewater treatment systems.

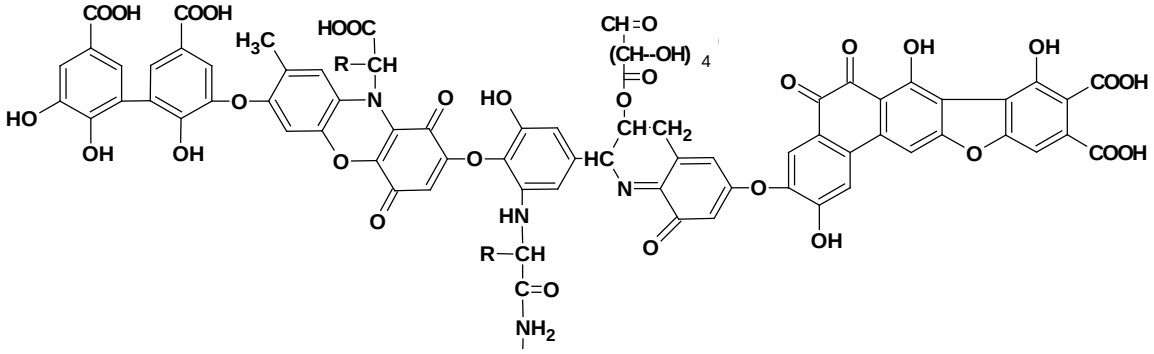

Figure 2.1 Model structure of humic acid proposed by Stevenson [80].

On the other hand, nanotechnology (NT) is an emergent area of science and technology focused to development, synthesis, and application of materials at nanometric scale (1-100 nm). Recent applications of nanoparticles (NP) include areas such as electronics, materials engineering, food, transportation, cosmetic, energy, pharmaceutical, biomedical, consumers goods, and environmental. The use of NT in environmental applications could be effective in prevention, treatment, and remediation of the pollution, and also for sustainable energy

production. Application of NT in wastewater treatment systems is an undeveloped area, but in the near future could be useful to enhance the current processes. The objective of this chapter is to show both the recent advances on the application of RM during the reductive transformations of priority pollutants (sections 2.2 and 2.3), and the use of NT to treat pollution in wastewater (section 2.4). This thesis presents the use of NP as immobilizing material of HS, and their application as a solid-phase RM.

2.2 The use of HS as RM

Many studies have indicated that the main groups responsible for the electron transferring capacity (ETC) in HS are quinones [24], but also other non-quinone groups are responsible for their redox capacity [72]. The capacity of HS to act as RM is due to redox reactions between quinones and an electron donor and/or a final electron acceptor. Therefore, quinones can be recycled by the reaction of their reduced form with oxidized compounds or minerals (Figure 2.2).

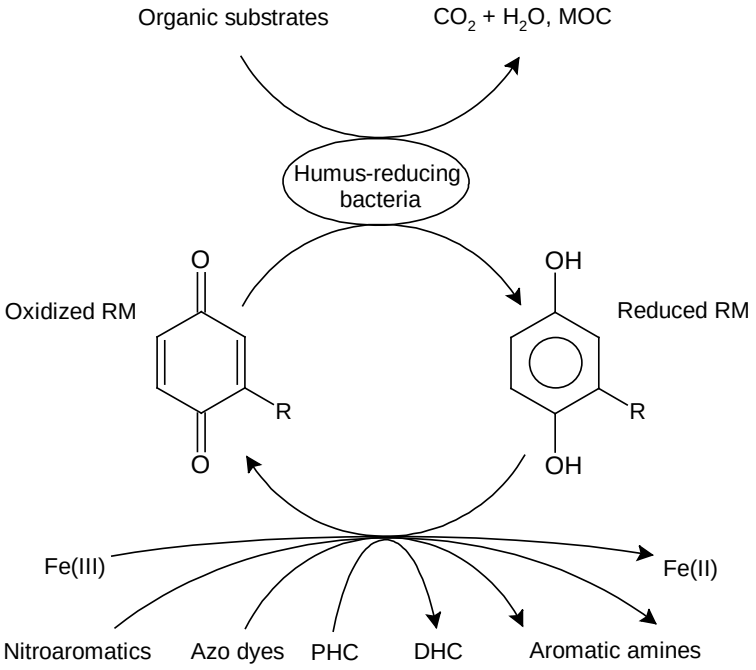

Figure 2.2 Proposed mechanism for anaerobic reduction of electron-accepting contaminants and Fe(III) using redox mediators. MOC, more oxidized compounds; PHC, polyhalogenated compounds; DHC, dehalogenated compounds.

The ETC of quinones in humus can be used to support the reductive biotransformation of electron-accepting contaminants (EAC) such as azo dyes, polyhalogenated compounds, nitrobenzenes, and radionuclides, acting as RM (Figure 2.2). The presence of RM accelerates the rate of reduction of EAC in several orders of magnitude and in some cases is a requisite for the reaction to take place. Van der Zee and Cervantes [87] published an interesting review research paper showing important aspects about the impact and application of RM during the biotransformation of contaminants. These authors indicate that factors such as pH, temperature, redox potential, electron donors, and source of HS, are directly involved with the role of RM on redox biotransformations. For instance, adequate redox potential of HS to act as RM should ideally be in between those of the two eventual half reactions of EAC and primary electron donor. Thus, redox potential of HS should to be ideally lower or more negative than that of EAC, but ideally higher or less negative than primary electron donor [87]. Table 2.1 shows a brief list with examples about the use of HS or quinones acting as RM during redox biotransformations of azo dyes, nitrobenzenes, and halogenated compounds.

Table 2.1 Impact of quinoid redox mediators in reductive biotransformations.

Pollutant[a]	Redox mediator[b]	Microorganisms	Results[c]	Ref.
Azo dyes				
AO52, AO7	AQS	*Issatchenkia occidentalis*	AO52: Max. reduction rate was 3-fold higher compared to the control without RM AO7: adverse effect of RM	71
P-O5	AQDS	*Shewanella* strain J18 143	Reduction rate was 4-fold higher respect to the control lacking RM	66
RR2	RF	*Methanothermo-bacter sp.*, *Methanosarcina barkeri*	Thermophilic strains: only dye reduction in the presence of RF Mesophilic strain: RF accelerates dye reduction	20
RO14	RF	Anaerobic granular sludge	Reduction rate was 1.5 to 2-fold higher respect to the control lacking RM	11

Table 2.1 Continued.

Pollutant[a]	Redox mediator[b]	Microorganisms	Results[c]	Ref.
RO14, DB53, DB71	AQDS, LAW, RF	Anaerobic granular sludge	Max. reduction rate was 3.8-fold higher compared to the control without RM	21
Nitrobenzenes				
RDX	AQDS	*Geobacter metallireducens*	Addition of AQDS increased the rate and extent of mineralization of RDX	49
TNT	AQDS	*Cellulomonas sp*. strain ES6	Up to 3.7-fold increase in first order rate constant of reduction of TNT in AQDS-amended assays compared to controls lacking RM	9
RDX	AQDS, HA	*Geobacter sp.*	Addition of HA or AQDS to Fe(III)-containing microbial cultures increased 5- to 66-fold the reduction rate of RDX compared to unamended controls	50
Halogenated compounds				
CT	CNB12	*Shewanella alga* strain BrY	No conversion of CT by *Shewanella alga* strain BrY in the absence CNB12; whereas 92% of CT conversion to CO within 3 weeks of incubation	92
CDD	CAT, RES	Contaminated sediment	4- to 6-fold higher conversion in RM amended cultures compared to control	8
CT	AQDS, HA	Anaerobic sludge or *Geobacter sp.*	6-fold higher first-order reduction rates in AQDS amended sludge incubations compared to controls. AQDS and HA stimulated the reduction of CT by *Geobacter sp*., which did not convert CT in the absence of RM	14
CT	AQDS, RF, CNB12, HOB12	Anaerobic sludge	3.8-, 4.0, 13.3- and 13.6-fold higher first-order reduction rates in AQDS, RF, CNB12 and HOB12 amended cultures, respectively, compared to controls	30

[a] AO52, Acid Orange 52; AO7, Acid Orange 7; P-O5, pigment Orange 5; RR2, Reactive Red 2; RO14, Reactive Orange 14; DB53, Direct Blue 53; DB71, Direct Blue 71; TNT, Tri-nitro-toluene; RDX, hexahydro-1,3,5-trinitro-1,3,5-triazine; HMX, octahydro-1,3,5,7-tetranitro-1,3,5,7-tetrazocine; CT, carbon tetrachloride; CDD, chlorinated dibenzo-p-dioxins.

[b] AQS, anthraquinone-2-sulfonate; AQDS, anthraquinone-2,6-disulfonate; RF, rivoflavine; LAW, lawsone; HA, humic acids; CNB12, cyanocobalamin; CAT, catechol; RES, resorcinol; HOB12, hydroxycobalamin.

Although quinones and HS have extensively been studied in redox biotransformations acting as RM, their potential to treat pollutants in groundwater and wastewaters generated by several industrial sectors has not been exploited. There are important tasks that should be completed in order to apply RM at real scale; among them, cost-effective sources of redox active groups, engineered HS, and overcoming limitations during catalysis involving RM could been considered. In addition, the solubility of RM is probably the main limitation for their application by the fact they could be washout from bioreactors. For this reason, immobilization of RM is also one of the most important tasks to do. In section 2.3 will be presented the recent advances on immobilization of RM and their use in reductive biotransformations.

2.3 Impact of immobilized RM

Evidence has been accumulated indicating that HS and quinoid analogues can act as RM during the reductive biotransformation of EAC [87]. Nevertheless, one of the main limitations for applying RM in wastewater treatment systems is that continuous addition of HS or quinones should be provided to increase conversion rates, which is economically and environmentally unviable. However, quinoid RM not necessarily have to be supplied abundantly in bioremediation processes to accelerate the redox transformation of different contaminants, as they are being recycled during the transfer of electron from an electron donor to the terminal electron acceptor, as is illustrated in Figure 2.2. An approach to eradicate the requisite of continuous supply of RM in anaerobic bioreactors is to create a niche for their immobilization [87]. Currently, there are significant advances about immobilization of RM for the reductive biotransformation of EAC (Table 2.2 and 2.3); nevertheless, no one of the immobilizing techniques reported have been implemented at full scale yet.

2.3.1 Immobilization of model quinones

Most of studies to elucidate the role of immobilized RM during the biotransformation of EAC have been conducted using model quinones. Anthraquinone-2,6-disulfonate (AQDS), illustrated in Figure 2.3, is the commonly studied RM in both soluble [87] and immobilized

form. Table 2.2 give a review of the studies reporting the different materials used to immobilize model quinones. According to the materials tested, different immobilization mechanisms such as adsorption, entrapment, ion exchange, covalent binding, and doping were observed (Table 2.2). In addition, most of these studies were focused to the biotransformation of azo dye compounds.

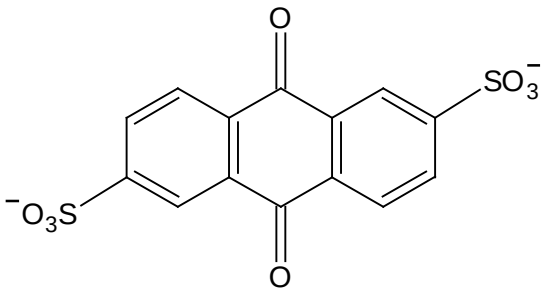

Anthraquinone-2,6-disulfonate (AQDS)

Figure 2.3 Model quinone commonly studied as redox mediator.

Calcium alginate has been used for the immobilization of RM through an entrapment process of anthraquinone [31-33, 82]. Briefly, a suspension anthraquinone was mixed with sodium alginate at a 0.05% (w/w) ratio; and was then pressured to drop into a 5% (w/w) $CaCl_2$ solution to form beads of 3.0–4.0 mm in diameter. Finally, the beads were suspended in a solution of $CaCl_2$ during 4 h in order to enhance their mechanical stability. Guo et al. [33] tested the catalytic effect of this material during the biological reduction of different azo dyes, achieving an increment in the rate of decolorization ranging between 1.5-2-fold compared to the control lacking RM. Also, color removal efficiency near to 100% and 34% for treatments with and without RM, respectively, was observed during decolorization of Acid Red 3R by an anaerobic sludge using these beads containing quinones [82]. The denitrification process was also studied using immobilized quinones into calcium alginate; the rate of denitrification was 2-times higher respect to the control without quinones [32]. Some disadvantages of using this material could be: 1) mass transfer limitations since a

major part of the RM is embedded within the polymeric material making its accessibility dependent on diffusion; 2) gradual loss of redox catalysts due to disruption of the polymeric material owing to weak mechanical strength of the materials explored.

Functionalized polypyrrole (PPy) composites were also enriched with AQDS during the electropolymerization of pyrrole monomer on activated carbon felt (ACF) electrode. This composite (PPy/AQDS/ACF) was used as catalyst for reduction of nitroaromatics compounds [52] and azo dyes [53, 89]. Biotransformation of nitroaromatics compounds using PPy/AQDS/ACF achieved an increased rate of reduction of 5.1, 5.7, and 4.8 times higher for nitrobenzene, 2,4- and 2,6-dinitrotoluene, respectively, compared to the control lacking RM [52]. On the other hand, the composite was also used as a RM for the azo dye biodecolorization, reaching an increment between 1-3.2-fold on the rate of decolorization in relation to the control without PPy/AQDS/ACF, with color removal efficiencies ≥65% for all the twelve different azo compounds tested [53, 89]. Thus, this immobilizing approach seems to be more attractive for full-scale applications than the previously described method involving entrapment within a polymer.

Another approach to immobilize RM is through the adsorption of AQDS and 1,2-naphthoquinone-4-sulfonate (NQS) on anion exchange resins (AER), proposed by Cervantes et al. [12]. The maximum adsorption capacities of RM on AER were 1.42 mmol NQS/g and 1.87 mmol AQDS/g, and were similar under the three different pH (6, 7, 8) conditions evaluated. In this study, three azo compounds were selected in order to evaluate the catalytic capacity of immobilized RM. Compared to the control where RM was not provided, an increase on the rate of decolorization of 8.8-fold was observed for Methyl Orange reduction, respect to the control unsupplied with RM. The adsorption of AQDS on AER was very stable at 25 °C; nevertheless, under conditions of high temperature and high anions (e.g., phosphate and sulfate) concentration, a competition for adsorption sites of AER may occur between quinones and anions [12]. Adsorption of AQDS was also conducted on metal-oxides nanoparticles (MONP) [4]. Among all MONP tested, $Al(OH)_3$ was the most appropriated material for immobilization of AQDS. For instance, an adsorption capacity of 0.105 mmol of AQDS/g was achieved, representing a capacity of 67-times higher respect to others MONP tested. AQDS (4.8 mM) immobilized on $Al(OH)_3$ was used as RM during decolorization of RR2 by anaerobic sludge. The rate of

decolorization increased up to 7.52-fold respect to control lacking quinones [4]. The use of NP to adsorb RM presents the disadvantage that a possible washout of NP can occur from continuous bioreactors. Nevertheless, the process of anaerobic granulation appears to be a niche opportunity for the co-immobilization of humus-reducing microorganisms and NP covered with RM in order to prevent washout of this solid-phase RM [2].

2.3.2 Immobilization of HS

Utilization of immobilized HS for anaerobic biotransformation of priority pollutants has scarcely been studied. There are only two reports showing the impact of immobilized HS (Table 2.2). For instance, fulvic acids (FA) were extracted from a soil of temperate pine forest located in San Luis Potosí, México. Then, FA were adsorbed on particles (45-63 μm) of $Al(OH)_3$, γ-Al_2O_3, and TiO_2 at pH 1. Adsorption tests indicated that particles of γ-Al_2O_3 showed the highest adsorption capacity followed by TiO_2, and $Al(OH)_3$. Immobilized FA on γ-Al_2O_3 demonstrated good catalytic capacity during dehalogenation of carbon tetrachloride (CT) by anaerobic sludge, with a rate of dehalogenation 10.4-fold higher in relation to the control without FA [3]. On the other hand, Cervantes et al. [12] immobilized HA (from the International Humic Substances Society, Catalogue No. 1BS104L) on AER for the anaerobic reduction of RR2 and CT. Prior to adsorption on AER, HA were chemically modified by insertion of sulfonic groups using chlorosulfonic acid ($HClSO_3$), according to the method described by Yudov et al. [99]. Sulfonation of HA increased up to 10.4- and 5.5-fold the solubility of HA at pH 7 and 10, respectively, as compared with not sulfonated HA. In addition, adsorption capacity of sulfonated HA on AER was 2-fold higher compared with not sulfonated HA. Immobilized HA increased ~4-fold the extent of CT reduction to chloroform, by anaerobic consortium, in comparison to incubations lacking HA. Moreover, immobilized HA increased 2-fold the second-order rate constant of decolorization of RR2 as compared with sludge incubations lacking RM [12].

Table 2.2 Impact of immobilized quinones and humic substances on the redox biotransformation of contaminants.

Redox mediator[a]	Immobilizing material	Immobilization mechanism	Pollutants[b]	Results[c]	Ref.
DTB, DR, DV, DB	Terylene and cotton fibers	Chemical	10 different azo dyes	With DTB, a reduction rate of 1.5-3-fold was achieved compared to unamended controls for all azo dyes.	31
AQS	Polyurethane foam	Covalent	Amaranth	Reduction rate of 5-times higher compared to control. CRE of 98.7% after 10 repeated exp.	54
Anthraquinone	Calcium alginate	Entrapment	Nitrate	Denitrification rate was 2-times higher compared to control	32
Anthraquinone	Calcium alginate	Entrapment	AB, RBR, AS, ARB, ARG, RBRK	Reduction rate of 1.5-2 times higher compared to control, for all dyes. With a good reusability after 4 cycles	33
AQDS	Polypyrrole	Doping in pyrrole	NB, DNT	The increment on reduction rate was 4.8 to 5.7-fold respect to the control lacking AQDS.RE >90% after six cycles for 2,4-DNT	52
AQDS, NQS	Ion exchange resin	Anion exchange	RR2, MO, MR	With AQDS, the reduction rates were 1.9-3.4. With NQS, the reduction rates were 3.5-8.8. In all cases respect to the control.	12
AQDS	$Al(OH)_3$ (15 nm)	Adsorption	RR2	Reduction rate was 7.5-fold higher respect to the control, with a CRE of 43% after 12 h	4
AQDS	Polypyrrole	Doping in pyrrole	11 Dyes	CRE ranging between 65-92%, reduction rate was 1-3 times higher respect to the control.	89

Table 2.2 Continued.

Redox mediator[a]	Material	Immobilization mechanism	Pollutants[b]	Results[c]	Ref.
AQDS	Polypyrrole	Doping	RR120	Reduction rate was 3.2-fold higher compared to the control, and 80% of CRE after six repeated experiments	53
AQDS	Calcium alginate	Entrapment	AR3R	CRE of ~100% and 34% with and without AQDS respectively	82
Humic acids	Ion exchange resin	Anion exchange	CT, RR2	CT: reduction rate was 4.0-fold higher respect to the control. RE of ~74% to CF. RR2: decoloriozation rate was 2.0-fold higher respect to the control. CRE of ~69%	13
Fulvic acids	γ-Al_2O_3 (63 μm)	Adsorption	CT	Adsorption and reduction of CT was observed. Reduction rate was 10.4 times compared to the control. RE of 90%	3

[a] DTB, Disperse Turquoise blue S-GL; DR, Disperse Red S-GL3B; DV, Disperse Violet S-GLHFRL; DB, Disperse blue S-GL2BLN; AQS, anthraquinone-2-sulfonate; AQDS, anthraquinone-2,6-disulfonate; NQS, 1,2-Naphthoquinone-4-sulfonate.

[b] AB, Acid Black 10B; RBR, Reactive Brilliant Red X-3B; AS, Acid Scarlet GR; ARB, Acid Red B; ARG, Acid Red G; RBRK, Reactive Brilliant Red K-2BP; NB, Nitrobenzene; DNT, 2,4- and 2,6-dinitrotoluene; RR2, Reactive Red 2; MO, Methyl Orange; MR, Methyl Red; RR120, Reactive Red 120; AR3R, Acid Red 3R; CT, Carbon tetrachloride.

[c] CRE, color removal efficiency; RE, reduction efficiency; CF, Chlroform.

It is well know that HS can be immobilized through physical and chemicals mechanisms using different materials. Nevertheless, many of these materials have not been used in redox reactions yet, but seem to fulfill the requirements to serve as a solid-phase RM for reductive biotransformations of EAC. For instance, Perminova et al. [69] developed a procedure to immobilize covalently HS on silica gel by alkoxysilylation. This material was

shown to efficiently remove actinides in high valence states such as Np(V) and Pu(V) by the sequestering properties of the immobilized HS. In addition, Klavins and Apsite [47] developed a method for the covalent immobilization of FA and HA on various polymers such as styrene-divinylbenzene, cellulose, and silica. These materials were initially designed as adsorbent materials for groundwater remediation through the construction permeable reactive barriers [69]; but also could be applied as solid-phase RM during reductive biotransformations in anaerobic reactors (e.g., UASB reactors) and in groundwater treatment systems.

2.3.3 Carbon-based materials as RM

Carbon-based materials (CBM) such as activated carbon and graphite have been used as RM for the chemical or biological reduction of recalcitrant pollutants (Table 2.3). Unlike of the immobilization processes described in sections 3.1 and 3.2, the use of CBM does not require external RM by the fact that they contain different functional groups at their surface, including quinones structures [25]. Moreover, CBM can be modified chemically in order to enhance their catalytic properties by introduction of different oxygenated active groups. Mainly, oxidization of CBM is through chemical (with HNO_3 or O_2) and/or thermal methods.

Modified surface chemistry of CBM promoted a better redox capacity during reduction of different EAC. For example, Pereira et al. [68] found that thermal modification of activated carbon (AC) in the presence of H_2 (AC_{H2}) was more effective than other oxidation methods for EAC reduction, which was evidenced by an increment of 8.6-fold in the rate of decolorization of the azo dye Mordant Yellow 10 (MY10) at pH 7, in the presence of sulfide, as compared with unmodified AC. Nevertheless, optimum decolorization rates were obtained at pH 5 for the other three azo dyes tested. In a biological system, AC_{H2} also duplicated and increase 4.5-fold the decolorization rates of MY10 and RR2, respectively. On the other hand, reduction of Orange II and Red Black 5 was conducted in upflow stirred packed-bed reactors using modified AC and anaerobic microorganisms [58]. These authors found that conversion values above 88% were achieved in the case of both azo dyes at a space time of 0.23 min or higher, using the AC with the highest surface area. Others azo dye compounds have also been reduced using unmodified AC (Table 2.3).

Table 2.3 Impact of CBM on the redox biotransformation of contaminants.

Material	Chemical modification[a]	Pollutants[b]	Results[c]	Ref.
Activated carbon	With HNO_3, O_2.Thermal with H_2 and N_2	RR2, AO7, MY10, DB71	Chemical reduction: Max. reduction rate was 9-fold higher compared to the control, using sulphide and 0.1 g AC/L Biological reduction: reduction rate were between 2 to 4.5-times higher compared to the control, with AC modified with H	68
Activated carbon	Oxidation with HNO_3 and thermal treatment	OII, RB5	>88% of conversion for both dyes using the AC with highest surface area	58
Activated carbon	WM	TT, OII, OG, AR, RB5, SY	High reduction rates with ≥80% of CRE in ~2 min	57
Activated carbon	WM	AO7	99% of CRE at 2 min	59
Activated carbon	WM	RR2, AO7	CRE in the control without AC ~35%, CRE using AC ~45% and ~95% with 0.4 and 10 g AC/L, respectively	88
Graphite	WM	DNT, RDX	DNT: ~95% and ~16% of RE; RDX: 94% and 26% of RE (with and without graphite, respectively)	64
Graphite	WM	NG, RDX	≥ 90% RE for NG and RDX with both graphite and sulfide	93
Graphite, activated carbon	WM	RDX	Almost a complete destruction of RDX after 2 h. RDX decay rates are favored increasing sulphide, pH and activated carbon	44
Graphite	WM	DNT	93.5% of DNT reduction	63

[a] WM, carbon-based material used without previous modification.

[b] RR2, Reactive Red 2; AO7, Acid Orange 7; MY10, Mordant Yellow 10; DB71, Direct Blue 71; OII, Orange II; RB5, Reactive Black 5; DNT, 2,4-dinitrotoluene; RDX, hexahydro-1,3,5-trinitro-1,3,5-triazine; OG, Orange G; SY, Sunset Yellow FCF; AR, Acid Red 88; TT, Tartrazine; NG, nitroglycerine

[c] AC, Activated carbon; CRE, color removal efficiency; RE, reduction efficiency.

Different nitroaromatic compounds could also be biotransformated using CBM without previous modification (Table 2.3). Oh and Chiu [64] used graphite powder (20-84 mesh) for the chemical reduction of 2,4-dinitrotoluene (DNT) and hexahydro-1,3,5-trinitro-1,3,5-

triazine (RDX) in the presence of dithiothreitol as reductant agent. DNT was firstly adsorbed on graphite, then a effective reduction (~89%) occurred from day two to seven; conversely, the control lacking graphite only achieved ~12% of reduction. Results from others studies indicated that the preferable pathway for the chemical reduction of adsorbed DNT on graphite occurred trough reduction of the *ortho* nitro group to form 2-amino-4-nitrotoluene, using a dialysis cell provided with iron powder [63]. On the other hand, the chemical reduction of RDX using graphite and AC as RM has also been studied [44, 64, 93]. These authors found higher reduction efficiencies (≥90%) as compared with those efficiencies obtained in the controls without CBM. Reduction rates of RDX were improved with the increasing of sulphide concentration, graphite concentration [44, 93], and pH [44].

2.4 The use of NT in wastewater treatment processes

Wastewater treatment can be defined as the manipulation of water from various sources to achieve a water quality in order to meet standards established by different agencies [18]. The treatment of wastewater is an increasingly complicated task due to the large list of contaminants. Nowadays, the United States Environmental Protection Agency (EPA) includes more than 85 compounds in its list of drinking water contaminants [23], and 104 chemicals compounds and 12 microbial agents are included in the third contaminant candidate list [22]; both lists include 126 priority pollutants. Nevertheless, more than 280,000 chemical compounds are currently used around the world [15], and these may eventually contaminate different water bodies or industrial effluents, and consequently require a treatment. Among these pollutants, fuel oxygenates (e.g. methyl *tert*-butyl ether), N-nitrosodimethylamine, perchlorate, chromate, veterinarian medications, NP, and pharmaceutical and personal care products are emerging [18].

The different physicochemical strategies currently used for water treatment such as chemical oxidation, membrane filtration, sorption and ion exchange, solvent extraction, and electrolysis, are time-consuming and expensive technologies [51, 65, 74]. Biological treatment is cost-effective and commonly without generation of undesirable products, but is usually time-consuming [65]. NT could play a significant role in resolving the problems associated with water treatment and remediation. Compared with their bulk forms, NP

offer: 1) affinity, capacity, and selectivity with heavy metals and other contaminants [84]; 2) exceptional physical, mechanical, and electronic properties [83]; and 3) enhanced reactivity, surface area and sequestration characteristics [102].

2.4.1 Physicochemical processes

Different physicochemical processes have been developed in order to treat water pollution. Among these processes are: adsorption, ion exchange, filtration, catalysis, reduction, advanced oxidation, chelation, degradation, photocatalysis, electrocatalysis, and photoelectrocatalysis. Table 2.4 shows a brief list of the different nanomaterials used for water treatment during the removal of different contaminants by physicochemical methods.

Adsorption studies using modified and unmodified carbon-based NP have been conducted to remove organic and inorganic pollutants. Many pollutants such as, azo dyes [60], polyaromatic hydrocarbons [81], nitroaromatics and polyhalogenated aromatics [17]; as well as heavy metals, such as Cd, Cu, Co, Ni, Zn, Mn, and Pb [5, 16, 79], can be adsorbed by carbon NP. The results obtained using carbon-based NP as adsorbents are significant. For instance, Mishra et al. found adsorption capacities (mg/g) of 148, 152 and 141 for direct congo red, reactive green, and golden yellow, respectively, using multi walled carbon nanotubes as adsorbent [60]. These results are similar or higher compared with those obtained using bulk-carbonaceous materials and others adsorbents [34]. On the other hand, Yang et al. examined the adsorption of phenanthrene on alumina NP coated with four sequentially extracted HA [97]. These authors found that the maximum adsorption capacities of AH on alumina at pH 5, were approximately 80, 90, 110, and 150 mg Total Organic Carbon (TOC)/g for the first, second, third, and fourth group of extracted HA. In addition, the adsorption capacity of phenanthrene by alumina NP was enhanced two orders of magnitude when this metal oxide was coated with 1500 mg/L of HA.

Degradation of contaminants using metallic NP as catalysts has also been widely studied. Dechlorination of halogenated compounds such as trichloroethene (TCE) was conducted using bimetallic NP of Pd-Au [62]. The first order rate constant value of 943 L/g Pd/min obtained with the most active composition of Pd-Au was >10-, >70-, and >2000-fold higher compared with monometallic Pd, Pd/Al_2O_3, and Pd black, respectively, with ethane as the

main product [62]. Iron NP have also been applied for the transformation of a large number of contaminants, including chlorinated organic compounds and metal ions [102].

Table 2.4 Physicochemical, biological and hybrid methods to treat water pollution using nanotechnology.

Nano-materials[a]	Process involved	Pollutants removed[b]	Results[c]	Ref.
Physicochemical methods				
MWCNT	Adsorption	Azo dyes	Q_{max} of 148, 152 and 141 was obtained for adsorption of direct congo red, reactive green, and golden yellow, respectively	60
CNx	Adsorption	Cadmium	Q_{max} at pH 7 were 31, and 20 for bamboo-type carbon nanotubes, and cup-stacked-type carbon nanofibres, respectively.	5
CNT	Adsorption	BTEX	Q_{max} were 200, 225, 250, and 270 for BTEX, respectively	81
CNT	Filtration	*E. coli*	Filtered solution not showed growth compared with unfiltered solution ($\sim 10^6$ organisms/mL)	78
ZVI	Reductive immobili-zation	Chromate	90% of Cr(IV) reduction with a dose of 0.12 g L^{-1} of nano-ZVI	94
ZVI	Adsorption	Arsenic(III)	Q_{max} calculated by Freundlich adsorption isotherm was 3.5.	42
TiO_2	Photoelec-trocatalysis	2-NP, 4-NP	95% of 4-NP and 85% of 2-NP was removed over a 2 h period from a 0.1 mM solutions.	85
PCA-SC	Filtration	Organic pollutants	Removal of PCA (up to 99%), of MAH (up to 93%), THM (up to 81%), MTBE (up to 46%).	1
Anion-SAMMS	Adsorption	Anions	Adsorption of Chromate and Arsenate	43
PH-SAMMS	Adsorption	LA, AC	High efficiency for LA and AC sequestration	27 28

Table 2.4 Continued.

Nano-materials[a]	Process involved	Pollutants removed[b]	Results[c]	Ref.
Biological and hybrid methods				
Single-enzime	Degradation	Organic pollutants	Phenols, polyaromatics, dyes, PCC, organophos-phorous pesticides, and explosives are suspect to be degraded	46
Bio-Pd	Reduction	TCE	The dechlorination rate up to 2,515 mg TCE day^{-1} g^{-1} Pd using hydrogen as electron donor	37
Bio-Pd	Reduction	TCE, DTZ	An increment of 20% in the rate of reduction of TCE using Bio-Pd. Reduction efficiencies of DTZ were ~48% and ~93% for the treatments without and with bio-Pd, respectively	36
Bio-Pd, Bio-Mn	Reduction/ oxidation	PHMC, BC, ICM	Reduction with Bio-Pd was higher than 90% for four compounds. Oxidation with Bio-MnOx was variable, but 14 of 29 compounds were eliminated achieving values ranging between 52%-95%.	26
Fe_3O_4	Desulfuri-zation	DBTP	56% higher of desulfurization compared with the control lacking NP	6
Quinones on $Al(OH)_3$	Reduction	RR2	Immobilized quinone increased up to 7.5-fold the rate of decolorization by anaerobic sludge as compared with incubations lacking RM	4
PEG-UC	Sequestra-tion and biodegra-dation	PHT	Nanoparticles enhanced the release of adsorbed and sequestered PHT, also increase its mineralization rate.	86

[a] CNT, carbon nanotubes; MWCNT, multi-walled CNT; CNx, CNT doped with nitrogen; ZVI, zero valent iron; PCA-SC, Polymer-impregnated ceramic alumina and silicon-carbon; SAMMS, Self-assembled monolayer on mesoporous supports; PH-SAMMS, phosphonate and hydroxypyridone SAMMS; PEG-UC, poly(ethylene) glycol modified urethane acrylate.

[b] BTEX, Benzene, toluene, ethylbenzene, p-xylene; 2-NP and 4-NP, 2-, 4-nitrophenol; LA, lantinides; AC, actinides; TCE, trichloroethene; DTZ, diatrizoate; PHMC, pharmaceuticals; BC, biocides; ICM, iodinated contrast media; DBTP, Dibenzothiophene; RR2, Red Reactive 2; PHT, phenanthrene.

[c] Q_{max}, maximum adsorption capacity; PCA, polycyclic aromatic hydrocarbons; MAH, monocyclic aromatic hydrocarbons; THM, trihalogen methanes; MTBE, methyl-tert-butyl ether; PCC, polychlorinated compounds; NP, nanoparticles; RM, redox mediator.

2.4.2 Biological processes

Biological water treatment systems using NT have been probably less extensively studied compared with physicochemical processes; nevertheless, important researches have been conducted in this direction (Table 2.4). Hennebel et al. [37] describes the use of microbially produced Pd(0) NP (bio-Pd) for dechlorination of TCE. Bio-Pd particles were deposited on *Shewanella oneidensis*, which dechlorinated TCE with a rate up to 2,515 mg TCE/day/g Pd using hydrogen as electron donor. Also, dehalogenation of TCE and diatrizoate using bio-Pd in microbial electrolysis cell (MEC) was carry out by Hennebel et al. [36] TCE dehalogenation using bio-Pd (5 mg/g graphite) to coat cathode granules, reaches a removal rate of 151 g TCE/m total cathode compartment (TCC)/day; and using bio-Pd free MCE the rate was 120 g TCE/m TCC/day, applying a power of -0.8 V. In addition, reduction efficiencies of diatrizoate were ~48% and ~93% for the treatments without and with bio-Pd, respectively [36]. Application of biogenically produced metals was also conducted by Forrez et al. [26]. These authors tested bio-Pd in lab-scale membrane bioreactor, and they found that iomeprol, iopromide and iohexol were removed by >97%, and diatrizoate by 90%. Moreover, with biogenic manganese oxides (bio-MnOx), 14 of 29 substances (pharmaceutical and personal care products) detected in the secondary effluents of sewage treatment plants were eliminated; achieving different values of removal for each substance, ranging between 52%-95% [26].

Another application of NT in biological processes was conducted by Ansari et al. [6]. These authors decorated *Rhodococcus erythropolis* with NP of Fe_3O_4 for the degradation of dibenzothiophene (DBT). Unlike of the biologically obtained metals described before, Fe_3O_4 NP were chemically synthesized. Nevertheless, important results were obtained when NP were adsorbed on the bacterial surface, achieving 56% higher of DBT desulfurization compared with the control lacking NP.

2.4.3 Hybrid processes

Hybrid processes involve two or more mechanisms during the degradation of pollutants in a wastewater treatment system. Combination of processes can enhance, promote and/or facilitate the degradation of contaminants. For instance, Tungittiplakorn et al. [86] investigated the usefulness of NP of poly(ethylene) glycol modified urethane acrylate

(PMUA), in enhancing the bioavailability of phenanthrene. Solubilization, adsorption and biodegradation were the three roles identified by using PMUA in the process. The extent of the solubilization was evidenced by the distribution coefficients of 780 mL/g and 3260 mL/g observed in the absence and presence of PMUA, respectively. In addition, biodegradation of phenanthrene was promoted due to the accessibility of adsorbed contaminant on PMUA NP for *Comamonas testosterone* [86]. Immobilization of metallic NP on cellulose acetate membrane for degradation of chlorinated compounds is also a reported hybrid process. Cellulose acetate allows the incorporation of 24-nm NP of Fe and Ni to membrane films; and this hybrid films demonstrated a greater than 75% reduction of TCE in 4.25 h, adding only 10% of the metal used in others studies reported in the literature [56].

On the other hand, it is well know that quinones and HS can serve as RM to accelerate the rate of reduction of several electron accepting contaminants [87] (Figure 2.2). Nevertheless, one of the main limitations for applying RM in wastewater treatment systems is that continuous addition of HS should be supplied to increase conversion rates, which is economically and environmentally unviable. An approach to eradicate the requisite of continuous supply of RM in anaerobic bioreactors is to create a system for their immobilization. For this reason, a hybrid process with immobilized RM and its consequent use as solid-phase catalyst, could eradicate the requisite of continuous addition. Alvarez et al. [4] used NP of $Al(OH)_3$, as adsorbents to immobilize anthraquinone 2,6-disulfonate (AQDS) for its application in the anaerobic reduction of Reactive Red 2 (RR2). Immobilized AQDS increased up to 7.5-fold the rate of decolorization of RR2 by anaerobic sludge as compared with sludge incubations lacking AQDS. Immobilization of AQDS on NP was very stable under the applied experimental conditions and spectrophotometric screening did not detect any detachment of AQDS during the time period reduction, confirming that immobilized AQDS served as an effective solid-phase RM [4].

Although the catalytic effect of immobilized RM on metal oxide NP (MONP) has been demonstrated, several important topics should be considered in order to use immobilized RM on NP in wastewater treatment systems. Some considerations are the following: 1) the evaluation of different NP, not only MONP, capable to effectively adsorb RM; 2) identify the most appropriated mechanism to immobilize RM, this is important in order to prevent

its release from the NP (see below); 3) test the catalytic capacity of immobilized RM to reduce different electron accepting contaminants; 4) evaluate the immobilization of HS on NP, not only model quinones (see below); 5) identify the most appropriated strategy to prevent the washout of NP covered with RM (NP-RM) from the bioreactors (e.g. upflow anaerobic sludge blanket, UASB). This last point is described below.

2.4.3.1 Adsorption of HS on NP

The interaction of HA with different MONP was evaluated by Yang et al. [96]. In this study it was documented that the adsorption of HA on TiO_2, α-Al_2O_3, γ-Al_2O_3 and ZnO was limited by the surface area of NP and was pH-dependent. The highest adsorption capacity was achieved by TiO_2 and γ-Al_2O_3, with values of ~95 and ~80 mg TOC/g respectively, at pH 5. These authors suggested that the adsorption of HA on MONP is affected by three main factors: (1) large surface area of NP; (2) low hydrophilicity and few negative charges on MONP surface, allowing HA to approach to their surface; and (3) strong interactions such as electrostatic attraction and ligand exchange between HA and MONP surfaces [96]. In addition, the most suitable mechanisms to describe the interaction between MONP and HA are anion exchange (electrostatic interaction), ligand exchange, hydrophobic interaction, entropic effect, hydrogen bonding, and cation bridging [29, 77].

Utilization of immobilized HA or quinones on NP through electrostatic interaction, could have the disadvantage that these RM can be desorbed when this material is exposed to adverse conditions, such as pH and temperature changes. Perminova et al. developed a procedure to immobilize covalently HS on alumina particles by alkoxysilylation [70]. This material was shown to efficiently remove Np(V) and Pu(V) by the sequestering properties of the immobilized HS [69]. However, this immobilized material has not been tested in redox reactions yet, but seems to fulfill the requirements to serve as a solid-phase RM for reductive biotransformations.

2.4.3.2 Co-immobilization of humus reducing microorganisms and NP-RM

The core of UASB reactors are the aggregates of microorganisms called granular sludge. Due to the particles size (0.5-2 mm) and high settling capacity, granules resist their washout from the bioreactors permitting high hydraulic loads. Granulation is not clearly defined

nowadays; nevertheless, Hulshoff Pol et al. [39] list 17 theories, from different authors, about the mechanisms of granulation. Different factors such as microbiological, other biotic and abiotic factor are involved in the process. The granulation process appears to be a niche of opportunity for the co-immobilization of humus reducing microorganisms (HRM) and NP-RM in order to prevent the washout of this solid-phase RM.

Figure 2.4 shows a scheme of granulation process simultaneously immobilizing HRM and NP-RM. This model is based on the spaghetti theory proposed by Wiegant W. [91], which is probably the most accurate theory about sludge granulation. In this theory, the first step is the interaction of filamentous microorganisms, such as *Methanosaete*, which produce small aggregates due to the turbulence generated by biogas or for the attachment to finely dispersed matter. The initial pellets can serve as a surface of attachment for other anaerobic microorganisms or NP-RM. Abiotic factors such as slime layers and calcium can enhance the attachment of microorganisms and NP-RM to the pellet. Calcium can serve as a bridge between negative charges to generate bacteria/bacteria and bacteria/NP-RM interactions. Both, surface of microorganisms and HS adsorbed on NP are negatively charged at circumneutral pH conditions; for this reason, calcium addition could have an important impact during the co-immobilization of HRM and NP-RM. Additionally, particles coated with HS could be used as nuclei for sludge granulation or biofilms growth, as has previously been shown with zeolite particles [98].

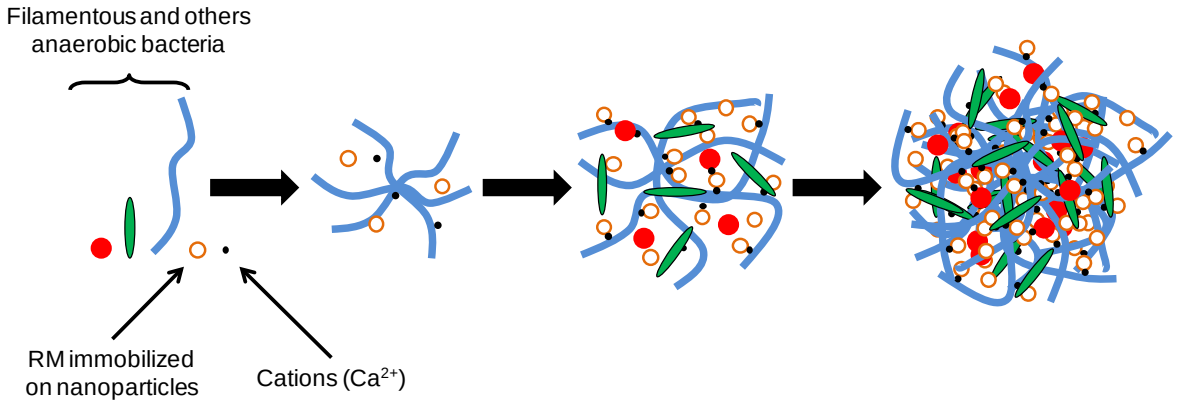

Figure 2.4 Proposed model for granulation co-immobilizing humus reducing microorganisms and nanoparticles coated with humic acids.

2.4.4 Presence of NP in environment

Although NT represents a promissory response for a better human life quality and for enhancing environment quality, it is very important to consider the impact of NP when they are introduced to ecosystems. There are many research and review papers considering that the actual knowledge about the impact, fate, and transport of NP in ecosystems is very limited. Nevertheless, during the last years, several studies have demonstrated the impact of NP in aquatic, air, and soil systems, including biotic and abiotic conditions; these processes are represented in Figure 2.5. NP can alter the environment by direct effect on biota (i.e. toxicity), changes in the bioavailability of toxins or nutrients, indirect effects on ecosystem (i.e. break-up of refractory natural organic substances), and changes of the environmental microstructures. In order to understand the impacts of NP in the environment, transport is a critical factor that needs to be considered. In some cases, those NP designed to be dispersed and intentionally introduced to the environment requires high mobility; conversely, those NP for other applications require low mobility [101]. Transport of NP is mainly dominated by Brownian diffusion, whereas forces such as the London-van der Waals and double-layered forces are responsible for attachment that ultimately determines their mobility [48]. The toxicity of several MONP have been evaluated on different bacteria including *Bacillus subtilis, Escherichia coli, Shewanella oneidensis, Cupriavididus metallidurans, Streptococcus aureus, and Pseudomonas fluorescens* [40, 67, 73, 76]. Toxicity of NP on bacteria can be attributed to the chemical composition of MONP, which can release toxic ions and particle surface catalyzed reactions, producing reactive oxygen species; or due to stress caused by physical characteristics of NP such as surface, size, and shape [10]. On the other hand, owing the presence of natural organic matter (i.e. HA) in aquatic environments, the surface of released NP can become negatively charged when HA are adsorbed, altering their fate and transport [96]. Moreover, adsorption of HA can increase the capacity of NP to adsorb organic contaminants, thus increasing also the toxicity of NP [90, 95]. Toxicity of NP on humans has also been studied. Cardiovascular and pulmonary effects as well as to other organs due to introduction of NP to human body were explained by Gwinn and Vallyathan [35]. The most common exposure routes of NP to human body are ingestion, ocular, inhalation, and dermal [41].

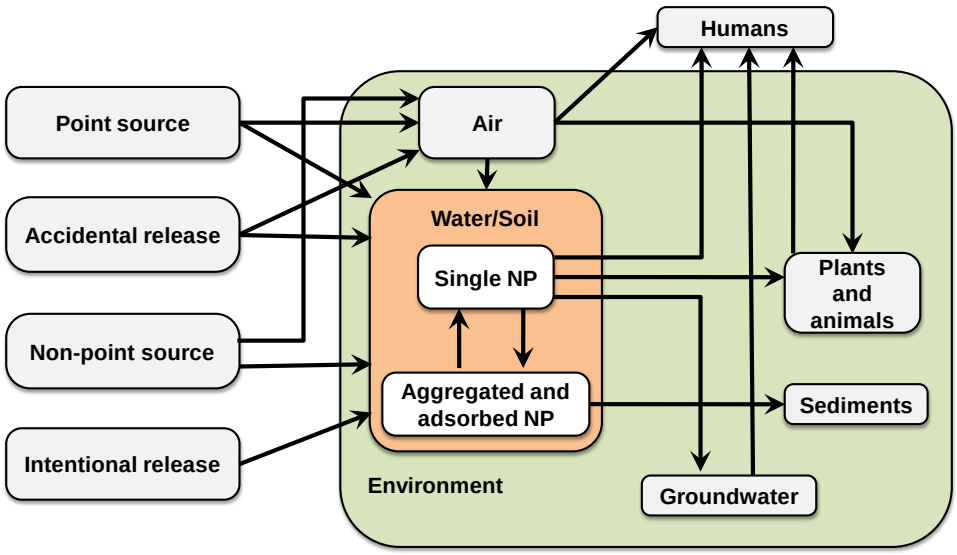

Figure 2.5 Release of NP from different sources into the environment, reactions in the environment and exposure of humans. Modified from reference 61.

Finally, Shah V. [75] showed a study conducted with data collected through April 2010 for articles (199 articles reporting 370 studies) published across all major scientific journals on ecotoxicological assessment of nanoparticles. This collection indicates that 42 NP has been tested in order to evaluate their ecotoxicological effects on several organisms, indicating that the most studied are microbial cultures (42%) , followed by daphnids and shrimp (20%), fish or fish cells (18%), plants (8%), worms (5%), and microbial and aquatic communities (3%). Regarding the use of NP, TiO_2 was the most widely tested (15%), followed by the C_{60} NP (12%), silver (11%), zinc oxide (11%), and others NP (<5% each). Some important tasks are still pending because there are no studies on several invertebrates, and no ecotoxicological studies have been carried out in the field. Also, many NP such as SiO_2, nanotubes, quantum dots, and transition metals have scarcely been studied [75].

References

1. Allabashi R, Arkas M, Hörmann G, Tsiourvas D, Removal of some organic pollutants in water employing ceramic membranes impregnated with cross-linked silylated dendritic and cyclodextrin polymers. *Wat Res* 41:476-486 (2007).

2. Alvarez LH, Cervantes FJ, Assessing the impact of alumina nanoparticles in an anaerobic consortium: methanogenic and humus reducing activity. *App Microbiol Biotechnol* (2012).

3. Alvarez LH, Jimenez L, Hernandez-Montoya V, Cervantes FJ, Enhanced dechlorination of carbon tetrachloride by immobilized fulvic acids on alumina particles. *Water Air Soil Pollut* (2012).

4. Alvarez LH, Perez-Cruz MA, Rangel-Mendez JR, Cervantes FJ, Immobilized redox mediator on metal-oxides nanoparticles and its catalytic effect in a reductive decolorization process. *J Hazard Mater* 184:268–272 (2010).

5. Andrade-Espinosa G, Muñoz-Sandoval E, Terrones M, Endo M, Terrones H, Rangel-Mendez JR, Acid modified bamboo-type carbon nanotubes and cup-stacked-type carbon nanofibres as adsorbent materials: cadmium removal from aqueous solution. *J Chem Technol Biotechnol* 84: 519–524 (2009).

6. Ansari F, Grigoriev P, Libor S, Tothill IE, Ramsden JJ, DBT degradation enhancement by decorating rhodococcus erythropolis IGST8 with magnetic Fe_3O_4 nanoparticles. *Biotechnol Bioeng* 102:1505-1512 (2009).

7. Baek YW, An YJ, Microbial toxicity of metal oxide nanoparticles (CuO, NiO, ZnO, and Sb_2O_3) to Escherichia coli, Bacillus subtilis, and Streptococcus aureus. *Sci Total Environ* 409:1603–1608 (2011).

8. Barkovskii AL, Adriaens P. Impact of humic constituents on microbial dechlorination of polychlorinated dioxins. *Environ Toxicol Chem* 17:1013–1020 (1998).

9. Borch T, Inskeep WP, Harwood JA, Gerlach R, Impact of ferrihydrite and anthraquinone- 2,6-disulfonate on the reductive transformation of 2,4,6-trinitrotoluene by a Grampositive fermenting bacterium. *Environ Sci Technol* 39:7126–33 (2005).

10. Brunner TJ, Wick P, Manser P, Spohn P, Grass RN, Limbach LK, Bruinink A, Stark WJ, In vitro cytotoxicity of oxide nanoparticles: comparison to asbestos, silica, and the effect of particle solubility. *Environ Sci Technol* 40:4374–4381 (2006).

11. Cervantes FJ, Enriquez JE, Mendoza-Hernandez MR, Razo-Flores E, Field JA, The role of sulphate reduction on the reductive decolorization of the azo dye reactive orange 14. *Water Sci Technol* 54:171–177 (2006).

12. Cervantes FJ, Garcia-Espinosa A, Moreno-Reynosa MA, Rangel-Mendez JJ, Immobilized redox mediators on anion exchange resins and their role on the reductive decolorization of azo dyes. *Environ Sci Technol* 44:1747-1753 (2010).

13. Cervantes FJ, González-Estrella J, Márquez A, Alvarez LH, Arriaga S, Immobilized humic substances on an anion exchange resin and their role on the redox biotransformation of contaminants. *Bioresour Technol* 102:2097-2100 (2011).

14. Cervantes FJ, Vu-Thi-Thu L, Lettinga G, Field JA, Quinone-respiration improves dechlorination of carbon tetrachloride by anaerobic sludge. *Appl Microbiol Biotechnol* 64:702–11 (2004).

15. CHEMLIST Database. American Chemical Society. http://www.cas.org/ASSETS/15B4DC7AD24B4F6BA38AEEE76214190E/chemlist.pdf [accessed 15 October 2011].

16. Chen C, Wang X, Adsorption of Ni(II) from Aqueous Solution Using Oxidized Multiwall Carbon Nanotubes. *Ind Eng Chem Res* 45:9144-9149 (2006).

17. Chen W, Duan L, Zhu D, Adsorption of polar and nonpolar organic chemicals to carbon nanotubes. *Environ Sci Technol* 41:8295-8300 (2007).

18. Crittenden JC, Trussell RR, Hand DW, Howe KJ, Tchobanoglous G, Water treatment: principles and design (2nd Edition), John Wiley & Sons (2005).

19. Diallo MS, Balogh L, Shafagati A, Johnson JH, Goddard WA, Tomalia DA, Poly(amidoamine) dendrimers: a new class of high capacity chelating agents for Cu(II) ions. *Environ Sci Technol* 33:820–824 (1999).

20. Dos Santos AB, De Madrid MP, De Bok FAM, Stams AJM, Van Lier JB, Cervantes FJ, The contribution of fermentative bacteria andmethanogenic archaea to azo dye reduction by a thermophilic anaerobic consortium. *Enzyme Microb Technol* 39:38–46 (2006).

21. Encinas-Yocupicio AA, Razo-Flores E, Sanchez-Diaz F, Dos Santos AB, Field JA, Cervantes FJ, Catalytic effects of different redox mediators on the reductive decolorization of azo dyes. *Water Sci Technol* 54:165–70 (2006).

22. EPA, Final third drinking water contaminant candidate list. http://water.epa.gov/scitech/drinkingwater/dws/ccl/upload/fs_cc3_final.pdf [accessed January 2011].

23. EPA, National primary drinking water regulations. http://water.epa.gov/drink/contaminants/ [accessed January 2011].

24. Field JA, Cervantes FJ, van der Zee FP, Lettinga G, Role of quinones in the biodegradation of priority pollutants: a review. *Wat Sci Technol* 42:215-222 (2000).

25. Figueiredo JL, Pereira MFR, Freitas MMA, Órfão JMM, Modification of the surface chemistry of activated carbons. *Carbon* 37:1379-1389 (1999).

26. Forrez I, Carballa M, Fink G, Wick A, Hennebel T, Vanhaecke L, Ternes T, Boon N Verstraete W, Biogenic metals for the oxidative and reductive removal of pharmaceuticals, biocides and iodinated contrast media in a polishing membrane bioreactor. *Water Res* 45:1763-1773 (2011).

27. Fryxell GE, Lin Y, Fiskum S, Birnbaum JC, Wu H, Actinide sequestration using self–assembled monolayers on mesoporous supports. *Environ Sci Technol* 39:1324–1331 (2005).

28. Fryxell GE, Wu H, Lin Y, Shaw WJ, Birnbaum JC, Linehan JC, Nie Z, Kemner K, Kelly S, Lanthanide selective sorbents: self assembled monolayers on mesoporous supports (SAMMS). *J Mater Chem* 14:3356-3363 (2004).

29. Gu BH, Schmitt J, Chen ZH, Liang LY, McCarthy JF, Adsorption and desorption of natural organic matter on iron oxides: mechanisms and models. *Environ Sci Technol* 28:38-46 (1994).

30. Guerrero-Barajas C, Field JA, Riboflavin- and cobalamin-mediated biodegradation of chloroform in a methanogenic consortium. *Biotechnol Bioeng* 89:539–50 (2005).

31. Guo J, Kang L, Lian J, Yang J, Yan B, Li Z, Liu C, Yue L, The accelerating effect and mechanism of a newly functional bio-carrier modified by redox mediators for the azo dyes decolorization. *Biodegradation* 21:1049-1056 (2010).

32. Guo J, Kang L, Yang J, Wang X, Lian J, Li H, Guo Y, Wang Y, Study on a novel non-dissolved redox mediator catalyzing biological denitrification (RMBDN) technology. *Bioresour Technol* 101:4238-4241 (2010).

33. Guo J, Zhou J, Wang D, Tian C, Wang P, Salah Uddin M, Yu H, Biocatalyst effects of immobilized anthraquinone on the anaerobic reduction of azo dyes by the salt-tolerant bacteria. *Water Res* 41:426-432 (2007).

34. Gupta VK, Suhas, Application of low-cost adsorbents for dye removal: A review. *J Environ Manage* 90:2313–2342 (2009).

35. Gwinn MR, Vallyathan V, Nanoparticles: health effects-pros and cons. *Environ Health Persp* 114:1818-1825 (2006).

36. Hennebel T, Benner J, Clauwaert P, Vanhaecke L, Aelterman P, Callebaut R, Boon N, Verstraete W, Dehalogenation of environmental pollutants in microbial electrolysis cells with biogenic palladium nanoparticles. *Biotechnol Lett* 33:89–95 (2011).

37. Hennebel T, Simoen H, Windt W, Verloo M, Boon N, Verstraete W, Biocatalytic dechlorination of trichloroethylene with bio-palladium in a pilot-scale membrane reactor. *Biotechnol Bioeng* 102:995-1002 (2009).

38. Hu J, Chen G, Lo IMC, Selective removal of heavy metals from industrial wastewater using maghemite nanoparticle: performance and mechanisms. *J Envir Engrg* 132:709-715 (2006).

39. Hulshoff Pol LW, Castro Lopes SI, Lettinga G, Lens PNL, Anaerobic sludge granulation. *Water Res* 38:1376–1389 (2004).

40. Jiang W, Mashayekhi H, Xing B, Bacterial toxicity comparison between nano- and micro-scaled oxide particles. *Environ Pollut* 157:619-1625 (2009).

41. Kandlikar M, Ramachandran G, Maynard A, Murdock B, Toscano WA, Health risk assessment for nanoparticles: A case for using expert judgment. *J Nanopar Res* 9:137-156 (2007).

42. Kanel SR, Manning B, Charlet L, Choi Hm, Removal of arsenic(III) from groundwater by nanoscale zero-valent iron. *Environ Sci Technol* 39:1291–1298 (2005).

43. Kelly S, Kemner K, Fryxell GE, Liu J, Mattigod SV, Ferris KF, X-ray absorption fine structure spectroscopy study of the interactions between contaminant tetrahedral anions to selfassembled monolayers on mesoporous supports. *J Phys Chem* 105:6337–6346 (2001).

44. Kemper JM, Ammar E, Mitch WA, Abiotic degradation of hexahydro-1,3,5-trinitro-1,3,5-triazine in the presence of hydrogen sulfide and black carbon. *Environ Sci Technol* 42:2118-2123 (2008).

45. Khaydarov RA, Khaydarov RR, Gapurova O, Water purification from metal ions using carbon nanoparticle-conjugated polymer nanocomposites. *Wat Res* 44:1927-1933 (2010).

46. Kim J, Grate JW, Single-enzyme nanoparticles armored by a nanometer-scale organic/inorganic network. *Nano Lett* 3:1219–1222 (2003).

47. Klavins M, Aspite E, Immobilization of humic substances, in: Drozd J, Gonet SS, Senesi N, Weber J Eds. The role of humic substances in the ecosystems and in

environmental protection. PTSH-Polish Society of Humic Subtances, Wroclaw, Poland, (1997).

48. Kulkarni P, Sureshkumar R, Biswas P, Multiscale simulation of irreversible deposition in presence of double layer interactions. *J Colloid Interf Sci* 260:36-48 (2003).

49. Kwon M, Finneran K, Biotransformation products and mineralization potential for hexahydro-1,3,5-trinitro-1,3,5-triazine (RDX) in abiotic versus biological degradation pathways with anthraquinone-2,6-disulfonate (AQDS) and Geobacter metallireducens. *Biodegradation* 19:705–715 (1998).

50. Kwon MJ, Finneran KT, Microbially mediated biodegradation of hexahydro-1,3,5-trinitro-1,3,5- triazine by extracellular electron shuttling compounds. *Appl Environ Microbiol* 72:5933–5941 (2006).

51. Langwaldt JH, Puhakka JA, On-site biological remediation of contaminated groundwater: A review. *Environ Pollut* 107:187–197 (2000).

52. Li L, Wang J, Zhou J, Yang F, Jin C, Qu Y, Li A, Zhang L, Enhancement of nitroaromatic compounds anaerobic biotransformation using a novel immobilized redox mediator prepared by electropolymerization. *Bioresour Technol* 99:6908-6916 (2008).

53. Li L, Zhou J, Wang J, Yang F, Jin C, Zhang G, Anaerobic biotransformation of azo dye using polypyrrole/anthraquinonedisulphonate modified active carbon felt as a novel immobilized redox mediator. *Sep Purif Technol* 66:375-382 (2009).

54. Lu H, Zhou J, Wang J, Si W, Teng H, Liu G, Enhanced biodecolorization of azo dyes by anthraquinone-2-sulfonate immobilized covalently in polyurethane foam. *Bioresour Technol* 101:7185–7188 (2010).

55. Mattigod SV, Fryxell GE, Feng X, Parker KE, Piers EM, Removal of mercury from aqueous streams of fossil fuel power plants using novel functionalized nanoporous sorbents. In Coal combustion by-products and environmental issues, ed by Sajwan KS, Twardowska I, Punshon T and Alva AK, New York, Springer, pp. 99–104 (2006).

56. Meyer DE, Wood K, Bachas LG, Bhattacharyya D, Degradation of chlorinated organics by membrane-immobilized nanosized metals. *Environmental Progress* 23:232-242 (2004).

57. Mezohegyi G, Fabregat A, Font J, Bengoa C, Stuber F, Fortuny A, Advanced bioreduction of commercially important azo dyes: modeling and correlation with electrochemical characteristics. *Ind Eng Chem Res* 48:7054-7059 (2009).

58. Mezohegyi G, Goncalves F, Órfão JJM, Fabregat A, Fortuny A, Font J, Bengoa C, Stuber F, Tailored activated carbons as catalysts in biodegradation of textile azo dyes. *Appl Catal B: Environ* 94:179–185 (2010).

59. Mezohegyi G, Kolodkin A, Castro UI, Bengoa C, Stuber F, Font J, Fabregat A, Effective anaerobic decolorization of azo dye acid orange 7 in continuous upflow packed bed reactor using biological activated carbon system. *Ind Eng Chem Res* 46:6788–6792 (2007).

60. Mishra AK, Arockiadoss T, Ramaprabhu S, Study of removal of azo dye by functionalized multi walled carbon nanotubes. *Chem Eng J* 162:1026-1034 (2010).

61. Nowack B, Bucheli TD, Occurrence, behavior and effects of nanoparticles in the environment. *Environ Pollut* 150:5-22 (2007).

62. Nutt MO, Hughes JB, Wong MS, Designing Pd-on-Au bimetallic nanoparticle catalysts for trichloroethene hydrodechlorination. *Environ Sci Technol* 39:1346–1353 (2005).

63. Oh SY, Cha DK, Chiu PC, Graphite-mediated reduction of 2,4-dinitrotoluene with elemental iron. *Environ Sci Technol* 36:2178-2184 (2002).

64. Oh SY, Chiu PC, Graphite- and soot-mediated reduction of 2,4-dinitrotoluene and hexahydro-1,3,5-trinitro-1,3,5-triazine. *Environ Sci Technol* 43:6983-6988 (2009).

65. Patterson JW, Industrial wastewater treatment technology. 2nd Edition. Butterworth Publishers, Boston (1985).

66. Pearce CI, Guthrie JT, Lloyd JR, Reduction of pigment dispersions by Shewanella strain J18 143. *Dyes Pigm* 76:696–705 (2008).

67. Pelletier DA, Suresh AK, Holton GA, McKeown CK, Wang W, Gu B, Mortensen NP, Allison DP, Joy DC, Allison MR, Brown SD, Phelps TJ, Doktycz MJ, Effects of Engineered Cerium Oxide Nanoparticles on Bacterial Growth and Viability. *Appl Environ Microb* 76:7981–7989 (2010).

68. Pereira L, Pereira, R, Pereira MFR, van der Zee FP, Cervantes FJ, Alves MM, Thermal modification of activated carbon surface chemistry improves its capacity as redox mediator for azo dye reduction. *J Hazard Mater* 183:931-939 (2010).

69. Perminova I, KarpioukL, Shcherbina N, Ponomarenko S, Kalmykov S, Hatfield K, Preparation and use of humic coatings covalently bound to silica gel for Np(V) and Pu(V) sequestration. *J Alloy Compd* 444-445:512-517 (2007).

70. Perminova I, Ponomarenko S, Karpiouk L, Hatfield K, PCT application RU2006/000102, Humic derivatives, methods of preparation and use (2006).

71. Ramalho PA, CardosoMH, Cavaco-Paulo A, Ramalho MT, Characterization of azo reduction activity in a novel ascomycete yeast strain. *Appl Environ Microbiol*, 70:2279–2288 (2004).

72. Ratasuk N, Nanny MA, Characterization and quantification of reversible redox sites in humic substances. *Environ Sci Technol*, 41:7844–7850 (2007).

73. Sadiq IM, Chowdhury B, Chandrasekaran N, Mukherjee A, Antimicrobial sensitivity of Escherichia coli to alumina nanoparticles. *Nanomedicine: NBM* 5:282-286 (2009).

74. Schwarzenbach RP, Escher BI, Fenner K, Hofstetter TB, Johnson CA, von Gunten U, Wehrli B, The challenge of micropollutants in aquatic systems. *Science* 313:1072–1077 (2006).

75. Shah V, Environmental impacts of engineered nanoparticles. *Environ Toxicol Chem* 29:2389–2390 (2010).

76. Simon-Deckers A, Loo S, Mayne-L'hermite M, Herlin-Boime N, Menguy N, Reynaud C, Gouget B, Carrire M, Size-, composition- and shape-dependent toxicological impact of metal oxide nanoparticles and carbon nanotubes toward bacteria. *Environ Sci Technol* 43:8423-8429 (2009).

77. Sposito G, The Surface Chemistry of Soils. Oxford University Press, Nueva York, (1984).

78. Srivastava A, Srivastava ON, Talapatra S, Vajtai R, Ajayan PM, Carbon nanotube filters. *Nat Mat* 3:610-614 (2004).

79. Stafiej A, Pyrzynska K, Adsorption of heavy metal ions with carbon nanotubes. *Sep Purif Technol* 58:49-52 (2007).

80. Stevenson FJ, Humus Chemistry: Genesis, Composition, Reactions. John Wiley & Sons, Inc., New York (1994).

81. Su F, Lu C, Hu S, Adsorption of benzene, toluene, ethylbenzene and p-xylene by NaOCl-oxidized carbon nanotubes. *Colloid Surface A* 1:83-91(2010).

82. Su Y, Zhang Y, Wang J, Zhou J, Lu X, Lu H, Enhanced bio-decolorization of azo dyes by co-immobilized quinone-reducing consortium and anthraquinone. *Bioresour Technol* 100:2982-2987 (2009).

83. Tenne R, Inorganic nanotubes and fullerene-like nanoparticles. *Nat Nanotechnol* 1:103–111 (2006).

84. Theron J, Walker JA, Cloete TE, Nanotechnology and water treatment: applications and emerging opportunities. *Crit Rev Microbiol* 34:43–69 (2008).

85. Tian M, Wu G, Adams B, Wen J, Chen A, Kinetics of photoelectrocatalytic degradation of nitrophenols on nanostructured TiO_2 electrodes. *J Phys Chem C* 112:825–831 (2008).

86. Tungittiplakorn W, Cohen C, Lion LW, Engineered polymeric nanoparticles for bioremediation of hydrophobic contaminants. *Environ Sci Technol* 39:1354–1358 (2005).

87. Van der Zee FP, Cervantes FJ, Impact and application of electron shuttles on the redox (bio)transformation of contaminants: A review. *Biotechnol Adv* 27:256–277 (2009).

88. Van der Zee FP, Bisschops IA, Lettinga G, Field JA, Activated carbon as an electron acceptor and redox mediator during the anaerobic biotransformation of azo dyes. *Environ Sci Technol* 37:402-408 (2003).

89. Wang J, Li L, Zhou J, Lu H, Liu G, Jin R, Yang F, Enhanced biodecolorization of azo dyes by electropolymerization-immobilized redox mediator. *J Hazard Mater* 168:1098-1104 (2009).

90. Wang X, Lu J, Xu M, Xing B, Sorption of pyrene by regular and nanoscaled metal oxide particles: influence of adsorbed organic matter. *Environ Sci Technol* 42:7267-7272 (2008).

91. Wiegant WM, The spaghetti theory on anaerobic sludge formation, or the inevitability of granulation, in *Granular anaerobic sludge: Microbiology and technology*, ed by Lettinga G, Zehnder AJB, Grotenhuis JTC and Hulshoff Pol LW. The Netherlands: Pudoc. Wageningen (1987).

92. Workman DJ, Woods SL, Gorby YA, Fredrickson JK, Truex MJ, Microbial reduction of vitamin B12 by Shewanella alga strain BrY with subsequent transformation of carbon tetrachloride. *Environ Sci Technol* 31:2292–2297 (1997).

93. Xu W, Dana KE, Mitch WA, Black carbon-mediated destruction of nitroglycerin and rdx by hydrogen sulfide. *Environ Sci Technol* 44:6409-6415 (2010).

94. Xu Y and Zhao D, Reductive immobilization of chromate in water and soil using stabilized iron nanoparticles. *Wat Res* 41:2101-2108 (2007).

95. Yang K, Xing B, Adsorption of fulvic acid by carbon nanotubes from water. *Environ Pollut* 157:1095-1100 (2009).

96. Yang K, Lin D, Xing B, Interactions of humic acid with nanosized inorganic oxides. *Langmuir* 25:3571-3576 (2009).

97. Yang K, Zhu L, Xing B, Sorption of phenanthrene by nanosized alumina coated with sequentially extracted humic acids. *Environ Sci Pollut Res* 17:410–419 (2010).

98. Yoda M, Kitagawa M, Miyaji Y, Granular sludge formation in the anaerobic expanded micro carrier process. *Water Sci Technol* 21:109–122 (1989).

99. Yudov MV, Zhilin DM, Pankova AP, Rusanov AG, Perminova IV, Petrosyan VS, Matorin DN, Synthesis, metal-binding properties and detoxifying ability of sulphonated humic acids, in: Perminova IV, Hatfield K, Hertkorn N Eds. Use of humic substances to remediate polluted environments: from theory to practice. Springer, Dordrecht, The Netherlands, pp. 485-498 (2005).

100. Zhang K, Meng Z, OH W, Degradation of rhodamine B by Fe-carbon nanotubes/TiO_2 composites under UV light in aerated solution. *Chinese J Cat* 31:751-758 (2010).

101. Zhang W, Wang C, Nanoscale metal particles for dechlorination of PCE and PCBs. *Environ Sci Technol* 31:2154-2156 (1997).

102. Zhang WX, Nanoscale iron particles for environmental remediation: An overview. *J Nanopart Res* 5:323–332 (2003).

3

Reduction of quinone and non-quinone redox functional groups in different humic acid samples by *Geobacter sulfurreducens*

Abstract

Humic substances constitute the most abundant organic fraction in the biosphere, which have extensively been studied for more than 200 years; however, much remains unknown regarding their structure and properties. In the present study, 12 different samples of humic acids (HA) were extracted from a wide diversity of organic rich environments, including soil from different forests and plantations, and were characterized based on their elemental composition, carboxyl and phenolic content, FTIR spectra and their electron transferring capacity (ETC). The total ETC determined in a H_2/Pd reaction system greatly varied (112–392 μmol g^{-1}) depending on the origin of the organic bulk material. Further analysis indicated that non-quinone (NQ) redox functional groups in HA accounted for an important fraction (25–44%) of the total quantified ETC. Results derived from the present study constitute the first demonstration that humus-reducing microorganisms are capable of reducing both quinone and NQ redox functional groups in different HA samples. HA samples derived from leonardite in a coal mine and from different organic rich soils and composts emerged as promising natural feedstock of HA, which could be applicable as catalysts in remediation processes involving the redox biotransformation of contaminants.

A modified version of this chapter has been published as: Hernández V, Alvarez LH, Montes-Moran MA, Cervantes FJ (2012) *Geoderma* 183–184:25–31

3.1 Introduction

Humic substances (HS) are composed of recalcitrant decomposition products derived from plants and animal biomass. The climate (temperature and moisture conditions), chemical and physical characteristics of litter (particularly lignin and phenolic constituents) and the abundance and composition of soil microbial population, are the three major causes of their incomplete decomposition that lead to accumulation of humus in soil [2, 11, 19]. HS are classified by their aqueous solubility in three fractions: humin, fulvic acids (FA) and humic acids (HA). Humic and fulvic acids have extensively been studied for more than 200 years; however, much remains unknown regarding their structure and properties [30]. The reports indicate that HS usually include a skeleton of alkyl and aromatic units with functional groups, such as carboxylic acid, phenolic hydroxyl, and quinone attached to them [28, 35].

HS transfer electrons to poorly crystalline Fe(III) minerals [13] and even to crystalline minerals [1]. Furthermore, during the last years evidence has been collected indicating that HS can also play important roles in abiotic and microbial reactions involved in the redox transformation of several distinct priority pollutants, such as azo dyes, nitroaromatics, polychlorinated compounds, among others [31]. Quinone moieties, which are very abundant in HS, have been identified as the main functional groups conferring the electron transferring capacity (ETC) to HS [7, 12, 25, 29]. However, recent reports suggest that other functional groups, such as nitrogen and sulfur functional groups, could also account for an important fraction of the ETC in HS [8, 20]. The microbial reduction of HS has been reported in a wide phylogenetic diversity of bacteria and archaea including iron-reducing [10, 13, 14], fermentative [3], sulfate-reducing, halorespiring, and methanogenic microorganisms [4]. However, the redox mediating functional groups, which serve as terminal electron acceptors during microbial humus reduction have not been fully identified, but several reports indicate that quinone moieties account for a major fraction of the ETC of HS during microbial incubations [13, 14, 22, 25]. Furthermore, most studies documenting the microbial reduction of HS have been conducted with quinone model compounds or with commercially available HS reservoirs. Thus, further research is needed in order to document the microbial reduction of ecologically relevant humic samples.

As underlined by Perminova et al. [18], one of the main factors limiting the application of HS in remediation technologies is the intrinsic variability in redox properties observed

among HS and their fractions. Therefore, characterization of HS, including their ETC, is required in order to identify suitable natural sources of HS, which subsequently could serve as redox mediators in remediation processes. In fact, most studies documenting the role of HS in redox reactions have been conducted with quinone model compounds [31] or with commercially available samples from the International Humic Substances Society (IHSS) *e.g.* soil, leonardite, peat, Suwannee River, and Summit Hill humic acids) and from other sources [2, 13, 20, 25]. The main disadvantage of using these materials is their high cost. Furthermore, considering that the properties of HS, such as size, molecular weight, elemental composition, structure and the number and position of functional groups vary depending on the origin and age of the precursor material, it is very important to identify what kind of materials (*e.g.* soil samples, composts and mine deposits) have a high content of HS and to determine the physicochemical characteristics and the ETC of these materials for their possible use as an economic and effective source of redox mediator for remediation processes.

The aims of this study were (1) to extract and characterize HA from a wide variety of organic rich natural samples; (2) to determine their ETC by two methods: chemical and biological; and (3) to determine if the humus-reducing microorganism, *Geobacter sulfurreducens*, is capable of reducing non-quinone redox functional groups in different HA samples. *G. sulfurreducens* is of interest because *Geobacter* spp. has the capacity of transferring electrons both to Fe(III) and to HA and have been demonstrated as predominant organisms responsible for metal reduction in subsurface environments [6, 10]. HA were selected from the humic organic bulk since they have previously been reported as the humic fraction having the largest ETCs from humic samples derived from different organic rich environments [20].

3.2 Materials and methods

3.2.1 Sources of HA

Twelve different materials of natural and commercial origin were used as precursors (bulk materials) for the extraction of HA. Natural precursors can be divided in four categories: 1)

four different forests soils; 2) three plantations soils; 3) three composts; and 4) soil from a volcanic zone and from coal mine. The sites where the precursors were taken were selected according to some factors affecting humification such as climate, time, vegetation, topography, and effect of cropping, as described by Stevenson [28]. Those samples originated from soil were taken from the humus layer (15-30 cm). Samples were mixed and sieved to obtain a particle size of 1 mm. The general characteristics of the precursors of HA are shown in Tables 3.1 and 3.2. As a reference, a standard of leonardite was purchased from the IHSS (STD-1S104H) and the physicochemical characteristics of this material were compared with the properties of HA isolated in the present study.

3.2.2 Extraction procedure of HA

HA were extracted according to the standardized procedure of the IHSS. Briefly, the sample was dissolved in NaOH 0.1 M (Sigma-Aldrich, solution titrated to 0.0987 M) under stirring in a nitrogen atmosphere. Then, the alkaline suspension settled overnight and the supernatant was collected by means of decantation. HCl 6 M was used to acidify the solution, with constant stirring, to pH = 1.0. After to allow the suspension to stand for 16 h, the HA was collected by centrifugation. HA fractions (precipitates) were purified with an acid mixture of 0.1 M HCl/0.3 M HF and dialyzed against distilled water until the dialysis water gave a negative chloride test with $AgNO_3$ 0.1 M (Sigma-Aldrich, solution titrated to 0.10014 M). A Spectra/Por 7 (MWCO 1000) dialysis membrane was used during the dialysis process. Finally, a freeze dry of all HA samples was conducted with a freeze drier system (Labconco, model 7753000).

3.2.3 Physicochemical characterization of HA

The content of carbon, hydrogen, nitrogen and sulfur in the HA samples was obtained with an elemental analyzer (LECO CHNS-932); and the content of oxygen was calculated by the difference. HA particles were observed in a scanning electron microscope (Philips XL-30 SFEG) equipped with an X ray energy detector (EDX XL-30). Solid particles were dispersed on a graphite adhesive tab placed on an aluminum/magnesium stub and covered with a thin layer of gold. The morphology and chemical composition was determined in three points of each sample and an average of the composition was obtained.

Table 3.1 Nomenclature and general characteristics of soil precursors of humic acids

Sample	Localization (state) and geographic coordinate	Typical Vegetation		Soil pH
		Specie	Genus	
CFA	Aguascalientes 22° 15′ 30″ S, 102° 26′ 40″ W	*Pinus Leiophylla*	*Pinus*	4.18
CFSLP	San Luis Potosí 22° 5′ 0″ N, 100° 38′ 0″ W	*Pinus cembroides Zucc*	*Pinus*	7.00
DFSLP	San Luis Potosí 22° 10′ 0″ N, 101° 08′ 0″ W	*Quercus rugosa Neé*	*Quercus*	5.65
DTFA	Aguascalientes 21° 46′ 45″ N, 102° 22′ 16″ W	*Leucaena esculenta*	*Leucaena*	6.52
SCOF	Huitiupán, Chiapas 17º10’ N, 92º41’ W	*Coffea arabica*	*Coffea*	7.38
SCOC	Pichucalco, Chiapas 17º 30’ N, 93º 07’ W	*Theobroma cacao*	*Theobroma*	5.23
SAVO	Atlixco, Puebla 18º 49` 30" y 18º 58` 30" N	*Persea americana*	*Persea*	6.90
SVM	Mexico, Puebla and Morelos 19° 1′ 0″ N, 98° 37′ 0″ W	-	.	5.00
MLE	Esperanzas, Coahuila	-	-	4.03

CFA, Coniferous forest of Aguascalientes
CFSLP, Coniferous forest of San Luis Potosi
DFSLP, Deciduous forest of San Luis Potosi
DTFA, Deciduous tropical forest of Aguascalientes;
SCOF, Soil from coffee plantation;
SCOC, Soil from cocoa plantation;
SAVO, Soil from avocado plantation;
SVM, Soil with volcanic matter (Popocatepetl volcano);
MLE, Leonardite from a carbon mine.
pH was determined directly on the sample with a soil pH electrode

Table 3.2 General characteristics of composts used as precursors of humic acids

Sample	Description	Origin/supplier	Compost pH[a]
CCO	Commercial compost	Querétaro compost	8.00
CAW	Compost of agave wastes	Pilot station at University of Guadalajara	5.87
CGW	Compost of gardening wastes	Pilot station at University of Guadalajara	6.69

[a]Determined directly on the sample with a soil pH electrode

Quantification of acidic groups (carboxyl and phenolic) was determined by potentiometric titration according to Ritchie and Perdue [21] and a pH meter (Hanna Instruments Co.) was employed with continuous deaeration with nitrogen. The presence of bulk functional groups in HA was determined directly in samples using a Nicolet-6700 FTIR spectrometer (Thermo Scientific) equipped with a Smart iTR accessory, which is a versatile accessory of attenuated total reflectance (ATR) with ZnSe crystal. A deuterated triglycine sulfate (DTGS) detector was used to collect the IR spectra in the 4000-650 cm^{-1} spectral range.

3.2.4 Electron transferring capacity of HA

The ETC of all HA were determined by chemical and biological methods, using solutions of HA at 0.5 g L^{-1} and 1 g L^{-1}, respectively. The chemical method was based on that of Ratasuk and Nanny [20], which comprises the measurement of reversible redox sites in HA by consecutive reduction and oxidation of the same samples. Two catalytic systems were used: (1) reduction of HA using H_2 and Pd (powder) at pH 8 and the re-oxidation of the sample with air; (2) reduction of HA with H_2 and Pd at pH 6.5 employing Pd supported on alumina as catalyst and the re-oxidation of the sample with air. The pH values were controlled by using phosphate buffers, prepared by mixing different volumes of 0.3 M NaH_2PO_4 and 0.3 M Na_2HPO_4, and then bubbling N_2 for 15 min. The ETC quantified at pH 8 account for the total amount of electrons transferred to HA samples, whereas the ETC quantified at pH 6.5 account for the electrons transferred to non-quinone (NQ) redox functional groups as previously demonstrated [20]. ETC measurements were conducted by

the ferrozine technique in a N_2/H_2 (95%/5%) anoxic chamber following the protocol described by Lovley et al. [13] as detailed below.

The biological method to determine ETC of HA samples was based on the reduction by *G. sulfurreducens*. An appropriate basal medium (pH 7.0) was prepared as previously reported by [36] with acetate as electron donor (10 mM), and 1.7 mg of protein (*G. sulfurreducens*) mL^{-1}. Incubations were placed in the dark at 30 °C. All ETC measurements were conducted by the ferrozine technique in a N_2/H_2 (95%/5%) anoxic chamber following the protocol described by Lovley et al. [13]. Briefly, Fe(III) citrate was mixed with samples to obtain a final concentration of 10 mM, and allowed to react for 15 min. Then, equal volume of 0.5 M HCl was added to the sample, and an aliquot was mixed with the ferrozine solution for spectrophotometric (562 nm) determination of Fe(II). The Fe(II) concentration was used to calculate the ETC from HA samples to Fe(III) under all experimental conditions. All ETC measurements were corrected for intrinsic Fe(II) present in HA samples by using a control untreated with Fe(III) citrate. Thus, interference of this redox-active element on the ETC measurements can be dismissed.

3.3 Results and discussion

3.3.1 Characterization of HA samples

Table 3.3 shows the yield of HA obtained from the different precursors after the extraction and purification procedures. In general, the yield of HA was low (up to 0.04%) for most samples analyzed following the order: coniferous forest soil of Aguascalientes (CFA) < commercial compost (CCO) < soil from cocoa plantation (SCOC) < soil with volcanic matter (SVM) < soil from coffee plantation (SCOF) < deciduous tropical forest soil of Aguascalientes (DTFA) < compost of agave wastes (CAW) < soil from avocado plantation (SAVO) < compost of gardening wastes (CGW) < deciduous forest soil of San Luis Potosi (DFSLP) < Coniferous forest soil of San Luis Potosi (CFSLP). However, leonardite derived from a carbon mine (MLE) was the parental material with the highest content of HA showing a yield of 12% (12 g HA extracted from 100 g of bulk material).

Table 3.3 Yield and elemental composition of humic acids extracted from different organic rich environments.

Sample[a]	Yield (%)	Ultimate analysis (%)					
		C (±0.05)	H (±0.05)	N (±0.05)	S (±0.05)	O (±1.0)	Fe[c]
CFA	0.04	28.06	3.30	1.73	0.37	35.55	11.90
CFSLP	2.27	22.87	2.75	1.58	0.34	29.93	10.28
DFSLP	2.01	48.13	4.84	3.19	0.71	37.91	6.07
DTFA	0.97	4.34	1.93	0.46	0.19	15.76	10.66
SCOF	0.50	29.76	3.67	2.79	0.54	33.35	3.92
SCOC	0.20	41.62	4.57	3.28	0.62	39.50	9.12
SAVO	1.90	20.03	3.23	1.47	0.39	45.68	9.95
SVM	0.34	48.20	4.01	2.75	0.48	34.62	8.36
MLE	12.48	59.36	2.80	1.22	0.41	29.13	2.76
CCO	0.18	51.86	5.29	4.20	1.31	30.96	2.34
CAW	1.45	51.17	5.20	4.91	0.76	33.21	1.36
CGW	1.90	51.12	4.76	4.40	0.81	38.67	1.90
1S104H[b]	-	63.81	3.7	1.23	0.76	31.27	-

[a] Codes are described in Tables 3.1 and 3.2.
[b] Data obtained from the IHSS web page (http://ihss.gatech.edu/ihss2/).
[c] Determined by EDX analysis.

The elemental composition of all HA samples is also listed in Table 3.3; which agree, in most cases, to the elemental composition described by Stevenson [28]. The carbon content (C) was found in the range of 20–59%; hydrogen (H), 1.93–5.29 %; nitrogen (N), 0.46–4.91%; sulfur (S), 0.19–1.31; and oxygen (O), 35–87 %; in addition, Fe content measured by EDX ranged from 1.36% to 11.90%. The total weight (%) of each sample of HA can be completed by ash content, since it can reach up 35% [45]; especially because Table 3.3

shows results considering both organic and inorganic fractions. The highest C content was found in the HA from MLE and, in general, the elemental composition of this HA sample was very similar to the composition of leonardite standard sample obtained from the IHSS (STD-1S104H). The IHSS leonardite sample is derived from a mine localized in Bowman County, North Dakota, USA. The comparison of these HA samples is provided as an evidence that the extraction process of HA made in the present study was conducted in a proper manner and that whatever the origin of leonardite, the elemental composition of their HA is very similar. Another interesting case is the group of HA extracted from different composts which, despite being prepared from different materials (Table 3.2), their elemental composition is almost identical among them (Table 3.3) and to the elemental composition of HA obtained from composts of Egypt and The Netherlands [9, 32].

EDX analysis indicate that most humic materials have a significant content of inorganic elements (aluminum <4%, silicon <2%, potassium <0.8%, and calcium <1.3%) despite the purification process. HA obtained from CFA, CFSLP and DTFA showed a higher content of these inorganic elements. This may be explained by the composition of the soils used as precursor of these HA, which are rich in inorganic elements in contrast to the content of inorganic elements found in the other bulk materials.

Table 3.4 shows the acidic groups quantified in all HA samples. In general, carboxylic groups were more abundant than phenolic groups in all HA samples. The results are consistent with previous studies documenting these functional groups by potentiometric titration or by Near Edge X-Ray Absorption Structure Spectroscopy [16, 21, 27]. Moreover, the content of carboxylic and phenolic groups detected for the standard leonardite HA (STD-1S104H) was very similar to that found in MLE in the present study (Table 3.4).

Figure 3.1 shows the FTIR-ATR spectra of all HA samples, which were divided and analyzed in four different groups according to the similarity of the spectra obtained. The spectra were grouped as follows: (A) HA obtained from forests soil; (B) HA derived from plantations soil; (C) HA extracted from volcanic matter and leonardite samples; and (D) HA obtained from composts. All spectra were analyzed and two signals were identified in groups A and B. The first band detected between 1588 and 1614 cm^{-1} is characteristic of stretching vibrations C=C of aromatic compounds. The second band at ~1010 cm^{-1} could be assigned to stretching vibration C–O of polysaccharides (Table 3.4). FTIR-ATR spectra of

groups C and D are more complex and additional bands were observed. The band at ~1710 cm^{-1} corresponding to the stretching vibrations C=O of carboxylic acids, ketones or aldehydes, which was only observed in leonardite samples.

Table 3.4 Functional groups determined in humic acids extracted from different organic rich environments

Sample	Acidic groups (mmol g^{-1})		FTIR-ATR interpretation			
	Carboxyl	Phenolic	Wavenumber cm^{-1}	Type of vibration	Functional group	Ref.
Group A and B						
CFA	not quantified		1588, 1614	C=C *v*	Aromatic compounds	15, 34
CFSLP	25.7	3.7	1009, 1015	C-O *v* or Si-O *v*	Polysaccharides or impurities	
DFSLP	6.7	5.3				
DTFA	123.4	24.1				
SCOF	106.0	17.8				
SCOC	4.2	4.1				
SAVO	46.6	10.0				
Group C and D						
SVM	9.1	5.0	1592	C=C *v*	Aromatic compounds	26, 34
MLE	6.9	2.3	1640	C=O *v*	Amide I or quinones	23
1S104H	7.5	2.3	1710	C=O *v*	COOH, ketones or aldehydes	
			1233, 1227	C-O *v* or O-H	COOH, aryl ethers or phenols	
CCO	5.3	4.9	757	=C–H γ	Aromatic compounds	
CAW	5.6	3.3				
CGW	5.9	3.2				

γ: deformation out-of-plane; *v*: stretching; def: deformation; δ: deformation in plan.
Codes are described in Tables 3.1 and 3.2.

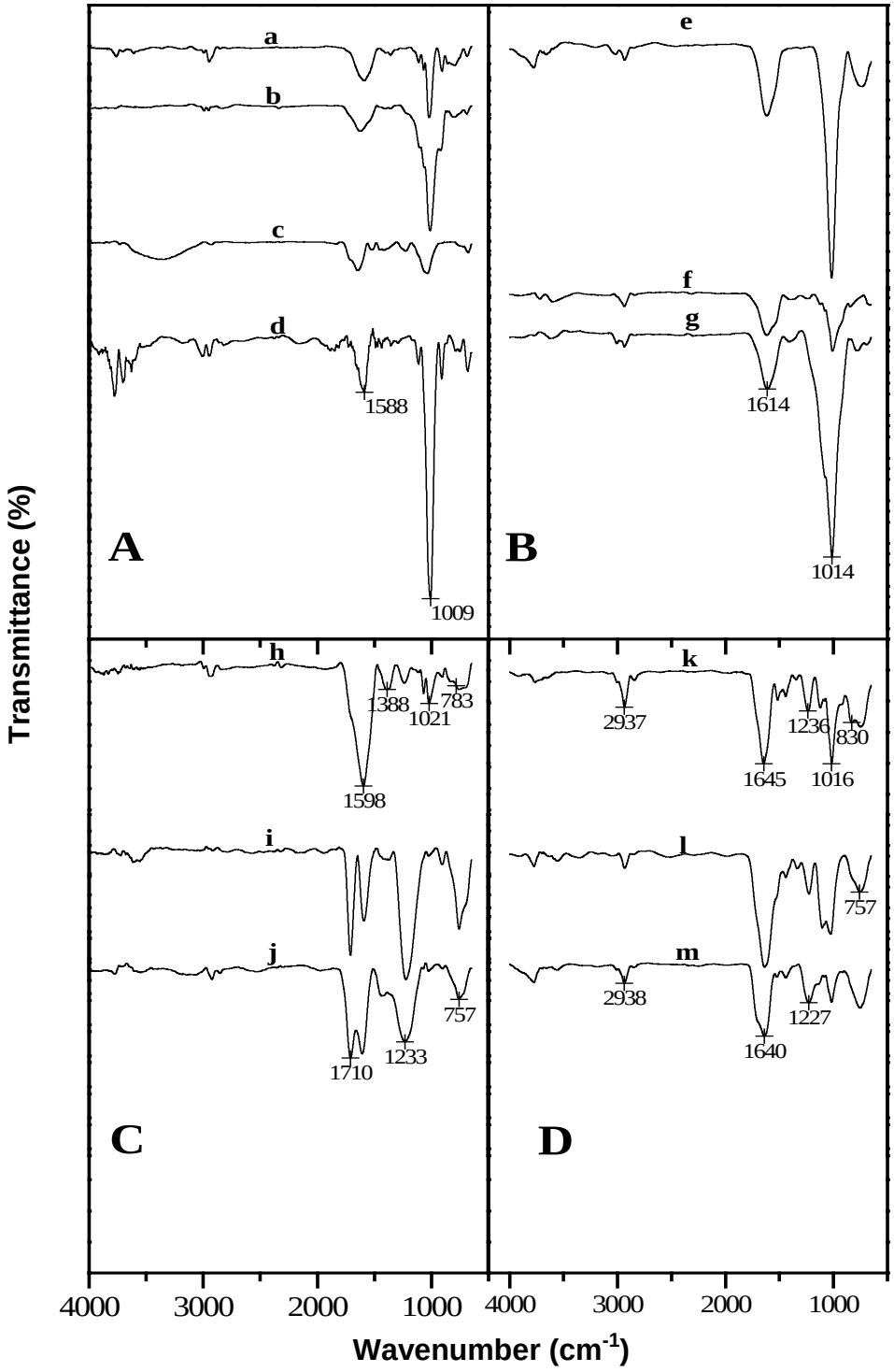

Figure 3.1 FTIR-ATR spectra of humic acids derived from A) forests soil, B) plantations soil, C) volcanic matter and leonardite samples, and D) composts. (a) CFA, (b) CFSLP, (c) DFSLP, (d) DTFA, (e) SCOF, (f) SCOC, (g) SAVO, (h) SVM, (i) MLE, (j) 1S104H, (k) CCO, (l) CAW, (m) CGW.

The band at ~1233 cm^{-1} (C-O stretching or O-H deformation) was observed in all spectra of the groups C and D and this signal is characteristic of carboxylic acids, aryl ethers or phenols. An additional band at 2938 cm^{-1} (stretching C-H vibration of aliphatic compounds) was observed in all spectra of group D. Furthermore, HA derived from composting material (group D) also showed a band at 1640 cm^{-1}, which was identified as a stretching vibration C=O of amide I or quinones (Table 3.4).

3.3.2 Electron transferring capacity of HA

The ETC of all HA samples was determined by a chemical method using a Pd/H_2 system [20]. The ETC was also determined with the humus-reducing microorganism *Geobacter sulfurreducens* frequently found in a wide variety of environments [5, 6]. All ETC determined were corrected for intrinsic Fe(II) present in HA samples by using subsamples in which Fe(III) citrate was not added. Thus, interference of this redox-active element on the ETC measurements can be dismissed. In general, the ETC quantified by the chemical method was higher than that obtained with *Geobacter sulfurreducens* (Figure 3.2) probably due to the presence of some inhibitory components in various HA samples, which affected the reducing capacity of this strain. Otherwise, *Geobacter sulfurreducens* may not have suitable electron carriers in its electron transport chain so that some redox mediating functional groups might have remained unaffected during the incubation period for some HA samples, particularly for those derived from DTFA, SCOF, SAVO and CCO, which showed remarkable difference between the ETC obtained with the two methods applied (Figure 3.2). Previous reports have documented the inhibitory effects of HA extracts [37] and humic model compounds [38, 39] on different microbial processes, such as methanogenesis and sulfate reduction. However, the mechanisms by which HA inhibit these microbial activities remain unclear and demand further elucidation in future studies.

An association was found between the ETC data and the FTIR-ATR spectra. For instance, HA isolated from the sample of leonardite (MLE) showed the highest ETC (Figure 3.2), whereas HA isolated from soil with volcanic matter showed the lowest ETC within this classified group (Figure 3.1 and 3.2). These results can be related to the groups identified by the FTIR-ATR spectra of the two samples, in which the characteristic band of carboxylic acids, ketones or aldehydes (C=O) is present in MLE (1710 cm^{-1}), but absent in

SVM, indicating that oxygenated groups can significantly account for the ETC obtained. Furthermore, HA isolated from DTFA and from SCOF had more content of oxygen than carbon (Table 3.3) and showed high ETC (Figure 3.2). Moreover, according to Veeken et al. [32] materials with low content of hydrogen, such as DTFA (Table 3.3), have a lower amount of aliphatic groups and a higher content of aromatic groups, which can participate in redox reactions. Likewise, a significant correlation (R^2 = 0.738) was found for the quantified ETC against the FTIR-ATR peak intensity at ~1600-1700 cm^{-1} (Figure 3.3), which agrees with previous studies suggesting that quinone moieties play an important role in the ETC of humic substances [7, 12, 25, 29]. Nevertheless, HA derived from SVM, CCO and CAW deviated from this correlation, probably because redox mediating functional groups distinct from quinones account for an important fraction of the ETC quantified in these samples (see below).

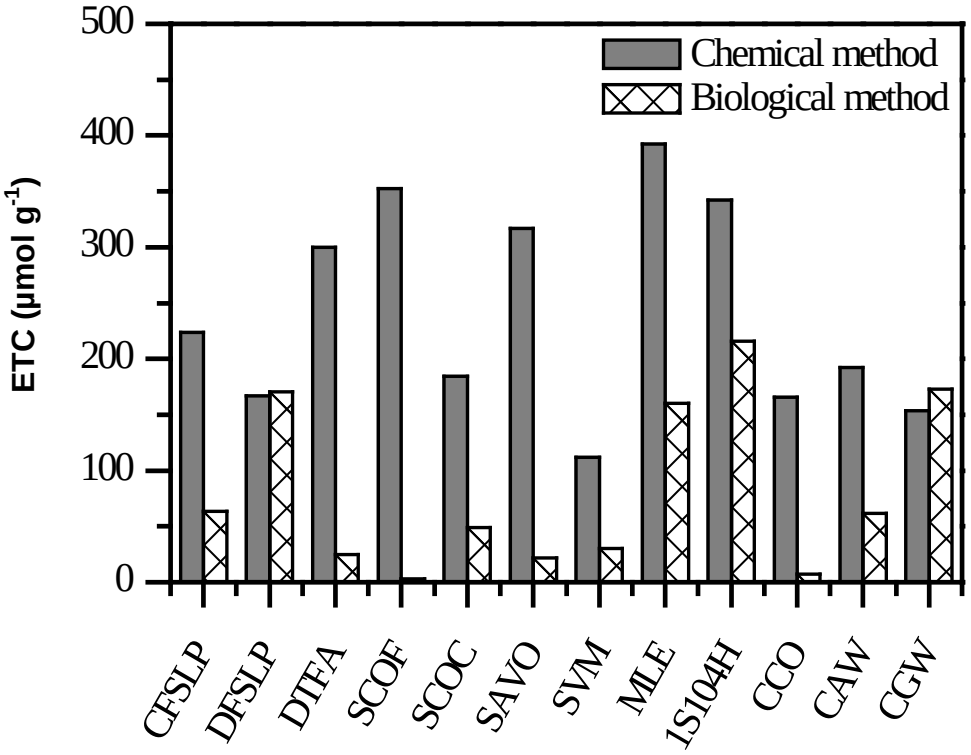

Figure 3.2 ETC of humic acids extracted from different organic rich environments determined by two methods: Chemical (H_2/Pd, pH 8) and biological (*G. sulfurreducens*).

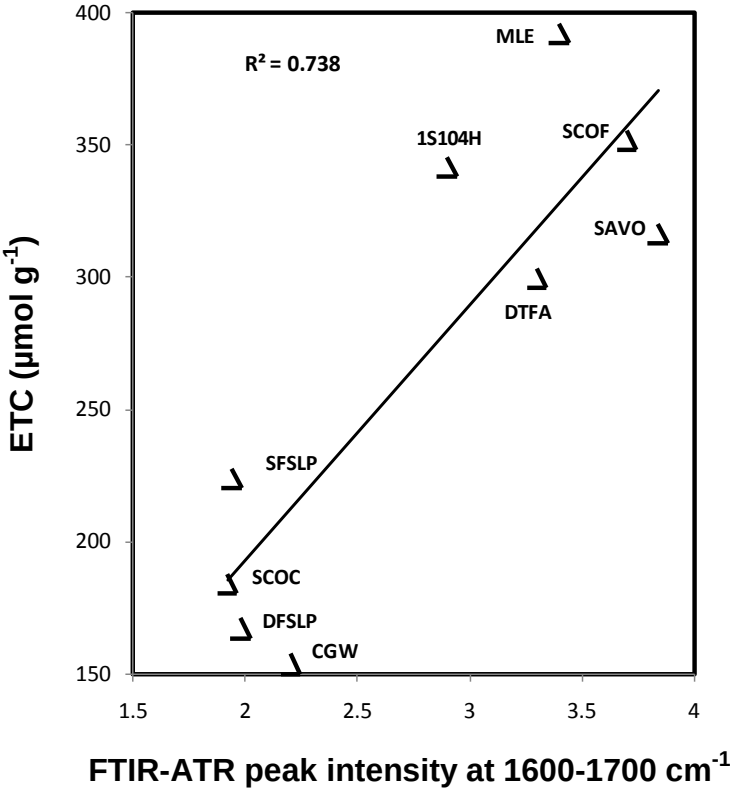

Figure 3.3 Correlation of ETC against FTIR-ATR peak intensity at ~1600-1700 cm^{-1} for different humic acids extracted from organic rich environments.

In order to elucidate the main functional groups accounting for the ETC of HA samples showing the highest ETC within the four different groups classified (Figure 3.1), further experiments were conducted. For that purpose, HA samples derived from DFSLP, SAVO, CGW and MLE were selected and compared with the results obtained with the standard of leonardite HA from the IHSS (STD-1S104H). In order to distinguish between the ETC attributable to quinone moieties and the ETC linked to non-quinone (NQ) redox mediating functional groups, the methodology of Ratasuk and Nanny [20] was followed. By selectively reducing HA samples at pH 6.5 in a H_2/Pd reaction system, aromatic ketone groups (C=O) are not longer available because they are protonated forming phenolic groups (pKa = 9.9) [24], thus blocking the ETC attributable to quinone moieties. Direct evidence of this blocking mechanism avoiding quinone reduction was revealed by FTIR-ATR spectra. Indeed, HA samples previously reduced with H_2-Pd at pH 8 showed the typical

spectral signal associated with hydroquinone groups at ~1360 cm^{-1} [33], (see Figure 3.4-A - B). On the contrary, HA samples previously reduced with H_2-Pd at pH 6.5 did not show the hydroquinone spectral signal, but aromatic ketone groups remain intact (signal at ~1650 cm^{-1} in Figure 3.4-C -D).

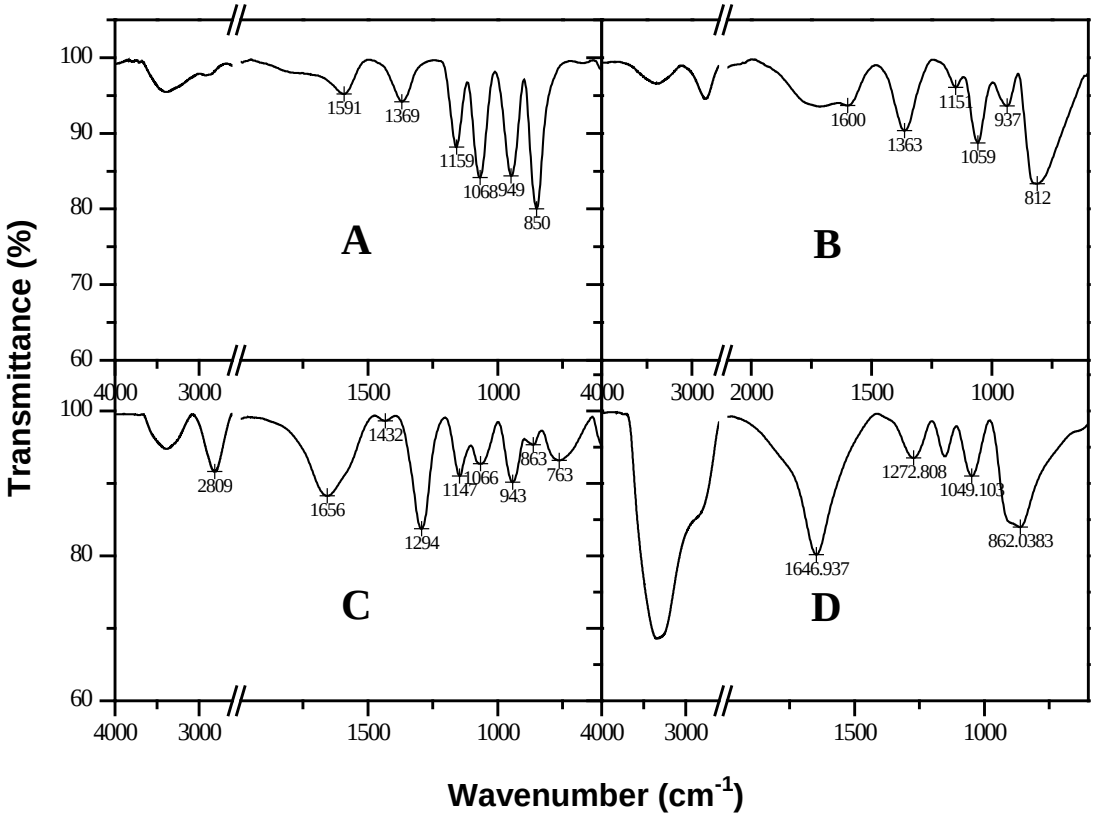

Figure 3.4 FTIR-ATR spectra of humic acids previously reduced chemically with H_2/Pd at pH 8 (A and B) and reduced chemically with H_2/Pd at pH 6.5 (C and D). Samples: 1S104H (A and C), MLE (B and D).

The two samples of HA derived from leonardite (MLE and STD-1S104H), which showed the highest ETC during the previous screening (Figure 3.2) did not show significant ETC attributable to NQ redox functional groups (Table 3.5), suggesting that the quantified ETC can mainly be linked to quinone groups. In contrast, HA samples derived from DFSLP, SAVO and CGW had significant ETC linked to NQ redox functional groups (Table 3.5). In

fact, the ETC linked to NQ groups in these HA samples accounted for 25–44% of the total ETC quantified at pH 8 with the same reaction system (Table 3.5). Among the HA samples described in Table 3.5, HA extracted from DFSLP, SAVO and CGW showed the highest content of nitrogen and sulfur in their elemental composition (Table 3.3). Previous reports have documented the participation of nitrogen and sulfur (thiols and disulfides) functional groups as redox sites [43, 8]. According to Szulczewski et al. [44], among 26% to 60 % of the total sulfur content in HS is represented by thiols and disulfides. If it is assumed that the content of thiols and disulfides in the HA sample derived from SAVO is 30% (total sulfur content in this sample is 0.71%); then the estimated value of ETC for these NQ redox groups ranging between 73 μmol g^{-1} (2 electrons transferred from disulfide to sulfoxide) to 109 μmol g^{-1} (3 electrons transferred from thiol to sulfoxide), which is nearby to the ETC value measured for SAVO (79±30 μmol g^{-1}, Table 3.5) in this study. Among the HA samples described in Table 3.5, HA extracted from DFSLP, SAVO and CGW showed the highest content of nitrogen and sulfur in their elemental composition (Table 3.3). Therefore, the significant ETC detected in these HA samples linked to NQ redox mediating functional groups might be associated with nitrogenous and sulfurous redox mediating functional groups as previously reported [8]; however, due to the relatively low content of these functional groups in the analyzed HA samples, FTIR-ATR spectra could not detect them.

The ETC determinations conducted with the humus-reducing microorganism, *Geobacter sulfurreducens*, suggest that this ecologically relevant bacterial strain is capable of reducing both quinone and NQ redox mediating functional groups in the HA samples examined. Certainly, the total ETC quantified (H_2-Pd at pH 8) was very close to that obtained with *Geobacter sulfurreducens* for these samples (Table 3.5), except for HA derived from SAVO, which showed a remarkable difference between the biological and chemical ETC values (Figure 3.2) as explained above. To our knowledge, there is no direct evidence in the literature documenting the microbial reduction of NQ redox mediating functional groups in humic substances, although the high correlation of the ETC determined by a H_2-Pd reaction system against those determined with *Geobacter metallireducens* suggests this premise [20]. Further studies have documented a high correlation between the ETC determined by chemical and microbial methods [10, 17]. *Geobacter sulfurreducens* could also fully reduce

HA samples, in which quinone moieties were previously blocked during their reduction with H_2-Pd at pH 6.5 (data not shown), which revealed the reversibility of this blocking mechanism.

Table 3.5 Electron transferring capacity (ETC) of different humic acids samples determined by distinct methods[a]

Sample	ETC (μmol g^{-1})		
	Biological with *G. sulfurreducens*	Chemical with H_2/Pd, pH 8	Chemical with H_2/Pd, pH 6.5
DFSLP	170.6 ± 14	167.1± 16	73.6 ± 27
SAVO	21.7 ± 4	316.8 ± 28	79.4 ± 30
CGW	172.9 ± 14	153.6 ± 10	54.2 ± 0.01
MLE	160.2 ± 17	392.4 ± 14	5.9 ± 0.01
1S104H	215.8 ± 7	342.1± 23	0

[a]Data represent average from triplicate determinations ± standard deviation. DFSLP, deciduous forest of San Luis Potosi; SAVO, soil from avocado plantation; CGW, compost of gardening wastes; MLE, leonardite from a carbon mine; 1S104H, leonardite standard from the IHSS.

Considering that many aquatic environments have an acidic pH (pH<6.5), it is expected that quinone moieties will not be available as terminal electron acceptors (TEA) for microbial respiration in these ecosystems due to the blocking mechanism explained above and also demonstrated in previous studies [20]. Furthermore, beyond changing the protonation state of HA, pH (as well as ionic strength) can also impact the aggregation state and solubility of HA (i.e. more aggregated and less soluble at low pH), which may also restrict the role of HA as TEA [40, 41]. Nevertheless, the microbial reduction of solid-phase HA has previously been documented [22]. More recently, it has also been demonstrated that the microbial reduction of HA immobilized in alumina nanoparticles occurred 7.5-fold faster as compared to suspended HA due to the attachment of HA-coated nanoparticles on the surface of humus-reducing microorganisms [42]. Therefore, HA even

aggregated under acidic conditions could be effective TEA for microbial respiration. The demonstration that *G. sulfurreducens* is able to reduce NQ redox functional groups, which are expected to be responsible for the ETCs of HA under acidic conditions, in different HA samples further emphasizes the role of HA as TEA in acidic conditions.

3.4 Conclusion

The present study indicate that the ETC of HA greatly varies depending on the origin of the organic bulk material. The results obtained also suggest that NQ redox functional groups in HA account for an important fraction of the quantified ETC and that the humus-reducing microorganism, *Geobacter sulfurreducens*, is capable of reducing both quinone and NQ redox functional groups in different HA samples. HA samples derived from MLE, DFSLP, SAVO and CGW emerged as promising natural sources of HA to be used as RM because of their distinctive characteristics, namely the ETC as the most important parameter. HS characterized in this study were included in experimentation of chapters 4 and 6 of this dissertation. Chapter 4 present the capacity of HS, previously immobilized on microparticles of alumina, to serve as a solid-phase RM during the reductive dechlorination of carbon tetrachloride by an anaerobic sludge. In addition, chapter 6 includes the use of the sample MLE to be immobilized in nanoparticles of alumina, in order to evaluate their impact on specific methanogenic activity and humus reducing activity in an anaerobic consortium. Thus, the materials characterized in the present study could be applied in remediation processes involving the redox biotransformation of contaminants, as mentioned in chapter 4 and 6.

References

1. Bauer, I., Kappler, A., 2009. Rates and extent of reduction of Fe(III) compounds and O_2 by humic substances. Environ. Sci. Technol. 43, 4902-4908.

2. Bauer, M., Heitmann, T., Macalady, D.L., Blodau, C. 2007. Electron transfer capacities and reaction kinetics of peat dissolved organic matter. Environ. Sci. Technol. 41, 139-145.

3. Benz, M., Schink, B., Brune, A., 1998. Humic acid reduction by *Propionibacterium freudenreichii* and other fermentative bacteria. Appl. Environ. Microbiol. 64, 4507-4512.

4. Cervantes, F.J., De Bok F.A.M., Duong-Dac T., Stams, A.J.M., Lettinga G., Field J.A., 2002. Reduction of humic substances by halorespiring, sulphate-reducing and methanogenic microorganisms. Environ. Microbiol. 4, 51-57.

5. Cervantes, F.J., Duong-Dac, T., Ivanova, A., Roest, K., Akkermans, A.D.L., Lettinga, G., Field, J.A., 2003. Selective enrichment of *Geobacter sulfurreducens* from anaerobic granular sludge with quinones as terminal electron acceptors. Biotechnol. Let. 25, 39-45.

6. Coates, J.D., Ellis, D.J., Roden, E., Gaw, K., Blunt-Harris, E.L., Lovley, D.R., 1998. Recovery of humics-reducing bacteria from a diversity of sedimentary environments. Appl. Environ. Microbiol. 64,1504-1509.

7. Cory, R.M., McKnight, D.M., 2005. Fluorescence spectroscopy reveals ubiquitous presence of oxidized and reduced quinones in dissolved organic matter. Environ. Sci. Technol. 39, 8142-8149.

8. Fimmen, R.L., Cory, R.M., Chin, Y-P., Trouts, T.D., McKnight, D.M., 2007. Probing the oxidation –reduction properties of terrestrially and microbially derived dissolved organic matter. Geochim. Cosmochim. Ac. 71, 3003-3015.

9. Ghabbour, E.A., Khairy, A.H., Cheney, D.P., Gross, V., Davies, G., Gilbert, T.R., Zhang, X., 1994. Isolation of humic acid from the brown alga Pilayella littoralis. J. Appl. Phycol. 6, 459-468.

10. Jiang, J., Kappler, A., 2008. Kinetics and thermodynamics of microbial and chemical reduction of humic substances: implications for electron shuttling in natural environments. Environ. Sci. Technol. 42, 3563-3569.

11. Kappler, A., Ji, R., Schink, B., Brune, A., 2001. Dynamics in composition and size-class distribution of humic substances in profundal sediments of Lake Constance. Org. Geochem. 32, 3-10.

12. Klapper, L., McKnight, D.M., Fulton, J.R., Blunt-Harris, E.L., Nevin, K.P., Lovley, D.R., 2002. Fulvic acid oxidation state detection using fluorescence spectroscopy. Environ. Sci. Technol. 36, 3170-3175.

13. Lovley, D.R., Coates, J.D., Blunt-Harris, E.L., Phillips, E.J.P., Woodward, J.C. 1996. Humic substances as electron acceptors for microbial respiration. Nature 382, 445-448.

14. Lovley, D.R., Fraga, J.L., Blunt-Harris, E.L., Hayes, L.A., Phillips, E.J.P., Coates, J.D., 1998. Humic substances as a mediator for microbially catalyzed metal reduction. Acta Hydroch. Hydrob. 26, 152-157.

15. Mafra, A.L., Senesi, N., Brunetti, G., Miklós, A.A.W., Melfi, A.J., 2007. Humic acids from hydromorphic soils of the upper Negro river basin, Amazonas: Chemical and spectroscopic characterisation. Geoderma 138, 170-176.

16. Malcolm, R.L., 1986. Limitations in the use of commercial humic acids in water and soil research. Environ. Sci. Technol. 20, 904-911.

17. Peretyazhko, T., Sposito, G., 2006. Reducing capacity of terrestrial humic acids. Geoderma 137, 140-146.

18. Perminova, I.V., Kovalenko, A.N., Schmitt-Kopplin, P., Hatfield, K., Hertkorn, N., Belyaeva, E.Y., Petrosyan, V.S., 2005. Desing of quinonoid-enriched humic materials with enhanced redox properties. Environ. Sci. Technol. 39, 8518-8524.

19. Pettersson, C., Ephraim, J., Allard, B., 1994. On the composition and properties of humic substances isolated from deep groundwater and surface waters. Org. Geochem. 21, 443-451.

20. Ratasuk, N., Nanny, M.A., 2007. Characterization and quantification of reversible redox sites in humic substances. Environ. Sci. Technol. 41, 7844-7850.

21. Ritchie, J.D., Perdue, E.M., 2003. Proton-binding study of standard and reference fulvic acids, humic acids, and natural organic matter. Geochim. Cosmochim. Ac. 67, 85-96.

22. Roden, E., Kappler, A., Bauer, I., Jiang, J., Paul, A., Stoesser, R., Konishi, H., Xu, H., 2010. Extracellular electron transfer through microbial reduction of solid-phase humic substances. Nat. Geosci. 3, 417-421.

23. Salavagione, H.J., Arias, J., Garcés, P., Morallcuŕron, E., Barbero, C., Vázquez, J.L., 2005. Spectroelectrochemical study of the oxidation of aminophenols on platinum electrode in acid medium. J. Electroanal. Chem. 565, 375-383.

24. Schwarzenbach, R.P., Gschwend, P.M., Imboden, D.M., 2003. Environmental organic chemistry. John Wiley & Sons, Inc., New Jersey.

25. Scott, D.T., Mcknight, D.M., Blunt-Harris, E.L., Kolesar, S.E., Lovley, D.R., 1998. Quinone moieties act as electron acceptors in the reduction of humic substances by humic-reducing microorganisms. Environ. Sci. Technol. 32, 2984-2989.

26. Shirshova, L.T., Ghabbour, E.A., Davies, G., 2006. Spectroscopic characterization of humic acid fractions isolated fom soil using different extraction procedures. Geoderma 133, 204-216.

27. Solomon, D., Lehmann, J., Kinyangi, J., Liang, B., Schäfer, T., 2005. Carbon K-Edge NEXAFS and FTIR-ATR Spectroscopic Investigation of Organic Carbon Speciation in Soils. Soil Sci. Soc. Am. J. 69, 107-119.

28. Stevenson, F.J., 1994. Humus Chemistry: Genesis, Composition, Reactions. John Wiley & Sons, Inc., New York.

29. Struyk, Z., Sposito, G., 2001. Redox properties of standard humic acids. Geoderma 102, 329-346.

30. Sutton, R., Sposito, G., 2005. Molecular structure in soil humic substances: The new view. Environ. Sci. Technol. 39, 9009-9015.

31. Van der Zee, F.P., Cervantes, F.J., 2009. Impact and Application of Electron Shuttles on the Redox (Bio)Transformation of Contaminants: A Review. Biotechnol. Adv. 27, 256-277.

32. Veeken, A., Nierop, K., De Wilde, V., Hamelers, B., 2000. Charcarterisation of NaOH-extracted humic acids during composting of a biowaste. Bioresour. Technol. 72, 33-41.

33. Wu, X., Buden, D.W., Attygalle, A.B., 2007. Hydroquinones from defensive secretion from a giant Pacific millipede, *Acladocricus setigerus* (Diplopoda: Spirobolida). Chemoecology 17, 131-138.

34. Xu, D., Zhu, S., Chen, H., Li, F. 2006. Structural characterization of humic acids isolated from typical soils in China and their adsorption characteristics to phenanthrene. Coll. Surface A 276, 1-7.

35. Yudov, M.V, Zhilin, D.M., Pankova, A.P., Rusanov, A.G., Perminova, I.V., Petrosyan, V.S., Matorin, D.N., 2005. Synthesis, metal-binding properties and detoxifying ability of sulphonated humic acids. In Perminova, I.V., Hatfield, K., Herrtkorn, N. (Eds.), Use of humic substances to remediate polluted environments: From theory to practice. Springer, Dordrecht, Netherlands, pp 485-498.

36. Caccavo Jr, F., Lonergan, D.J., Lovley, D.R., Davis, M., Stolz, J.F., McInerney, M.J., 1994. *Geobacter sulfurreducens* sp. nov., a hydrogen- and acetate-oxidizing dissimilatory metal-reducing microorganism. Appl. Environ. Microbiol. 60, 3752–3759.

37. Minderlein, S., Blodau, C., 2010. Humic-rich peat extracts inhibit sulfate reduction, methanogenesis, and anaerobic respiration but not acetogenesis in peat soils of a temperate bog. Soil Biol. Biochem. 42, 2078–2086.

38. Cervantes, F.J., van der Velde, S., Lettinga, G., Field, J.A., 2000. Competition between methanogenesis and quinone respiration for ecologically important substrates in anaerobic consortia. FEMS Microbiology Ecology 34, 161–171.

39. Cervantes, F.J., Gutiérrez, C.H., López, K.Y., Estrada-Alvarado, M.I., Meza-Escalante, E.R., Texier, A.-C., Cuervo, F., Gómez, J., 2008. Contribution of quinone-reducing microorganisms on the anaerobic biodegradation of organic compounds under different redox conditions. Biodegradation 19, 235–246.

40. Kipton, H., Powell, J., Town, R.M., 1992. Solubility and fractionation of humic acid; effect of pH and ionic medium. Analytica Chimica Acta 267, 47–54.

41. Terashima, M., Fukushima, M., Tanaka, S., 2004. Influence of pH on the surface activity of humic acid: micelle-like aggregate formation and interfacial adsorption. Colloids and Surfaces A: Physicochemical and Engineering Aspects 247, 77–83.

42. Alvarez, L.H., Cervantes, F.J. in press. Assessing the impact of alumina nanoparticles in an anaerobic consortium: methanogenic and humus reducing activity. Appl. Microbiol. Biotechnol. DOI 10.1007/s00253-011-3759-4.

43. Larson, R.A., Weber, E.J. 1994. In Reaction Mechanisms in Environmental Organic Chemistry; Lewis Publishers: Boca Raton, FL.

44. Szulczewski, M.D., Helmke, P.A., Bleam, W.F. 2001. XANES spectroscopy studies of Cr(VI) reduction by thiols in organosulfur compounds and humic substances. Environ. Sci. Technol. 2001, 35, 1134-1141.

45. Malcolm, R.L., MacCarthy, P. 1986. Limitations in the use of commercial humic acids in water and soil research. Environ. Sci. Technol. 1986, 20, 904-911.

4

Enhanced dechlorination of carbon tetrachloride by immobilized fulvic acids on alumina particles

Abstract

Fulvic acids (FA) were immobilized on alumina particles in order to evaluate their catalytic effect as solid-phase redox mediator (RM) during the reductive dechlorination of carbon tetrachloride (CT) by anaerobic sludge. FA were extracted from three different soil samples and two commercial composts. Electron transferring capacity (ETC) was determined in all FA samples in order to select the appropriate source of redox-mediating compounds for CT dechlorination. TiO_2, $Al(OH)_3$, and γ-Al_2O_3 particles were tested as immobilizing materials for the extracted FA. FA extracted from a temperate pine forest soil showed the highest ETC (291.72 μmol g^{-1}). The highest adsorption capacity of FA, measured as total organic carbon (TOC), was achieved by alumina (γ-Al_2O_3) particles (12 mg TOC-FA g^{-1}). Results suggest that the transfer of electrons rather than their microbial generation through glucose fermentation was the rate-limiting factor during dechlorination of CT. Immobilized FA increase up to 10.4–fold the rate of CT dechlorination as compared with the control lacking FA. Immobilization of FA on alumina particles was very stable and spectrophotometric screening did not detect any detachment of FA during dechlorination of CT, thus confirming that the enhanced dechlorination achieved could exclusively be linked to the redox-mediating capacity of immobilized FA. The present study constitutes the first demonstration that immobilized FA on alumina particles could serve as a solid-phase RM in dechlorination reactions.

A modified version of this chapter has been published as: Alvarez LH, Jimenez L, Hernandez-Montoya V, Cervantes FJ (2012) *Water Air and Soil Pollution* 223:1911-1920

4.1 Introduction

As a result of improper disposal, leaking storage tanks, and spillage, carbon tetrachloride (CT) has become a common contaminant of soils and aquifers. Moreover, due to its relatively high water solubility, high vapor pressure, and low sorption to soil, CT is relatively mobile in the environment [11]. CT is a suspected carcinogenic compound listed as a priority pollutant by the United States Environmental Protection Agency. CT can produce liver and kidney damage in mammals by accidental acute exposure. Chronic exposure of humans to CT results in neurological effects and has lethal impacts on humans and animals at high doses [27, 29]. CT was the most common chlorinated solvent used as a dry-cleaning agent until it was banned in the 1950s when it was gradually replaced by trichloroethylene and perchloroethylene [36]. Furthermore, CT has been banned under the Montreal Protocol since 1996 in developed countries, and its use in developing countries ended in 2010. Nevertheless, CT is still produced, but only as an intermediate for the production of other chemical compounds nowadays [22]. Thus, industrial accidents may also account for its current incidence in different effluents.

CT generally prevails unaffected under aerobic biodegrading conditions because its carbon atom is highly oxidized. However, as a polychlorinated hydrocarbon, CT readily undergoes abiotic and microbial reductive dechlorination [33]. CT dechlorination has been documented under methanogenic [12-14, 32], denitrifying [6, 18], sulfate-reducing [7, 12, 13], iron-reducing [21, 25], humus-reducing [10] and fermenting conditions [7, 16].

During the last two decades, evidence has been accumulated indicating that humic substances (HS) and quinoid analogues can play important roles in the redox biotransformation of polychlorinated compounds accelerating their reductive dechlorination by anaerobic consortia [5, 10, 11, 17]. In fact, the capacity of HS and quinoid analogues to accelerate several redox reactions [30] has significant potential to develop strategies for enhancing the redox biotransformation of priority pollutants. One of the main limitations for applying HS as electron shuttles in wastewater treatment systems is that continuous addition of HS should be supplied to increase conversion rates, which is economically and environmentally unviable. Few attempts to apply immobilized redox mediators (RM) for the anaerobic conversion of priority pollutants have been reported. An immobilizing technique explored the incorporation of quinoid humic analogues within different materials

through polymerization procedure [15]. Through this immobilizing technique, quinones remain entrapped within the synthesized polymer keeping their redox mediating capacity, which has been shown to accelerate the reductive decolorization of azo dyes [15]. Functionalized polypyrrole (PPy) composites were enriched with the humic model compound, anthraquinone-2,6-disulfonate (AQDS), during the electro-polymerization of pyrrole monomer on activated carbon felt (ACF) electrode. The resulting composite (ACF/PPy/AQDS) exhibited good catalytic activity and stability and its addition effectively accelerated the reductive transformation of different nitroaromatics [19] and azo compounds [34] by anaerobic consortia. More recently, quinoid RM and HS were immobilized in anion exchange resins, which subsequently were demonstrated as an effective solid-phase RM accelerating the reductive biotransformation of azo dyes and CT [8-9].

The aim of the present study was to evaluate the capacity of fulvic acids (FA) extracted from a temperate pine forest soil, previously immobilized in alumina particles, to serve as a solid-phase RM during the reductive dechlorination of CT by an anaerobic sludge.

4.2 Materials and methods

4.2.1 Materials and inoculum

FA were extracted according to the protocol described by the International Humic Substances Society (IHSS) from five different sources. The extraction procedure was conducted as follows: the sample was dissolved in NaOH 0.1 M under stirring in a N_2 atmosphere. Then, the alkaline suspension settled overnight and the supernatant was collected by means of decantation. HCl 6 M was used to acidify the solution, with constant stirring, to pH = 1.0. After to allow the suspension to stand for 16 h, the FA fraction (supernatant) was separated by centrifugation. The sources of FA were: (1) compost made of agave bagasse from tequila production (Guadalajara, Mexico); (2) compost made of gardening wastes (Guadalajara, Mexico); (3) commercial compost produced from a variety of organic wastes by vermicomposting (Querétaro, Mexico); (4) soil from temperate pine

forest dominated (STPF) by *Pinus cembroides Zucc* (San Luis Potosí, Mexico); and (5) soil from deciduous forest (SDF) dominated by *Quercus rugosa Neé* (San Luis Potosí, Mexico). Three different materials were considered to immobilize FA in the present study: $Al(OH)_3$, γ-Al_2O_3, and TiO_2. $Al(OH)_3$ (>45 μm) and γ-Al_2O_3 (72% > 63 μm) were purchased from Merck, and TiO_2 was obtained from Sigma-Aldrich. These materials were used as received from suppliers without further purification.

The anaerobic granular sludge utilized during dechlorination of CT was collected from a full-scale upflow anaerobic sludge bed (UASB) reactor treating effluents from a factory of candies (San Luis Potosí, Mexico). The sludge was acclimated for 3 months in a lab-scale UASB reactor (1.5 L) operated at a hydraulic residence time (HRT) of 12 h and with an organic loading rate of 1 kg chemical oxygen demand (COD) m^{-3} d^{-1}. Glucose was used as a sole energy source for the UASB reactor, which showed stable efficiencies in terms of COD removal (>90%) during steady state conditions. The anaerobic granular sludge was sieved (pore size 1.5 mm) and washed with distilled water before batch experiments.

4.2.2 Surface charge distribution of metal (hydr)oxides

Batch experiments were conducted to determinate the surface charge distribution of all metal (hydr)oxide particles at different pH values under a CO_2-free atmosphere. N_2 was bubbled for 15 min into the solutions and also in the headspace of vials before sealing. First, 0.4 g of metal (hydr)oxide particles were dispensed in vials, and portions of 0.1 M NaCl was used to maintain a constant ionic strength. Initial pH values (2 to 12) were obtained by adding NaOH or HCl 0.1 M, for a total volume of 25 ml. After 4 days in stirring (150 rpm at 25 °C), the final pH was measure and the surface charge (expressed as the amount of ions released) was obtained with a mass balance based on pH change.

4.2.3 Immobilization of FA on alumina particles

FA were immobilized using the adsorption equilibrium technique in order to determine the adsorption capacity of metal (hydr)oxides particles. First, 0.14 g of metal (hydr)oxide particles were added to polypropylene vials (15 mL). Then, FA (10 mL) were added from the extracted solution without previous modification, at pH 1.0. After 3 days in stirring (150 at 25 °C), the initial and equilibrium concentration of total organic carbon (TOC) was

measured in order to determine the adsorption capacity by a mass balance relationship using Eq. (1):

$$q_e = V (C_0 - C_e) / W \quad (1)$$

Where q_e is the adsorption capacity (mg g^{-1}); V is the volume of FA solution (L); C_0 and C_e are the initial and equilibrium concentration of FA (mg TOC L^{-1}) respectively; and W the weight (g) of (hydr)oxides particles. Additionally, the adsorption strength of FA on (hydr)oxides was evaluated through desorption test in basal medium at pH . The basal medium was made according to the nutritional requirements of anaerobic wastewater treatment systems, with the composition described below.

4.2.4 Dechlorination of CT in the presence of FA

Dechlorination assays were conducted in 60 mL glass serum bottles using a basal medium with the following composition (g L^{-1}): $NaHCO_3$ (1.68); NH_4Cl (0.3); KH_2PO_4 (0.2); $MgCl_2 \cdot 6H_2O$ (0.03); $CaCl_2$ (0.1); and 1 mL L^{-1} of trace elements solution. The trace elements solution contained (mg L^{-1}): $FeCl_2 \cdot 4H_2O$, (2000); H_3BO_3, (50); $ZnCl_2$, (50); $CuCl_2 \cdot 2H_2O$,(38); $MnCl_2 \cdot 4H_2O$ (500); $(NH_4)_6Mo_7O_{24} \cdot 4H_2O$, (50); $AlCl_3 \cdot 6H_2O$, (90); $CoCl_2 \cdot 6H_2O$, (2000); $NiCl_2 \cdot 6H_2O$, (92); $Na_2SeO \cdot 5H_2O$, (162); EDTA, (1000); and 1 mL L^{-1} of HCl (36%). The pH was buffered at 7.2 with the amount of bicarbonate added and a head-space composed of N_2/CO_2 (80%/20%). Portions of basal medium (30 mL) were placed in serum bottles, which were immediately sealed with Teflon stoppers and aluminum caps. Anaerobic conditions were established by flushing the head-space (30 mL) of the bottles with a mixture of N_2/CO_2 (80%/20%) for 5 min. CT was added at the initial concentration of 50 µM from a sterilized anaerobic stock solution, then all bottles were pre-incubated for 24 h at 25 °C in order to obtain partition equilibrium of CT under these experimental conditions. Once equilibrium of CT concentration was reached, inoculation took place by adding 1 g volatile suspended solids (VSS) L^{-1} of the stabilized anaerobic sludge described above. The anaerobic granular sludge was previously disintegrated by pressing the sludge suspension through sterile needles with decreasing diameters (the smallest needle was a Microlance needle 3 [25G5/8, 0.5 by 16 mm]). Glucose was provided

as external electron donor (2 g L^{-1}). Sterile controls provided with nutrients (basal medium) and FA (suspended or immobilized), in the absence of glucose and microbial consortium, were also incubated. Endogenous controls included active consortium, provided with nutrients and FA (suspended or immobilized), but without external electron donor (glucose). Another control included active consortium, provided with nutrients and glucose, but in the absence of FA. Finally, different treatments containing active inoculum supplemented with nutrients, glucose and 100 or 200 mg TOC-FA L^{-1} in either suspended or immobilized form. All experimental treatments were carried out by triplicate and incubated at 25°C and 150 rpm. Spectrophotometric screening was conducted during the incubation period in order to verify detachment of FA from alumina particles. The concentration of CT, chloroform (CF) and dichloromethane (DCM) was also measured during the incubation period. CT reduction followed first-order kinetics. First-order conversion rates were calculated by fitting the CT removal from the batch incubations to Eq. (2) by using the least-squares method:

$$CT_t = CT_0 \bullet e^{-k_{CT} t} \quad (2)$$

Where k_{CT} is the first-order rate constant (h^{-1}); CTt is the concentration of CT (μM) at time t; CT_0 is the concentration of CT (μM) at $t = 0$; and t is incubation time (h).

4.2.5 Analytical Methods

The concentrations of CT, CF and DCM were measured by gas chromatography (GC, Agilent technologies 7890 series) coupled to a micro cell electron capture detector (μECD). Separation was achieved with a 5% phenyl-95% dimethyl-polysiloxane (30 m × 32 mm ID, 0.25μm (d_f)) HP-5 fused-silica capillary column from Agilent Technologies (Little Falls, DE). Helium was used as carrier gas at 1 mL min^{-1} column flow-rate and nitrogen was the makeup gas at 59 mL min^{-1}. The temperatures of injector and detector were maintained at 200 ºC and 260 ºC, respectively. Injection of 50 μL of headspace samples was made in split mode at 100:1 ratio. The oven temperature was programmed from 45 ºC (1 min hold) to 63 ºC (5 ºC min^{-1}). The identification of volatile chlorinated compounds (CT, CF and DCM) was confirmed in headspace samples using a gas chromatograph (Agilent technologies 7890)

coupled to a mass selective detector (Agilent technologies 5975-C), with the same column and chromatographic conditions. The temperatures of injector, transfer line, source and detector were maintained at 200 ºC, 250 ºC, 150 ºC and 230 ºC, respectively. Injection of 50 µL of gas samples was made in split mode at 100:1 ratio. The mass detector was operated in the electron impact mode at 70 eV. Identification was performed in full scan mode in the 20 to 200 mass/charge (m/z) range using also a mass spectral library data from N.I.S.T.-2005. Standards and samples were injected and analyzed under the same experimental conditions.

TOC concentrations were determined in previously filtered samples (0.22 µm) in a TOC-meter (Shimadzu Co. Model TOC-V_{CSN}). VSS concentrations were determined according to *Standard Methods* [2]. Glucose concentrations were measured using a capillary electrophoresis ion analyzer (Agilent G1600A, Waldbronn, Germany) equipped with a capillary column (50 µm ID × 72 cm) under the following conditions: temperature, 15 °C; current, 45 µA; negative polarity. A buffer composed of 25 mM of 2,6-pyridinecarboxylic acid and 5 mM of hexadecy-trimethyl ammonium bromide (pH 12) was used as eluant. Samples were also filtered (0.22 µm) before processing the electrophoresis analyses.

Fourier transformed infrared (FTIR) spectrometer (Thermo Scientific, Nicolet 6700) equipped with an attenuated total reflection (ATR) accessory was used to obtain ATR spectra at a resolution of 4 cm^{-1}. The (hydr)oxides coated with FA and those which were not coated were firstly dried overnight at 50 °C before obtaining their ATR spectra.

Electron transferring capacity (ETC) of all FA samples studied was determined chemically in an anaerobic chamber with an atmosphere composed of N_2-H_2 (95%/5%) following the protocol described by Lovley et al. [20]. Briefly, Fe(III) citrate was mixed with 0.5 mL of the sample to obtain a 10 mM final concentration and then allowed to react for 15 min before an aliquot was taken for Fe(II) determination by ferrozine assay. The Fe(II) concentration was used to calculate the number of mole equivalents of electrons transferred from FA samples to Fe(III). The difference between the Fe(II) concentration of the reduced and oxidized samples was defined as the sample ETC. For determining ETC, FA samples were reduced using a Pd-H_2 catalytic system at pH 8 and oxidized with air under the experimental conditions described by Ratasuk and Nanny [26]. ETC data were statistically analized by one-way analysis of variance (ANOVA) using STATGRAPHICS Centurion

XVI (Version 16.1.11) with a confidence level of 95%. Then a Fisher's Least Significant Differences (LSD) post-hoc test was done to verify differences between groups.

4.3 Results

4.3.1 Characterization and immobilization of FA

The ETC of five different samples of FA was measured in order to identify the most appropriated source of redox-mediating compounds for CT dechlorination. The LSD test showed no statistical difference ($P<0.05$) between the ETC values of those FA samples originated from SDF and from STPF (Table 4.1). Nevertheless, the sample of FA from STPF showed a statistically different value of ETC compared to the other three samples of FA. Furthermore, previous ETC determinations conducted with the humus-reducing microorganism, *Geobacter sulfurreducens*, revealed that FA extracted from STPF showed the highest ETC among the different FA samples tested (data not shown). Based on these results, FA extracted from STPF were selected as a source of RM for the reductive dechlorination of CT.

Table 4.1 Electron carrying capacity (ETC) of fulvic acids (FA) extracted from different sources

FA source	ETC ($\mu mol\ g^{-1}$)
Compost of agave bagasse	19.4 ± 13.7 a
Compost of grass residues	ND
Commercial compost	55.1 ± 41.2 a
Soil from deciduous forest	158.8 ± 50.4 ab
Soil from temperate pine forest	291.7 ± 91.6 b

Data represent average of duplicate ± standard deviation.
Different letters after ETC values indicate significantly different means ($P < 0.05$).
ND no detected.

The capacity of three different metal (hydr)oxides to adsorb the selected FA was evaluated. Surface charge distribution of these immobilizing materials revealed that all particles are positively charged at pH below 4.0; however, particles of γ-Al_2O_3 showed a wider pH range at which positive charges prevailed on their surface (Figure 4.1). The point of zero charge (pH_{pzc}) was 6.3, 8.9 and 7.4 for TiO_2, γ-Al_2O_3 and $Al(OH)_3$, respectively. Adsorption tests indicated that particles of γ-Al_2O_3 showed the highest adsorption capacity (12 mg TOC-FA g^{-1}) followed by TiO_2 (4.1 mg TOC-FA g^{-1}), and $Al(OH)_3$ (2.6 mg TOC-FA g^{-1}). In addition, after the desorption test in basal medium (pH 7.2), an important fraction of FA was desorbed from metal (hydr)oxides. The adsorption values (mg TOC-FA g^{-1}) after this test were to 6.16, 1.05, and 0.53 for γ-Al_2O_3, TiO_2, and $Al(OH)_3$, respectively. This indicates that the adsorption of FA in these materials could be partially attributed to electrostatic forces, but also to others type of interactions [38]; thus, adsorption-desorption of FA on metal (hydr)oxides is pH dependent.

Besides the superior adsorption capacity of γ-Al_2O_3 particles, they also showed better settling capacity (observational determination during the adsorption tests) compared to that observed with TiO_2 and $Al(OH)_3$. The settling capacity of particles could prevent their washout from up-flow anaerobic bioreactors such as UASB and EGSB (expanded granular sludge bed reactor), which also maintain the RM in the bioreactor. Thus, particles γ-Al_2O_3 were selected as immobilizing material of FA for their application as a solid-phase RM during the reductive dechlorination of CT (see below). FTIR-ATR spectra confirmed that quinone moieties (*e.g.* main redox-mediating functional groups in HS [30]) remained available once FA were adsorbed on γ-Al_2O_3 particles (Figure 4.2). Certainly, the spectral signal associated to quinone groups at ~1650 cm^{-1} appeared on the surface of γ-Al_2O_3 particles in which FA were previously immobilized.

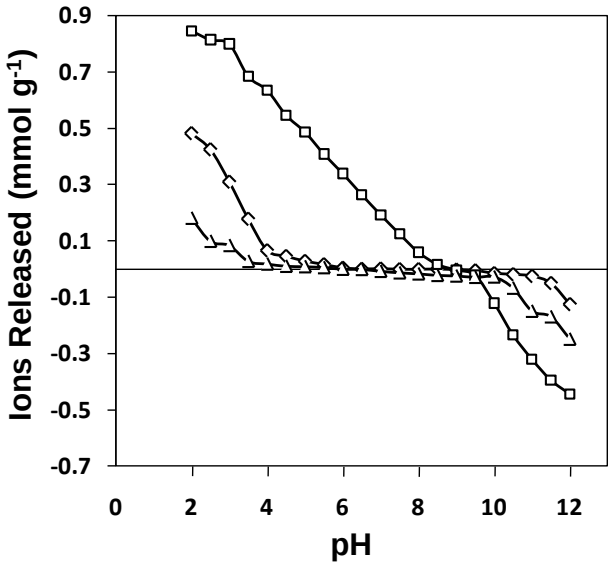

Figure 4.1 Surface charge distribution of (hydr)oxides at different pH values. Legends: (*square*) γ-Al_2O_3, (*diamond*) $Al(OH)_3$, and (*triangle*) TiO_2. The pH_{ZPC} values are 8.9, 7.4, and 6.3 respectively.

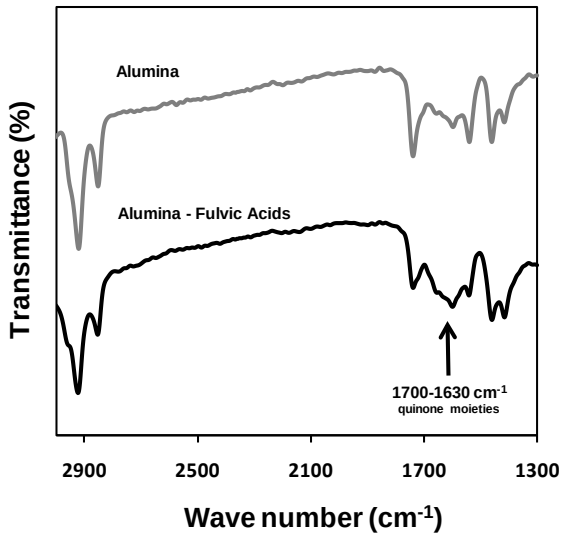

Figure 4.2 ATR spectra of alumina particles before and after of immobilize FA. Arrow shows the characteristic peak of quinone groups at 1700–1630 cm^{-1}.

4.3.2 Impact of FA on dechlorination of CT by anaerobic sludge

Reductive dechlorination of CT occurred without lag phase by the anaerobic consortium evaluated, which was evidenced by the concomitant reduction of CT and production of CF during microbial incubations, especially in those amended with FA (Figure 4.3). Nevertheless, the rate and extent of CT dechlorination greatly varied depending on the experimental conditions prevailing. For instance, sludge incubations performed in the absence of FA achieved only 16.6% of CT reduction to CF after 30 h of incubation with a k_{CT} value of 0.006 h^{-1}. Addition of suspended FA (FA_s) to sludge incubations increased up to 4.5–fold the k_{CT} value with respect to control incubations lacking FA (Table 4.2). The catalytic effect of FA_s was also evidenced by a higher extent of CT dechlorination in sludge incubations amended with FA_s as compared with controls lacking FA during the same incubations period (Figure 4.3c-d, Table 4.2). Indeed, the reduction of CT to CF in FA_s amended cultures ranged 23.7-26.9%, which is significantly higher than that achieved in the control lacking FA. Sterile controls including FA_s did not show significant (<1%) removal of CT (data not shown). However, sterile controls including FA immobilized on alumina particles (FA_i) showed major CT removal (up to ~50%) before inoculation, presumably due to adsorption on FA_i. However, a clear distinction between adsorption and reduction of CT could be established by measuring the production of CF (Figure 4.3a-b, Table 4.2). No CF production was detected in sterile controls amended with FA_i (data not shown).

Although CF was the unique chlorinated product detected during CT reduction in all sludge incubations, the relatively low recovery (72-73%) observed in FA_s-amended cultures suggests other unidentified chlorinated products might have been formed [10]. Experimental data revealed that FA_i could serve as an effective solid-phase RM during the reductive dechlorination of CT increasing up to 10.4–fold the rate of dechlorination. Moreover, the catalytic effect of FA_i was also favourably reflected in a higher extent of conversion of CT to CF (up to >90%, Figure 4.3a). Glucose was completely consumed in all sludge incubations, including the experimental control lacking FA, suggesting that dechlorination of CT was not limited by the generation of reducing equivalents, especially considering that 2 g L^{-1} of glucose was provided, which correponds to 267 milli-electron equivalents (mEq) L^{-1}, whereas the amount demanded for complete reduction of CT (~50

μM) is only 0.4 mEq L^{-1}. Spectrophotometric screening performed during CT dechlorination in the presence of FA_i did not detect any detachment of FA confirming that the enhanced dechlorination achieved can be attributable to the redox mediating capacity of FA_i.

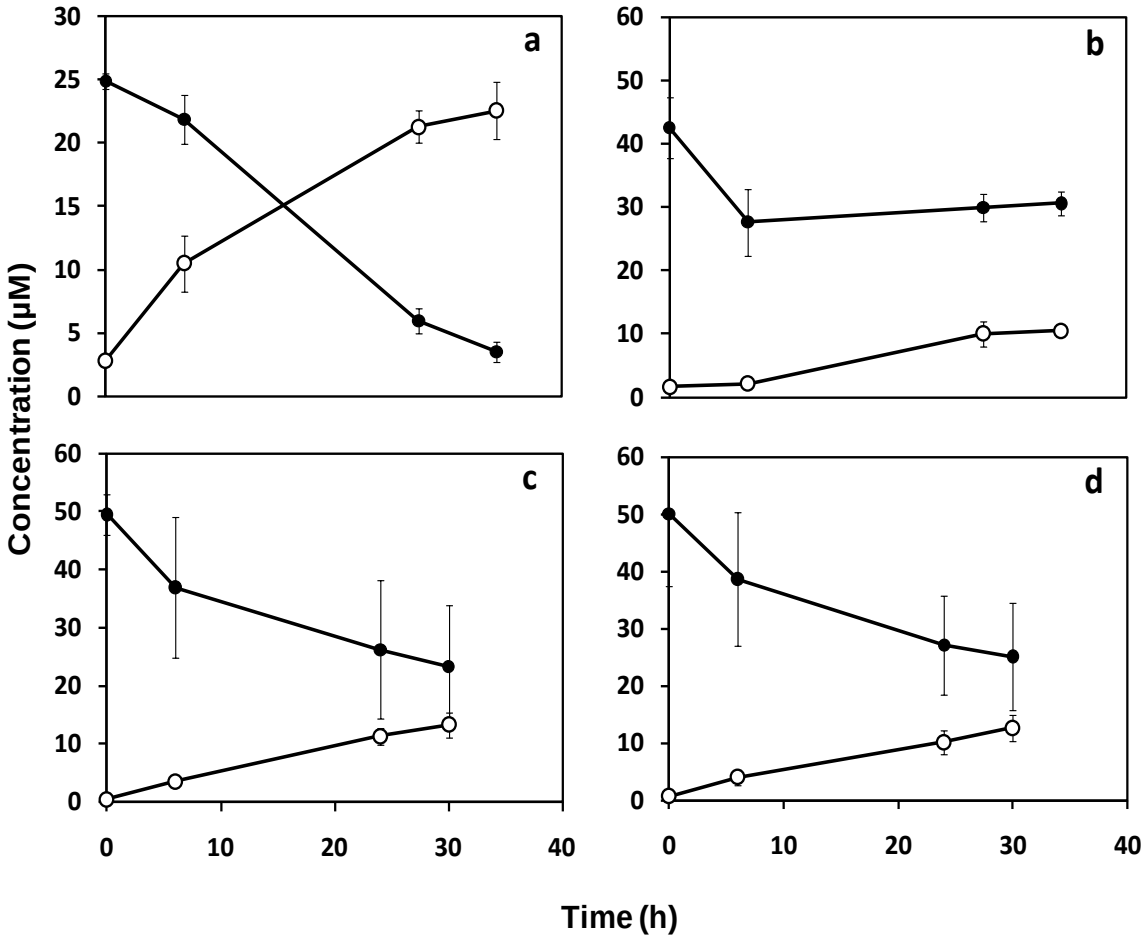

Figure 4.3 Time course of reductive dechlorination of CT (*filled circle*) linked to production of CF (*unfilled circle*) by anaerobic sludge. Panels a and b: sludge incubations amended with immobilized FA on γ-Al_2O_3 at 200 and 100 mg TOC-AF L^{-1} respectively. Panels c and d: sludge incubations amended with suspended FA at 200 and 100 mg TOC-AF L^{-1} respectively.

Table 4.2 Impact of suspended and immobilized FA on the Reductive Dechlorination of CT by anaerobic sludge[a]

Treatment	Increase in k_{CT}[b]	$[CT]_o$ (μM)	$[CT]_f$ (μM)	$[CF]_p$ (μM)	Reduction[c] (%)	Recovery[d] (%)
Control without FA		52.9±2.4	44.9±3.1	8.8±2.3	16.6	101.6
100 mg L^{-1} TOC-FA_s	4.2	53.5±12	25.1±9.4	12.7±0.7	23.7	72.7
200 mg L^{-1} TOC-FA_s	4.5	49.5±3.5	23.3±10	13.3±2.1	26.9	73.8
100 mg L^{-1} TOC-FA_i	1.7	42.5±4.7	30.6±1.9	10.5±0.2	24.7	97.7
200 mg L^{-1} TOC-FA_i	10.4	24.9±0.6	3.5±0.8	22.5±2.3	90.4	105.1

[a]Experimental conditions: Initial glucose concentration, 2 g L^{-1}; inoculum concentration, 1 g VSS L^{-1}.
[b]Increase respect to the control without FA.
[c]Extent of reduction of CT = $([CF]_p \times 100/[CT]_o$.
[d]Recovery = $([CT]_f + [CF]_p) \times 100/[CT]_o$.
FA, fulvic acids; FA_s, suspended FA; FA_i, immobilized FA; CT, carbon tetrachloride; TOC, total organic carbon; $[CT]_o$, initial CT concentration; $[CT]_f$, final CT concentration after 30 h of incubation; $[CF]_p$, produced chloroform after 30 h of incubation. Data represent average of triplicate determinations ± standard deviation.

4.4 Discussion

The aim of this study was to evaluate the redox-mediating capacity of FA immobilized on alumina particles during the reductive dechlorination of CT by anaerobic sludge. The results revealed that FA_i could increase up to 10.4–fold the rate of dechlorination of CT by anaerobic sludge. Sludge incubations supplied with 100 mg TOC-FA_i L^{-1} showed lower catalytic effect as compared with its counterpart including the same amount of FA, but suspended (Table 4.2). This decrease in the catalytic effect of FA_i could be associated with mass transfer limitations because microorganisms present in the anaerobic consortium might have required direct contact with FA_i to achieve the reduction of this solid-phase RM. Furthermore, some quinone moieties might have been sacrificed during the immobilizing procedure by serving as a link between alumina particles and FA, thus affecting the ETC of FA_i. Nevertheless, this limitation could be overcome by increasing the concentration of FA_i to 200 mg TOC-FA_i L^{-1}. Considering that glucose was completely

consumed during dechlorination of CT in all sludge incubations, it is conceivable that the generation of reducing equivalents was not the rate-limiting factor during the dechlorination of CT, but rather the transfer of electrons from the external electron donor to this polychlorinated pollutant. Certainly, the amount of glucose provided (2 g L^{-1}) was in large excess so that enough electrons would have been available to completely dechlorinate the amount of CT supplied (50 μM). Similar conclusion was obtained by Van der Zee et al. [31]; who found that the rate-limiting step during the reductive decolorization of azo dyes was not the production of reducing equivalents, but their transfer for azo dye reduction. Further indication that FA_i served as an effective solid-phase RM during the reductive dechlorination of CT is the capacity of the tested sludge to reduce HS and AQDS, suspended and immobilized, with glucose as an electron donor in the absence of CT (data not shown).

Previous reports evidenced the enhancement of CT dechlorination by anaerobic consortia when HS or AQDS were supplied as RM (in soluble form) increasing up to 6-fold the rate of CT-dechlorination [10, 14]. Collins and Picardal [11] reported the enhancement of CT conversion to CF by *Shewanella putrefaciens* 200 in the presence of different organic matter fractions including FA. Moreover, AQDS greatly accelerated the dechlorination of 2,4-dichlorophenoxyacetic acid by *Comamonas koreensis* strain CY01[35]. AQDS was also demonstrated as an effective electron shuttle in the electricity-driven microbial dechlorination of trichloroethene to *cis*-dichloroethene [4]. Further studies have also documented the role of immobilized RM on the redox biotransformation of azo dyes [1, 8, 15, 28, 34], nitroaromatics [19] and polychlorinated compounds [3]. However, in all these studies electron-shuttling model compounds were used, which implies costs limitations if these immobilizing methods are considered for full-scale applications. To our knowledge the present study constitutes the first demonstration that immobilized FA on alumina particles could serve as an effective solid-phase RM in dechlorination reactions.

Previously, Perminova et al. [24] developed a procedure to covalently bind HS to alumina particles by alkoxysilylation and this material was shown to efficiently remove Np(V) and Pu(V) by the sequestering properties of the immobilized HS [23]. However, this immobilized material has not been tested in redox reactions yet, but seems to fulfill the requirements to serve as a solid-phase RM feasible for remediation purposes.

Immobilized FA on alumina particles could constitute a new alternative for the treatment of industrial wastewaters containing recalcitrant pollutants by serving as solid-phase RM. Some important advantages could be underlined for applying alumina for the immobilization of FA. The high settling capacity of alumina particles could prevent the wash-out of RM when this (hydr)oxide is used as supporting material. Additionally, alumina particles coated with HS could be used as nuclei for sludge granulation or biofilms growth, as has previously been shown with zeolite particles [37].

The limited dechlorination of CT (*e.g.* incomplete reduction to CF) observed in the present study could be explained by the very low biomass concentration used in the assays (1 g VSS L^{-1}). Nevertheless, a wastewater treatment system co-immobilizing high concentrations of FA and biomass could be established for achieving complete dechlorination processes at full-scale. This will be the subject of an upcoming research using lab-scale UASB reactors in order to evaluate the treatment concept in long term experiments.

4.5 Conclusion

A novel technique to immobilize FA on alumina particles has been developed. Immobilized FA were subsequently demonstrated as effect solid-phase RM during the reductive dechlorination of CT. The rate of CT reduction to CF was increased up to 10.4–fold in the presence of immobilized FA, which was also reflected in a higher reduction efficiency (>90%) compared to the control lacking FA (only 16.6% of CT conversion to CF). A novel treatment concept involving the co-immobilization of high concentrations of FA and biomass is proposed for enhancing the redox biotransformation of priority pollutants in industrial effluents.

References

1. Alvarez, L. H., Perez-Cruz, M. A., Rangel-Mendez, J. R., & Cervantes, F. J. (2010) Immobilized redox mediator on metal-oxides nanoparticles and its catalytic effect in a reductive decolorization process. *Journal of Hazardous Materials, 184*, 268-272.

2. APHA (1985). *Standard Methods for Examination of Water and Wastewater*. American Public Health Association, Washington, D. C.

3. Aulenta, F., Canosa, A., De Roma, L., Reale, P., Panero, S., Rosseti, S., & Majone, M. (2009). Influence of mediator immobilization on the electrochemically assisted microbial dechlorination of trichloroethene (TCE) and *cis*-dichloroethene (*cis*-DCE). *Journal of Chemical Technology Biotechnology, 84*, 864-870.

4. Aulenta, F., Di Maio, V., Ferri, T., Majone, M. (2010). The humic acid analogue antraquinone-2,6-disulfonate (AQDS) serves as an electron shuttle in the electricity-driven microbial dechlorination of trichloroethene to *cis*-dichloroethene. *Bioresource Technology*, *101*, 9728-9733.

5. Barkovskii, A. L., & Adriaens, P. (1998). Impact of humic constituents on microbial dechlorination of polychlorinated dioxins. *Environmental Toxicology and Chemistry*, *17*, 1013-1020.

6. Bouwer, E. J., & McCarty, P. L. (1983). Transformations of halogenated organic compounds under denitrification conditions. *Applied and Environmental Microbiology*, *45*, 1295-1299.

7. Bouwer, E. J., & Wright, J. P. (1988). Transformations of trace halogenated aliphatics in anoxic biofilm columns. *Journal of Contaminant Hydrology*, *2*, 155-169.

8. Cervantes, F. J., Garcia-Espinosa, A., Moreno-Reynosa, M. A., & Rangel-Mendez, J. R. (2010). Immobilized redox mediators on anion exchange resins and their role on the reductive decolorization of azo dyes. *Environmental Science and Technology, 44*, 1747-1753

9. Cervantes, F. J., Gonzalez-Estrella, J., Marquez, A., Alvarez, L. H., & Arriaga, S. (2011). Immobilized humic substances on an anion exchange resin and their role on the redox biotransformation of contaminants. *Bioresource Technology, 102*, 2097-2100.

10. Cervantes, F. J., Vu-Thi-Thu, L., Lettinga, G., & Field, J. A. (2004). Quinone-respiration improves dechlorination of carbon tetrachloride by anaerobic sludge. *Applied Microbiology and Biotechnology, 64*, 702-711.

11. Collins, R., & Picardal, F. (1999). Enhanced anaerobic transformation of carbon tetrachloride by soil organic matter. *Environmental Toxicology and Chemistry, 18*, 2703-2710.

12. De Best, J. H., Hunneman, P., Doddema, H. J., Janssen, D. B., Harder, W. (1999). Transformation of carbon tetrachloride in an anaerobic packed-bed reactor without addition of another electron donor. *Biodegradation, 10,* 287-295.

13. Egli, C. R., Scholtz, R., Cook, A. M., & Leisinger, T. (1987). Anaerobic dechlorination of tetrachloromethane and 1,2-dichloroethane to degradable products by pure cultures of *Desulfitobacterium sp*. and *Methanobacterium sp*. *FEMS Microbiology Letters, 43,* 257-261.

14. Guerrero-Barajas, C., & Field, J. A. (2005). Riboflavin- and cobalamin-mediated biodegradation of chloroform in a methanogenic consortium. *Biotechnology and Bioengineering, 89,* 539-550.

15. Guo, J., Zhou, J., Wang, D., Tian, C., Wang, P., Salah Uddin, M., & Yu, H. (2007). Biocatalyst effects of immobilized anthraquinone on the anaerobic reduction of azo dyes by the salt-tolerant bacteria. *Water Research, 41,* 426-432.

16. Hashsham, S. A., & Freedman, D. L. (1999). Enhanced biotransformation of carbon tetrachloride by Acetobacterium woodii upon addition of hydroxocobalamin and fructose. *Applied and Environmental Microbiology, 65,* 4537-4542.

17. Kappler, A., & Haderlein, S. B. (2003). Natural organic matter as reductant for chlorinated aliphatic pollutants. *Environmental Science and Technology, 37,* 2714-2719.

18. Lee, C. H., Lewis, T. A., Paszczynski, A., Crawford, R. L. (1999). Identification of an extracellular catalyst of carbon tetrachloride dehalogenation from Pseudomonas stutzeri strain KC as pyridine-2,6-bis(thiocarboxylate). *Biochemical and Biophysical Research Communications, 261,* 562-566.

19. Li, L., Wang, J., Zhou, J., Yang, F., Jin, C., Qu, Y., Li, A., & Zhang, L. (2008). Enhancement of nitroaromatic compounds anaerobic biotransformation using a novel immobilized redox mediator prepared by electropolymerization. *Bioresource Technology, 99,* 6908-6916.

20. Lovley, D. R., Coates, J. D., Blunt-Harris, E. L., Phillips, E. J. P., & Woodward, J. C. (1996). Humic substances as electron acceptors for microbial respiration. *Nature, 382,* 445-448.

21. McCormick, M. L., Bouwer, E. J., & Adriaens, P. (2002). Carbon tetrachloride transformation in a model iron-reducing culture: relative kinetics of biotic and abiotic reactions. *Environmental Science and Technology, 36,* 403-410.

22. Penny, C., Vuilleumier, S., & Bringel, F. (2010) Microbial degradation of tetrachloromethane: mechanisms and perspectives for bioremediation. *FEMS Microbiology Ecology, 74*, 257-275.

23. Perminova, I., Karpiouk, L., Shcherbina, N., Ponomarenko, S., Kalmykov, S, Hatfield, K. (2007). Preparation and use of humic coatings covalently bound to silica gel for Np(V) and Pu(V) se-questration. *Journal of Alloys and Compounds, 444-445*, 512-517.

24. Perminova, I., Ponomarenko, S., Karpiouk, L., & Hatfield, K. (2006). *Humic derivatives, methods of preparation and use*. Patent application RU2006/000102. Filed on March 7, 2006.

25. Picardal, F. W., Arnold, R. G., Couch, H., Little, A. M., & Smith, M. A. (1993). Involvement of cytochromes in the anaerobic biotransformation of tetrachloromethane by Shewanella putrefaciens 200. *Applied and Environmental Microbiology, 59*, 3763-3770.

26. Ratasuk, N., & Nanny, M. A. (2007). Characterization and quantification of reversible redox sites in humic substances. *Environmental Science and Technology, 41*, 7844-7850.

27. Recknagel, R. O., & Glende, E. A. (1973). Carbon tetrachloride hepatotoxicity: an example of lethal cleavage. *Critical Reviews in Toxicology, 2*, 263-297.

28. Su, Y., Zhang, Y., Wang, J., Zhou, J., Lu, X., & Lu, H. (2009). Enhanced bio-decolorization of azo dyes by co-immobilized quinone-reducing consortium and anthraquinone. *Bioresource Technology, 100*, 2982-2987.

29. Van Agteren, M. H., & Keuning, S. (1998). *Handbook on biodegradation and biological treatment of hazardous organic compounds*. Kluwer Academic Publishers, Dordrecht.

30. Van der Zee, F. P., & Cervantes, F. J. (2009). Impact and Application of Electron Shuttles on the Redox (Bio)Transformation of Contaminants: A Review. *Biotechnology Advances, 27*, 256-277.

31. Van der Zee, F. P., Lettinga, G., & Field, J. A. (2001). Azo dye decolorization by anaerobic granular sludge. *Chemosphere, 44*, 1169-1176.

32. Van Eekert, M. H. A., Schröder, T. J., Stams, A. J. M., Schraa, G., & Field, J. A. (1998). Degradation and fate of carbon tetrachloride in unadapted methanogenic granular sludge. *Applied and Environmental Microbiology, 64*, 2350-2356.

33. Vogel, T. M., Criddle, C. S., & McCarty, P. L. (1987). Transformations of halogenated aliphatic compounds. *Environmental Science and Technology, 21,* 722-736.

34. Wang, J., Li, L., Zhou, J., Lu, H., Liu, G., Jin, R., & Yang, F. (2009). Enhanced biodecolorization of azo dyes by electropolymerization-immobilized redox mediator. *Journal of Hazardous Materials, 168,* 1098-1104.

35. Wang, Y., Wu, C., Wang, X., Zhou, S. (2009). The role of humic substances in the anaerobic reductive dechlorination of 2,4-dichlorophenoxyacetic acid by *Comamonas koreensis* strain CY01. *Journal of Hazardous Materials, 164*, 941-947.

36. Wentz, M. (1995). The evolution of environmentally responsible fabricate technologies. *American Drycleaner, 62,* 52-62.

37. Yoda, M., Kitagawa, M., & Miyaji, Y. (1989). Granular sludge formation in the anaerobic expanded micro carrier process. *Water Science and Technology, 21*, 109-122.

38. Yang, K., Lin, D., Xing, B. (2009) Interactions of humic acid with nanosized inorganic oxides. *Langmuir, 25*, 3571-3576

5

Immobilized redox mediator on metal-oxides nanoparticles and its catalytic effect in a reductive decolorization process

Abstract

Different metal-oxides nanoparticles (MONP) including α-Al_2O_3, ZnO, and $Al(OH)_3$, were utilized as adsorbents to immobilize anthraquinone-2,6-disulfonate (AQDS). Immobilized AQDS was subsequently tested as a solid-phase redox mediator (RMs) for the reductive decolorization of the azo dye Reactive Red 2 (RR2) by anaerobic sludge. The highest adsorption capacity of AQDS was achieved on $Al(OH)_3$ nanoparticles, which was ~0.16 mmol g^{-1} at pH 4. Immobilized AQDS increased up to 7.5–fold the rate of decolorization of RR2 by anaerobic sludge as compared with sludge incubations lacking AQDS. Sterile controls including immobilized AQDS did not show significant (<3.5%) RR2 decolorization suggesting that the physical-chemical processes (*e.g.* adsorption or chemical reduction) were not responsible for the enhanced decolorization achieved. Immobilization of AQDS on MONP was very stable under the applied experimental conditions and spectrophotometric screening did not detect any detachment of AQDS during the reductive decolorization of RR2, confirming that immobilized AQDS served as an effective RMs. The present study constitutes the first demonstration that immobilized quinones on MONP can serve as effective RMs in the reductive decolorization of an azo dye. The immobilizing technique developed could be applied in anaerobic wastewater treatment systems to accelerate the redox biotransformation of recalcitrant pollutants.

A modified version of this chapter has been published as: Alvarez LH, Perez MA, Rangel-Mendez JR, Cervantes FJ (2010) *Journal of Hazardous Materials* 184:268-272

5.1 Introduction

Several industrial sectors obtain great economical benefits due to the large and continuous production of different chemicals [1]. Nevertheless, linked to these economical benefits, several toxic and recalcitrant pollutants are discharged in large volumes of wastewater. Many of these contaminants are electron-accepting compounds, such as nitroaromatics, azo dyes, polyhalogenated compounds, and metalloids, due to the presence of electrophilic functional groups in their structures, making it difficult to treat them by convectional aerobic processes [2]. On the other hand, these pollutants can undergo anaerobic reductive biotransformation, producing compounds susceptible to aerobic biodegradation [3]. However, anaerobic reduction of recalcitrant pollutants occurs slowly as a result of toxicity effects on anaerobic consortia [4] or due to electron transfer limitations; consequently, anaerobic bioreactors could have deficient performance and can even collapse [5, 6].

In the last years, humic substances (HS) and quinones (main redox reactive functional groups in HS) have been tested as redox mediators (RM) during the reductive biotransformation of electron-accepting priority pollutants [7-9]. RM decrease electron transfer limitations, so that biotransformation of these contaminants is accelerated, which minimizes the toxic effects in the anaerobic microorganisms [4, 6]. Nevertheless, water soluble RM, such as anthraquinone-2,6-disulfonate (AQDS), need to be continuously added to achieve increased reduction rates in anaerobic wastewater treatment processes; the continuous addition of RM increases the cost of treatment and generates contaminated effluents.

Few studies have shown the use of solid-phase RM (RMs) during the reductive biotransformation of priority pollutants. For instance, activated carbon was tested as a RMs due to the presence of quinone moieties in this material [10]. Moreover, quinoid RM have been immobilized in polymeric matrixes [11], on anion exchange resins [12], and on composites of polypyrrole [13]. In all these cases, the immobilized catalysts were shown to enhance the anaerobic biotransformation of azo dyes [10-12] or nitroaromatics [13].

Few years ago, with the emergence of nanotechnology, new materials have been designed and aimed to improve environmental quality through pollution prevention, treatment, and remediation processes [14]. Mainly, nanoparticles are used as adsorbent of different organic and inorganic compounds for water treatment [14, 15], including HS [16] and natural

organic matter. Additionally, the adsorption of AQDS and HS has been conducted on ferrihydrite nanoparticles to evaluate the effect of adsorbed quinones on ferrihydrite reduction [17]. Furthermore, AQDS has also been adsorbed on hematite in order to understand geochemical variables during the reduction of iron oxides [18]. Nevertheless, to our knowledge, RM adsorbed on metal-oxides nanoparticles (MONP) has never been tested as RMs for the reductive biotransformation of priority pollutants, such as azo dyes. In this work, the capacity of different MONP to adsorb AQDS was evaluated. The catalytic properties of immobilized AQDS were subsequently tested in the reductive biotransformation of the azo model compound, Reactive Red 2 (RR2). RR2 is a very recalcitrant azo compound commonly used to represent reductive decolorization processes for textile wastewater treatment [6, 12, 19].

5.2 Materials and methods

5.2.1 Reagents and nanoparticles

AQDS (98% purity, Sigma Aldrich) was selected as a model RM. RR2 was purchased from Sigma Aldrich (purity of 40%) and used without further purification. Nanoparticles used for the immobilization of AQDS were the following metal-oxides: α-Al_2O_3, ZnO, and $Al(OH)_3$. All nanoparticles have a purity ≥99%, and were purchased from Nanostructured & Amorphous Materials Inc. (Houston, TX. USA).

5.2.2 Inoculum

Anaerobic granular sludge was used as inoculum, and was collected from a full-scale upflow anaerobic sludge bed (UASB) reactor treating effluents from a malt-processing factory (Lara-Grajales, Puebla, Mexico). The sludge was previously acclimated in a lab-scale UASB reactor (1.5 L) operated at a hydraulic residence time of 12 h. Glucose was used as a sole energy source for the UASB reactor, which showed stable efficiencies in terms of chemical oxygen demand (COD) removal (>90%) during steady state conditions. Prior to incubations, stabilized sludge was washed with distilled water and disintegrated with sterile needles (Microlance 3, 25G5/8, 0.5×16 mm); in the same step, the sludge was

stored in a glass serum bottle containing basal medium as describe in the section 2.4, and anaerobic conditions were established by saturating the inoculation bottle with a gas mixture of N_2/CO_2 (80%/20%).

5.2.3 Characterization of nanoparticles

Nanoparticles were characterized by nitrogen adsorption at 77 K, using a Physisorption equipment (Micromeritics ASAP 2020, Norcross, GA, USA) to calculate surface area (SA), applying the BET method. Before adsorption, samples were degassed at 383 K for 3 h. Pore volume (V_{Po}) was calculated from the maximum adsorption amount of nitrogen at p/p_0 = 0.99 applying the Harkins and Jura method. Additionally, batch experiments were used to determinate the surface charge of all nanoparticles at different pH values under a CO_2-free atmosphere. N_2 was bubbled for 15 min into the solutions and also in the headspace of vials before sealing. First, 30 mg of nanoparticles were dispensed in vials, and portions of 0.1 M NaCl were used to keep a constant ionic strength. Initial pH values (3 to 11) were obtained by adding NaOH or HCl 0.1 M, for a total volume of 15 mL. After 7 days in stirring, the final pH was measured and the surface charge (expressed as the amount of ions released) was obtained with a mass balance based on pH change.

5.2.4 Immobilization of AQDS on nanoparticles

The capacity of MONP to immobilize AQDS was conducted by adsorption isotherms using the batch equilibrium technique. Different concentrations (50, 100, 200, 300, 400, 500, and 600 mg L^{-1}) of AQDS were prepared and the pH was adjust to 4.0 using 0.1 M HCl. Then, 50 mg of nanoparticles and 10 mL of AQDS solution were mixed in vials. Vials were placed on a shaker (180 rpm at 25°C) until the equilibrium was accomplished. After centrifugation (5000 rpm, 10 min) the supernatant was analyzed in order to determine the equilibrium concentration of AQDS and the adsorption capacity.

The saturated materials were exposed several times to basal medium (pH 7.2) in order to verify the adsorption strength of AQDS on MONP. The basal medium was prepared according to the typical nutritional requirements for anaerobic wastewater treatment systems [4, 6, 10, 12], which composition was as follows (mg L^{-1}): $NaHCO_3$ (3000), NH_4Cl (280), K_2HPO_4 (250), $MgSO_4.7H_2O$ (100), $CaCl_2.2H_2O$ (10), and 1 mL L^{-1} of

trace element solution, which composition was as follows (mg L^{-1}): $FeCl_2.4H_2O$ (2000), H_3BO_3 (50), $ZnCl_2$ (50), $CuCl_2.2H_2O$ (38), $MnCl_2.4H_2O$ (500), $(NH_4)6Mo_7O_{24}.4H_2O$ (50), $AlCl_3.6H_2O$ (90), $CoCl_2.6H_2O$ (2000), $NiCl_2.6H_2O$ (92), $Na_2SeO.5H_2O$ (162), EDTA (1000), and 1 mL L^{-1} of HCl (36 %). The produced materials were characterized by Fourier transform infrared (FTIR) spectrometry and were compared with the FTIR spectra of AQDS and nanoparticles, as mentioned in the section 2.6. In addition, energy dispersive X ray (EDX) analysis was determined as previously established [12].

5.2.5 Decolorization assays of RR2

Decolorization assays were performed in 120 mL serum glass bottles with the basal medium described above; $NaHCO_3$ was change to 5000 mg L^{-1} to create the proper buffer capacity (pH 7.2). Portions of basal medium, for a total volume of 50 mL, were dispensed in the bottles, which were then sealed with rubber stoppers and aluminum caps. The atmosphere in the headspace (70 mL) of the bottles was changed with a mixture of N_2/CO_2 (80%/20%) in order to create anaerobic conditions. Once the atmosphere was changed, the bottles were inoculated with anaerobic sludge (disintegrated) at 1 g of volatile suspended solids (VSS) L^{-1}. All bottles were supplied with glucose (1 g COD L^{-1}) and pre-incubated during 12 h at 25°C and 180 rpm. After the pre-incubation period, the bottles were flushed again with the same gas mixture and supplied with a second glucose pulse (2 g COD L^{-1}). RR2 was added from a stock solution prepared with sterile basal medium, and the initial concentration in the incubations was 0.3 mM. Different treatments and controls were tested in order to elucidate the catalytic effect of immobilized AQDS on nanoparticles. The treatments included three different concentrations (1.2, 2.4, and 4.8 mM) of AQDS in soluble and immobilized form. The controls were: first, a control without AQDS in any form, but including glucose, basal medium and sludge. Second, sterile controls with soluble or immobilized AQDS at 4.8 mM and basal medium. Finally, a control with nanoparticles, basal medium, sludge, and glucose, but in the absence of AQDS. All conditions were carried out by triplicate and incubated at 25°C and 180 rpm.

5.2.6 Analytical methods

AQDS concentration was spectrophotometrically measured at 328 nm. Liquid samples were firstly centrifuged (10 min at 10 000 rpm) and diluted in bicarbonate buffer (60 mM, pH 7.2). RR2 decolorization was also documented spectrophotometrically at the maximum wavelength of visible absorbance (539 nm). Samples (0.75 mL) were centrifuged and diluted in a 0.1 M phosphate buffer at pH 7.0. FTIR spectra were obtained at a resolution of 4 cm^{-1} using a FTIR spectrometer (Thermo Scientific, Nicolet 6700) equipped with an attenuated total reflection (ATR) accessory. Samples were previously dried at 40 °C in an oven.

5.3 Results and discussion

5.3.1 Characterization of nanoparticles

Characterization of the evaluated MONP is summarized in Table 5.1. The highest particle diameter (D_P) corresponds to α-Al_2O_3-2, while the smallest D_P value was found for $Al(OH)_3$. SA of nanoparticles follows the order: $Al(OH)_3$ > ZnO > α-Al_2O_3-1 > α-Al_2O_3-2. Regarding V_{Po} data, nanoparticles showed different values from 0.018 to 0.159 $cm^3\ g^{-1}$. There is a relationship between the V_{Po} and SA values, but an indirect relationship between SA and DP values (e. g. the small SA found in α-Al_2O_3-2 (8.89 $m^2\ g^{-1}$) is attributed to its relatively large D_P and small V_{Po} value).

Table 5.1 Characterization and adsorption capacity of AQDS on nanoparticles tested.

Nanoparticle	D_P[a] (nm)	SA[b] ($m^2\ g^{-1}$)	V_{Po}[c] ($cm^3\ g^{-1}$)	pH_{PZC}[d]	Q_{des}[e] (mmol g^{-1})
α-Al_2O_3-1	35	10.05	0.018	7.9	$7.03x10^{-3}$
α-Al_2O_3-2	150	8.89	0.015	7.9	$1.56x10^{-3}$
ZnO	20	37.97	0.159	7.5	$6.31x10^{-3}$
$Al(OH)_3$	15	62.40	0.138	4.8	$1.05x10^{-1}$

[a]Particle diameter; [b]Surface area; [c]Porous volume; [d]pH of zero point charge; [e]Adsorption capacity after various desorption cycles in basal medium.

Surface charge data at different pH values are given in Figure 5.1. Surface charge of all MONP decreased with the increase of pH. Both, α-Al_2O_3-1 and α-Al_2O_3-2 had positive charges on their surfaces below its pH point of zero charge (pH_{PZC}), and negative charges over its pH_{PZC}; the pH_{PZC} of these nanoparticles was 7.9. The highest surface charge at pH 3.0 corresponds to $Al(OH)_3$, but relatively low surface charge values were observed at the pH range between 5 and 11. Finally, the pH_{PZC} identified for ZnO nanoparticles was 7.5.

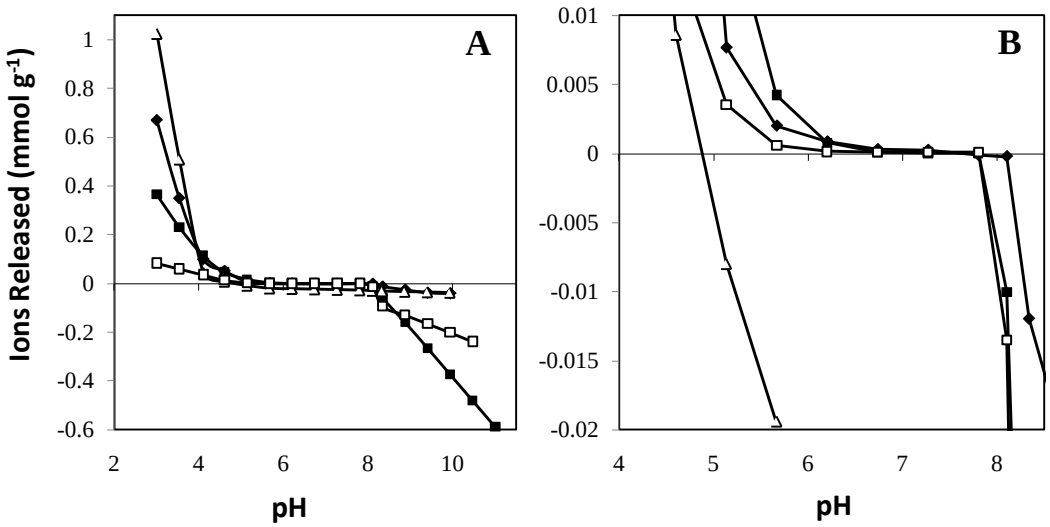

Figure 5.1 Surface charge of MONP using NaCl 0.1 mM to maintain a constant ionic strength. Panel A: Surface charge considering all pH values tested. Panel B: Approach of panel A, the pH_{PZC} of MONP is easily identified. Symbols: (■) α-Al_2O_3-1, (□) α-Al_2O_3-2, (♦) Zn, and (Δ) $Al(OH)_3$.

5.3.2 Adsorption of AQDS on nanoparticles

Adsorption isotherms of AQDS on nanoparticles are presented in Figure 5.2. The highest adsorption capacity was achieved on $Al(OH)_3$ nanoparticles, while similar adsorption capacity was observed for the two types of α-Al_2O_3 and ZnO. The isotherm with $Al(OH)_3$ showed an initial slope for the lower concentrations of AQDS tested, then a plateau and maximum adsorption capacity was observed (~0.16 mmol g^{-1}). AQDS adsorption on $Al(OH)_3$ is pH dependent (Figure 5.2); a lower adsorption capacity was achieved at pH 7.0 compared to that obtained at pH 4.0, with values of 0.099 mmol g^{-1} and 0.168 mmol g^{-1},

respectively. The adsorption of AQDS on the two types of α-Al_2O_3 and on ZnO was similar and within the range of 8.4×10^{-2} mmol g^{-1} to 1.2×10^{-2} mmol g^{-1}; one order of magnitude lower than the adsorption capacity accomplished with $Al(OH)_3$, and no plateau was found for these nanoparticles under the experimental conditions tested. The adsorption capacity of $Al(OH)_3$ is much higher than that achieved with previously tested materials such as hematite (~2 μmol g^{-1}) [18], α-alumina (~1.7 μmol g^{-1}), and ferrihydrite (≤10%) [17], which immobilized AQDS for different purposes to that aimed in the present study. The adsorption capacity of $Al(OH)_3$ is also higher than that obtained during the immobilization of AQDS on an anion exchange resin, which was subsequently shown to effectively increase the reductive decolorization of several azo dyes by serving as a RMs [12].

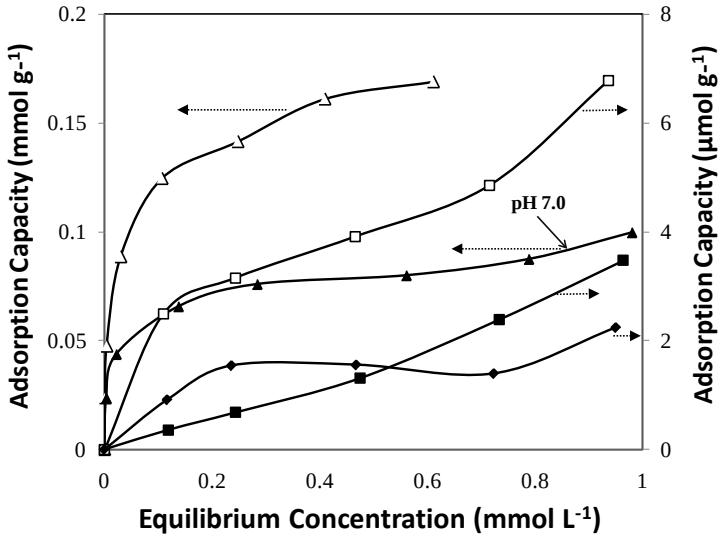

Figure 5.2 Adsorption capacity of AQDS on MONP at pH 4; the initials AQDS concentrations were 50 to 600 mg L^{-1}. Symbols: (■) α-Al_2O_3-1, (□) α-Al_2O_3-2, (♦) ZnO, (Δ) $Al(OH)_3$, and (▲) $Al(OH)_3$ at pH 7.0.

According to the surface charge values (Figure 5.1), AQDS adsorption could be attributed to electrostatic interaction between positive charges of the nanoparticles at pH 4.0, and negative charges of ionized sulfonate groups (SO_3^-) of AQDS, similar to the interaction of

AQDS with hematite [18]. Nevertheless, it could be possible that an additional mechanism such as affinity, might be involved for AQDS adsorption on $Al(OH)_3$; this is implied by the superior adsorption capacity observed with this material even though its surface charge, at the pH at which adsorption took place (4.0), is lower than that found on α-Al_2O_3-1, and ZnO (Figure 5.2).

In order to verify the strength at which AQDS was immobilized on the different MONP evaluated, the saturated materials were exposed to four desorption cycles with a basal medium, which resembles the typical nutritional conditions prevailing in anaerobic wastewater treatment systems. All saturated MONP showed desorption of AQDS during the first desorption cycle, probably due to detachment of quinones not electrostatically interacting with MONP, but forming multi-layers during the adsorption process. The amount of AQDS desorbed after the desorption cycles, was (%): $Al(OH)_3$ (37.8), ZnO (32.1), α-Al_2O_3-1 (16.8), and α-Al_2O_3-2 (85.8). Immobilized AQDS remained stable after this washing procedure and throughout its application during the reductive decolorization of RR2 (see below). The adsorption capacities of AQDS on MONP after desorption cycles are listed in Table 5.1.

Table 5.2 EDX analysis of $Al(OH)_3$ and AQDS-amended $Al(OH)_3$ after desorption test in basal medium[a]**.**

Element	% ± SD	
	$Al(OH)_3$ nanoparticles	AQDS-amended $Al(OH)_3$
Al	39.18 ± 0.18	36.51 ± 0.58
O	60.81 ± 1.37	34.52 ± 1.40
C	NI	12.87 ± 1.40
S	NI	2.61 ± 0.25

[a]Data represent average of triplicate determinations ± standard deviation.
NI no identified.

EDX analysis confirmed adsorption of AQDS on nanoparticles of $Al(OH)_3$ as an increase in the content of C and S was detected in the surface of AQDS-amended $Al(OH)_3$ nanoparticles, compared with their counterpart lacking this quinoid RM; whereas a decrease in the content of Al and O occurred once AQDS was adsorbed on this material (Table 5.2). Finally, FTIR spectra revealed that carbonyl groups of AQDS, which are the redox mediating groups of this catalyst, remained available once adsorbed on $Al(OH)_3$ (Figure 5.3). Certainly, the characteristic spectral signal of both carbonyl (C=O) and sulfonate (SO_3^-) groups at 1700-1630 cm^{-1} and 1200-1100 cm^{-1}, respectively, were detected in FTIR spectra of AQDS-amended $Al(OH)_3$ nanoparticles. These functional groups were also detected in the spectra of AQDS, but not in $Al(OH)_3$ nanoparticles lacking AQDS.

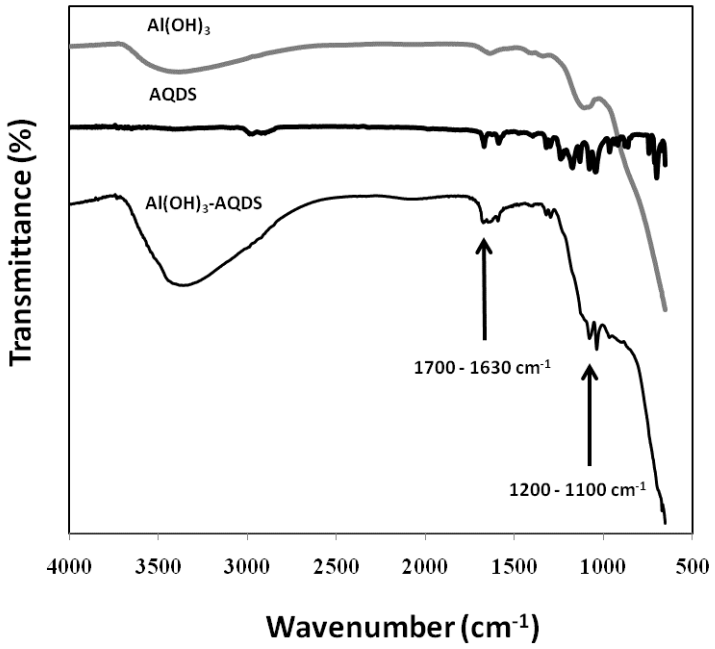

Figure 5.3 FTIR-ATR spectra of $Al(OH)_3$, and AQDS before and after to immobilize on nanoparticles of $Al(OH)_3$. The arrow show the characteristic peak signal of carbonyl and sulfonate groups of the quinone at 1700–1630 cm^{-1} and 1200-1100 cm^{-1}, respectively. Both groups are presents in AQDS and $Al(OH)_3$-AQDS.

5.3.3 Decolorization of RR2 with immobilized AQDS

Nanoparticles of $Al(OH)_3$ were selected as immobilizing material of AQDS to verify if the synthesized composite could efficiently increase the reductive decolorization of the azo model compound RR2 by serving as RMs in sludge incubations. Decolorization of RR2 followed first-order kinetics and the first-order rate constants of decolorization were calculated according to the following equation:

$$A = A_o \bullet e^{-kd \bullet t}$$

Where A is absorbance at a given time; A_o is the initial absorbance; k_d is the first-order rate constant of decolorization; and t is time.

Typical decolorization profiles are shown in Figure 5.4. Sterile controls provided with the highest concentration of AQDS tested (4.8 mM), either immobilized (AQDS-im) or free (AQDS-free), did not show significant (<3.5%) decolorization of RR2 indicating that physical-chemical processes (*e.g.* adsorption or chemical reduction) were not responsible for the reductive decolorization of RR2 achieved in sludge incubations. Controls including biologically active sludge incubated without AQDS achieved only 7.25% of RR2 decolorization. The catalytic effect of AQDS-im could be confirmed by the increased k_d values achieved during the reductive decolorization of RR2 by anaerobic sludge when the immobilized RM was included in sludge incubations (Table 5.3).

The rate of decolorization of RR2 was increased up to 7.5-fold in the presence of AQDS-im as compared with the biologically active control lacking AQDS. The catalytic effect of AQDS-im was also favorably reflected in a greater extent of decolorization of RR2. Indeed, up to 43.2% of RR2 decolorization occurred in sludge incubations supplied with AQDS-im after 12 hours of incubation, whereas only 7.25% of RR2 decolorization was achieved in sludge incubation without AQDS during the same incubation period. Spectrophotometric screening (Figure 5.5) performed during the decolorization of RR2 (and even after 5 days of incubation) in the presence of AQDS-im did not detect any detachment of AQDS confirming that the enhanced decolorization achieved could exclusively be attributed to the redox mediating capacity of the immobilized catalyst.

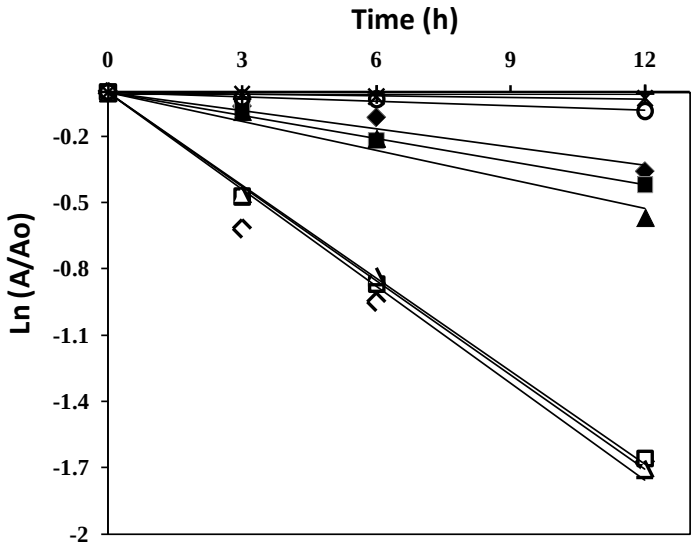

Figure 5.4 Catalytic effect of soluble and immobilized AQDS on nanoparticles of $Al(OH)_3$, on the reductive decolorization of RR2 (0.3 mM) by disintegrated anaerobic sludge (1 g SSV L^{-1}), and glucose as source of energy (2 g L^{-1}). Symbols: AQDS-im (mM) at (♦) 1.2, (■) 2.4, and (▲) 4.8, AQDS-so (mM) at (◊) 1.2, (□) 2.4, and (□) 4.8, control without AQDS (○), and sterile controls with soluble (+) and immobilized (x) AQDS at 4.8 mM.

Table 5.3 Rate of decolorization (*kd*) of reactive red 2 using immobilized redox mediators and anaerobic granular sludge[a].

Condition	RM concentration (mM)	*kd* (d^{-1})	Increase in *kd*[d]	Decolorization efficiency (%)
AQDS-im[b]	1.2	0.71 ± 0.01	4.77 ± 0.11	30.1 ± 0.60
	2.4	0.83 ± 0.05	5.57 ± 0.47	34.2 ± 1.65
	4.8	1.13 ± 0.01	7.52 ± 0.10	43.2 ± 0.43
AQDS-so[c]	1.2	3.47 ± 0.27	23.11 ± 1.81	81.2 ± 2.55
	2.4	3.31 ± 0.14	22.04 ± 0.97	80.9 ± 1.43
	4.8	3.41 ± 0.14	22.68 ± 0.95	81.8 ± 1.31

[a]Conditions: glucose concentration, 2 g COD L^{-1}; sludge concentration (disintegrated), 1 g VSS L^{-1}; RR2 concentration, 0.3 mM.

[b]AQDS immobilized on $Al(OH)_3$ nanoparticles.

[c]Refers to quinones, which were not immobilized, but provided in soluble form.

[d]Increase observed on k_d with respect to the control lacking AQDS (k_d in quinone-amended cultures/k_d in control), which was 0.119 d^{-1}. Data represent average of triplicate determinations ± standard deviation.

Previous studies reported different approaches to apply RMs during the redox biotransformation of azo dyes [10-12, 20] and nitroaromatics [13]. Some disadvantages of these immobilizing techniques are the gradual loss of the redox mediating capacity due to either wash out of the RMs from bioreactors [10] or disruption of the immobilizing material [11] and mass transfer limitations because a major fraction of the RMs remained entrapped within the immobilizing material [11]. To our knowledge the present study constitute the first demonstration that quinoid RM immobilized in MONP can serve as an effective RMs in a reductive decolorization process.

A series of experiments with AQDS-so was also conducted in order to compare with the results derived from sludge incubations provided with AQDS-im. As expected, the rates of decolorization achieved in incubations amended with AQDS-so were higher than those achieved with AQDS-im. AQDS-so increased up to 23.1-fold the decolorization rate of RR2 as compared with the control lacking AQDS, which allowed decolorization efficiencies of up 81.8% after 12 hours of incubation.

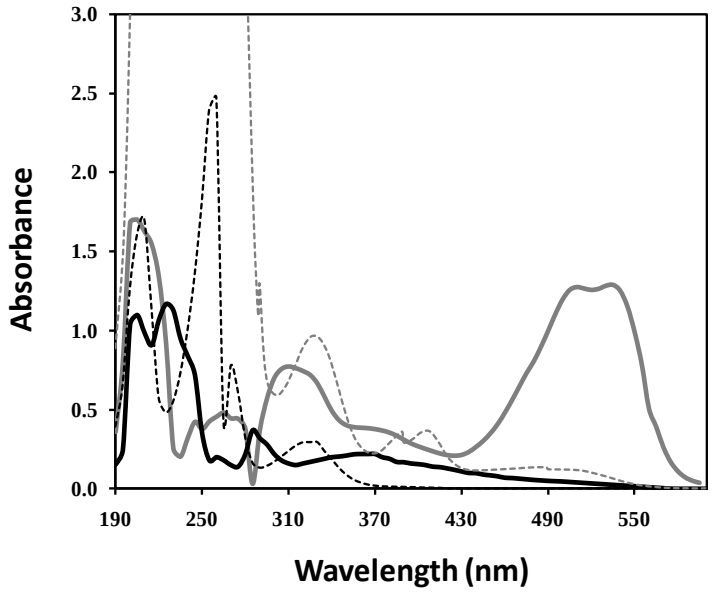

Figure 5.5 Spectra obtained during the reductive decolorization of RR2 (0.3 mM) by anaerobic granular sludge. The spectra were obtained from the culture with AQDS-im at 4.8 mM at initial (grey-solid) and final (black-solid) time. Black and grey lines (dash) represent spectra of oxidized and reduced AQDS (0.2 mM), respectively.

Despite the lower decolorization rates achieved with AQDS-im as compared with those obtained with AQDS-so, there are several advantages for considering MONP as immobilizing material of RM. Firstly, MONP can economically be synthesized. Secondly, MONP have a larger capacity to immobilize quinoid RM or HS compared to other materials [17-18]. Moreover, MONP have the proper physical-chemical properties to prevent disruption of the immobilized catalysts. Furthermore, mass transfer limitations occurring with other immobilizing materials could be overcome by using MONP to immobilize RM. Certainly, AQDS immobilized on an anion exchange resin and tested as a RMs, under the same experimental conditions applied in the present study, increased the rate of the decolorization of RR2 only by ~2-fold [12], whereas an enhancement of up to 7.5-fold was achieved in the present study by using nanoparticles of $Al(OH)_3$ as immobilizing material. The redox mediating capacity of AQDS immobilized in MONP is also superior to other RMs immobilized by different approaches [11, 13], which also have mass transfer limitations. Further experiments in our group has revealed that MONP can also serve as an effective matrix to immobilize HS and this immobilized material efficiently increase the redox biotransformation of different electron-accepting pollutants, such as azo dyes and carbon tetrachloride.

Perminova et al. [21] developed a procedure to covalently bind HS to alumina particles by alkoxysilylation and this material was shown to efficiently remove Np(V) and Pu(V) by the sequestering properties of the immobilized HS [22]. However, this immobilized material has not been tested in redox reactions yet, but seems to fulfill the requirements to serve as a RMs feasible for remediation purposes.

Finally, although the catalytic effect of AQDS-im was demonstrated in the present study, the use of MONP in anaerobic wastewater treatment systems requires some important considerations in order to prevent their wash-out. An alternative to warrant the maintenance of this RMs in anaerobic bioreactors is by creating granules in which HS-amended MONP and anaerobic sludge are simultaneously immobilized. This will be the subject of an upcoming research.

5.4 Conclusion

Immobilized AQDS on nanoparticles of $Al(OH)_3$ could serve as an effective RMs during the reductive decolorization of RR2 by an anaerobic sludge. Compared with the control lacking quinones, incubations with AQDS-im increased up to 7.5–fold the rate of decolorization of RR2. Spectrophotometric screening did not detect any detachment of AQDS during the reductive decolorization of RR2, indicating that the enhanced decolorization achieved could be exclusively attributed to the immobilized catalyst. Mass transfer limitations could be decreased by using nanoparticles to immobilize RM in comparison with other materials previously explored.

References

1. E. Razo-Flores, H. Macarie, F. Morier, Application of biological treatment systems for chemical and petrochemical wastewaters. In: F.J. Cervantes, S.G. Pavlostathis, A.C. Van Haandel, editors. Advanced biological treatment processes for industrial wastewaters: principles & applications. London, UK: IWA Publishing. (2006) 267–97.

2. F.P. Van der Zee, F.J. Cervantes, Impact and application of electron shuttles on the redox (bio)transformation of contaminants: A review, Biotechnol. Adv. 27 (2009) 256–277.

3. J.A. Field, A.J.M. Stams, M. Kato, G. Schraa, Enhanced biodegradation of aromatic pollutants in cocultures of anaerobic and aerobic bacterial consortia, Anton. Leeuw. Int. J. G. 67 (1995) 47–77.

4. F.J. Cervantes, M.I. López-Vizcarra, E. Siqueiros, E. Razo-Flores, Riboflavin prevents inhibitory effects during the reductive decolorization of Reactive Orange 14 by methanogenic sludge, J. Chem. Technol. Biotechnol, 83 (2008) 1703-1709.

5. J.D. Rodgers, N.J. Bunce, Treatment methods for the remediation of nitroaromatic explosives, Water Res. 35 (2001) 2101–11.

6. F.P. Van der Zee, R.H.M. Bouwman, D.P.B.T.B. Strik, G. Lettinga, J.A. Field, Application of redox mediators to accelerate the transformation of reactive azo dyes in anaerobic bioreactors, Biotechnol. Bioeng. 75 (2001) 691–701.

7. J. Rau, H.J. Knackmuss, A. Stolz, Effects of different quinoid redox mediators on the anaerobic reduction of azo dyes by bacteria, Environ. Sci. Technol. 36 (2002) 1497–1504.

8. T. Borch, W.P. Inskeep, J.A. Harwood, R. Gerlach, Impact of ferrihydrite and anthraquinone-2,6-disulfonate on the reductive transformation of 2,4,6-trinitrotoluene by a Grampositive fermenting bacterium, Environ. Sci. Technol. 39 (2005) 7126–7133.

9. A.L. Barkovskii, P. Adriaens, Impact of humic constituents on microbial dechlorination of polychlorinated dioxins, Environ. Toxicol. Chem. 17 (1998) 1013–1020.

10. F.P. Van der Zee, I.A. Bisschops, G. Lettinga, J.A. Field, Activated carbon as an electron acceptor and redox mediator during the anaerobic biotransformation of azo dyes, Environ. Sci. Technol. 37 (2003) 402-408.

11. J. Guo, J. Zhou, D. Wang, C. Tian, P. Wang, M.S. Uddin, H. Yu, Biocalalyst effects of immobilized anthraquinone on the anaerobic reduction of azo dyes by the salttolerant bacteria, Water Res. 41 (2007) 426- 432.

12. F.J. Cervantes, A. Garcia-Espinosa, M.A. Moreno-Reynosa, J.J. Rangel-Mendez, Immobilized redox mediators on anion exchange resins and their role on the reductive decolorization of azo dyes, Environ. Sci. Technol. 44 (2010) 1747-1753.

13. L. Li, J. Wang, J. Zhou, F. Yang, C. Jin, Y. Qu, A. Li, L. Zhang, Enhancement of nitroaromatic compounds anaerobic biotransformation using a novel immobilized redox mediator prepared by electropolymerization, Biores. Technol. 99 (2008**)** 6908-6916.

14. T. Masciangioli, Z. Wei-Xian, Environmental technologies at the nanoscale, Environ. Sci. Technol. 37 (2003) 102A-108A.

15. J. Theron, J. A. Walker, T. E. Cloete, Nanotechnology and water treatment: applications and emerging opportunities, Crit. Rev. Microbiol. 34 (2008) 43-69.

16. K. Yang, D. Lin, B. Xing, Interactions of humic acid with nanosized inorganic oxides, Langmuir. 25 (2009) 3571-3576.

17. M. Wolf, A. Kappler, J. Jiang, R. Meckenstock, Effects of humic substances and quinones at low concentrations on ferrihydrite reduction by geobacter metallireducens, Environ. Sci. Technol. 43 (2009) 5679-5685.

18. C. Liu, J.M. Zachara, N.S. Foster, J. Strickland, Kinetics of reductive dissolution of hematite by bioreduced anthraquinone-2,6-disulfonate, Environ. Sci. Technol. 41 (2007) 7730-7735.

19. S.G. Pavlostathis, M.I. Beydilli, Decolorization kinetics of the azo dye reactive red 2 under methanogenic conditions: effect of long-term culture acclimation, Biodegradation. 16 (2005) 135-146.

20. G. Mezohegyi, A. Kolodkin, U.I Castro, C. Bengoa, F. Stuber, J. Font, A. Fabregat, Effective anaerobic decolorization of azo dye Acid Orange 7 in continuous upflow packed-bed reactor using biological activated carbon system, Ind. Eng. Chem. Res. 46 (2007) 6788–6792.

21. I. Perminova, S. Ponomarenko, L. Karpiouk, K. Hatfield, PCT application RU2006/000102, Humic derivatives, methods of preparation and use, Filed on March 7, 2006.

22. I. Perminova, L. Karpiouk, N. Shcherbina, S. Ponomarenko, S. Kalmykov, K. Hatfield, Preparation and use of humic coatings covalently bound to silica gel for Np(V) and Pu(V) sequestration, J. Alloy Compd. 444-445 (2007) 512-517.

6

Assessing the impact of alumina nanoparticles in an anaerobic consortium: methanogenic and humus reducing activity

Abstract

The impact of γ-Al_2O_3 nanoparticles (NP) on specific methanogenic activity (SMA) and humus reducing activity (HRA) in an anaerobic consortium was evaluated. SMA in sludge incubations without γ-Al_2O_3 was always higher compared with those performed in the presence of 100 g/L of γ-Al_2O_3. Nevertheless, the SMA in incubations with γ-Al_2O_3 was not completely inhibited, indicating that some methanogenic microorganisms were physiologically active even in the presence of γ-Al_2O_3 NP during the incubation period (~400 h). SMA and HRA of the anaerobic consortium were also conducted in the presence of γ-Al_2O_3 NP coated with humic acids (HA). Microbial HA reduction occurred 3.7-fold faster using HA immobilized on γ-Al_2O_3 NP (HA_{Imm}), compared with the control with suspended HA (HA_{Sus}). Furthermore, immobilized HA decreased the toxicological effects of γ-Al_2O_3 NP on methanogenesis. SEM images revealed cell membrane damage in those sludge incubations exposed to uncoated γ-Al_2O_3 NP. In contrast, cell damage was not observed in incubations with HA-coated γ-Al_2O_3 NP. Methanogenesis out-competed microbial humus reduction regardless if HA was HA_{Imm} or HA_{Sus}. The present study provides clear demonstration that HA immobilized in γ-Al_2O_3 NP are effective terminal electron acceptor for microbial respiration and suggests that HA could mitigate the toxicological effects of metal oxides NP on anaerobic microorganisms. In addition, this study also provides a significant base for the feasibility of the co-immobilization of HA_{Imm} and humus reducing microorganisms trough the anaerobic granulation process, as mentioned in chapter 2.

A modified version of this chapter has been published as: Alvarez LH, Cervantes FJ (2012) *Applied Microbiology and Biotechnology* (doi: 10.1007/s00253-011-3759-4)

6.1 Introduction

In the last years, the use of materials at nanometric scale (1-100 nm) has allowed the development of nanotechnology. These nano-materials are also usually called nanoparticles (NP), and are extensively used for different purposes and applications. For instance, areas such as electronic, materials engineering, food, transportation, cosmetic, energy, pharmaceutical, biomedical, automotive, agriculture, fishing, manufacturing, security, consumers goods, and environmental have introduced the use of NP in their processes [5, 38]. NP offer a great number of advantages compared with their bulk forms [39-40, 46], and their use is constantly increasing. Nevertheless, little is known about the role of NP on the fate, transport, transformation, and bioavailability of environmentally relevant substances, and about their toxicity on living organisms in nature and in environmental bioprocesses.

The toxicity of several metal-oxides NP have been evaluated on different pure cultures, including *Bacillus subtilis, Escherichia coli, Shewanella oneidensis, Cupriavididus metallidurans, Streptococcus aureus, and Pseudomonas fluorescens* [4, 19, 31, 34, 37]. However, there are few reports showing the toxicological effects of NP on anaerobic sludge, as those obtained in upflow anaerobic sludge bed (UASB) reactors. For example, Luna-delRisco et al. [26], and Nyberg et al. [30] evaluated the effect of metal-oxides (CuO and ZnO), and fullerenes, respectively, on the production of biogas in anaerobic sludge. The toxicity of NP on bacteria can be attributed to their chemical composition, by the fact that they can release toxic ions [7] and particle surface catalyzed reactions [23], producing reactive oxygen species; or due to stress caused by their physical characteristics as surface, size, and shape.

Introduction of NP to ecosystems may also have a significant impact in relevant environmental processes, including biotic and abiotic systems. In aquatic environments, the surface of released metal-oxides NP can become negatively charged when natural organic matter (e.g. humic substances (HS)) is adsorbed, altering the fate and transport of both NP and HS [45]. On the other hand, it is well known that microorganisms can use dissolved HS as terminal electron acceptor (TEA) for the anaerobic oxidation of organic substrates [25]; and reduced HS can rapidly transfer electrons to reduce Fe(III) and Mn(IV) oxides [25, 29], acting as redox mediators (RM). In addition, the ability of microorganisms to reduce solid-

phase HS has recently been reported [33]. These authors showed that solid-phase HS significantly accelerated Fe(III) reduction, by shuttling electrons from bacteria to metal oxide surfaces, representing a new mechanism for extracellular electron transfer in sediments. Nevertheless, to our knowledge, the capacity of HS adsorbed on metal-oxides NP to act as TEA and RM has never been evaluated. However, previous studies, have reported the immobilization of quinoid model compounds (main redox functional groups in HS) on NP of $Al(OH)_3$, which were demonstrated as effective solid-phase RM accelerating the reductive decolorization of an azo dye by anaerobic consortia [2]. This report was the first demonstration that humic analogous immobilized on metal-oxide NP can act as RM. As mention by Van der Zee and Cervantes [43], immobilization of RM is a prerequisite for their use in anaerobic reactors in order to treat wastewaters containing electron-accepting contaminants. The results obtained from this study provide important evidence about the potential to use immobilized HS (on NP) as a solid-phase RM. Nevertheless, the impacts of NP on anaerobic consortium need to be considered prior to use them in wastewater treatment systems.

The two main goals of this study are: (1) evaluate the inhibitory effects of NP of alumina (γ-Al_2O_3) on specific methanogenic activity (SMA); and (2) evaluate the humus reducing activity (HRA) and SMA in the presence of γ-Al_2O_3 NP coated with humic acids (γ-Al_2O_3-HA). SMA and HRA experiments were conducted using a methanogenic consortium previously reported to have the ability to use HS as TEA.

6.2 Materials and methods

6.2.1 Humic acids and nanoparticles

HA were extracted from a soil of coal mine, according to the protocol described by the International Humic Substances Society (IHSS) (http://ihss.gatech.edu/ihss2/index.html). Briefly, the sample was dissolved in NaOH 0.1 M under stirring in a N_2 atmosphere. Then, the alkaline suspension settled overnight and the supernatant was collected by means of decantation. HCl 6 M was used to acidify the solution, with constant stirring, to pH = 1.0. After to allow the suspension to stand for 16 h, the HA (precipitate) was collected by

centrifugation. The yield of extraction was approximately 35% (unpurified); and its content (%) of carbon (59.36), hydrogen (2.8), nitrogen (1.22), sulfur (0.41), and oxygen (29.13) was similar to Standard Leonardite (1S104H) reported by IHSS. The electron carrying capacity (ECC) of extracted HA was evaluated by chemical [32] and biological (with *Geobacter sulfurreducens*) methods, using the ferrozina technique described by Lovley et al. [25]. The obtained ECC values were 392.4±14 micro-electron equivalents (µEq)/L and 160.2±17 µEq/L, respectively.

γ-Al_2O_3 NP was purchase from Inframat Advanced Materials (Manchester, CT. USA). According to the supplier, this material have a purity of 99.99%, average particle size of 20-50 nm, and surface area (BET) >150 m^2/g. γ-Al_2O_3 was used as received without previous modification. Surface charge distribution of γ-Al_2O_3 NP was determined using a mass balance based on pH change, as described by Alvarez et al. [2].

6.2.2 Anaerobic consortium

The anaerobic consortium studied was granular sludge collected from a full-scale UASB reactor treating effluents from a factory of candies (San Luis Potosí, Mexico). The sludge, which contains 6% of volatile suspended solids (VSS), was acclimated in a lab-scale UASB reactor (1.5 L) operated at a hydraulic residence time of 12 h and with an organic loading rate of 1 kg chemical oxygen demand (COD)/m^3•d. Glucose was used as a sole energy source for the UASB reactor, which showed stable efficiencies in terms of COD removal (>90%) during steady state conditions. The basal medium used during acclimatization was according to the following composition (g/L): $NaHCO_3$ (1.68); NH_4Cl (0.3); KH_2PO_4 (0.2); $MgCl_2$•$6H_2O$ (0.03); $CaCl_2$ (0.1); and 1 mL/L of trace elements solution. The trace elements solution contained (mg/L): $FeCl_2$•$4H_2O$, (2000); H_3BO_3, (50); $ZnCl_2$, (50); $CuCl_2$•$2H_2O$,(38); $MnCl_2$•$4H_2O$ (500); $(NH_4)_6Mo_7O_{24}$•$4H_2O$, (50); $AlCl_3$•$6H_2O$, (90); $CoCl_2$•$6H_2O$, (2000); $NiCl_2$•$6H_2O$, (92); Na_2SeO•$5H_2O$, (162); EDTA, (1000); and 1 mL/L of HCl (36%).

6.2.3 Adsorption of HA on γ-Al_2O_3 NP

The capacity of NP of γ-Al_2O_3 to adsorb HA was determined by adsorption isotherms using the batch equilibrium technique. Different concentrations of HA (100 to 5800 mg Total

Organic Carbon (TOC)/L) were prepared using deionized water, and then adjusting the pH to 4 with 0.1 M HCl. Then, 0.2 g of γ-Al_2O_3 and 10 mL of HA solution (previously filtered with 0.22 µm) were mixed in polypropylene vials. The vials were placed on a shaker (160 rpm at 27°C) during three days, until the equilibrium was accomplished. After centrifugation (3200 rpm, 10 min) the supernatant was analyzed in order to determine the equilibrium concentration of HA in terms of TOC; and the adsorption capacity determined by a mass balance.

According to the data obtained from adsorption isotherms, 40 g of γ-Al_2O_3 were prepared in order to evaluate SMA and HRA in the presence of immobilized HA. After this procedure, the material was washed with deionized water at pH 4 and dried in an oven at 40-45 °C. Then, in order to evaluate the adsorption strength of HA on NP, the saturated material was exposed several times to the basal medium described above. Finally, the material was characterized by Fourier transform infrared (FTIR) spectrometry and energy dispersive X ray (EDX) analysis, according to previously described methods [9].

6.2.4 SMA and HRA of anaerobic sludge

Activity assays of sludge incubations in the presence of γ-Al_2O_3 were conducted in serum glass bottles of 120 mL and 60 mL, with a working volume of 50 mL and 10 mL for SMA and HRA, respectively. The concentration of $NaHCO_3$ in the basal medium was change to 5000 mg/L to create the proper buffer capacity (pH 7.2). Glucose, acetate, and hydrogen at 1 g COD/L were used as model substrates during SMA assays and different concentrations (25, 50, 75, and 100 g/L) of γ-Al_2O_3 were also tested. On the other hand, experiments with 100 g/L of γ-Al_2O_3 uncoated (only for SMA) and coated with HA (for HRA and SMA), were also conducted using 7 g COD/L of acetate in order to evaluate microbial activity under conditions not limited by substrate. The HA concentration used in HRA and SMA either soluble or immobilized form was ~3750 mg TOC/L, which was establish according the adsorption capacity achieved on γ-Al_2O_3 NP. After sealing the bottles with rubber stoppers and aluminum caps, anaerobic conditions were established by saturating the headspace with a gas mixture of N_2/CO_2 (80%/20%). Then, the bottles were inoculated with 2 g VSS/L for SMA, and 1 g VSS/L for HRA, with anaerobic sludge previously disintegrated with sterile needles (Microlance 3, 25G5/8, 0.5×16 mm). The controls for

SMA were: a control in the absence of γ-Al_2O_3 and an endogenous control incubated without external electron donor. The HRA was conducted with sacrificial bottles, including controls with suspended HA (not attached to NP of γ-Al_2O_3). All experiments were carried out by triplicate, and were incubated at 27 °C and 160 rpm. Incubation conditions were selected in order to resemble realistic scenarios commonly found in anaerobic digesters. For instance, pH and temperature values correspond to those commonly prevailing in anaerobic wastewater treatment facilities [28]. No stabilizers were used to prevent NP agglomeration in sludge incubations supplied with NP of γ-Al_2O_3 so that exposure of the microbial consortium to NP could be performed at conditions expected in anaerobic digesters. Agglomeration of NP can prevent their washout from bioreactors, and could be caused by the presence of organic compounds and pH variations [22]; which is desirable into the context of the present study. SMA and HRA were determined on the maximum slope observed on linear regressions considering at least three sampling points. The coefficient of determination (R^2) was higher than 0.95 for most of activities calculated.

6.2.5 Analytical methods

Concentration of produced methane was measured by injecting 100 µL with a gas-tight syringe (Hamilton Co., Reno, NV, USA) in a gas chromatograph (GC, 6890N Network GC System, Agilent Technologies, Waldbronn, Germany) equipped with a thermal conductivity detector, and a column Hayesep D (Alltech, Deerfield, Illinois, USA) with the following dimensions: 10’ x 1/8” x 0.085”. Temperatures of the injection port, oven and the detector were 250, 60 and 250 °C, respectively. Nitrogen was used as carrier gas with a flow-rate of 12 mL/min. HA reduction of immobilized and suspended samples was measured in an anaerobic chamber with an atmosphere composed of N_2-H_2 (95%/5%) and using the ferrozine method described by Lovley et al. [25]. Briefly, Fe(III) citrate was mixed with the sacrificial samples to obtain a final concentration of 10 mM, and allowed to react for 15 min. Then, equal volume of 0.5 M HCl was added to the sample, and an aliquot was taken for spectrophotometric (562 nm) determination of Fe(II). The Fe(II) concentration was used to calculate the number of mole equivalents of electrons transferred from HA samples to Fe(III). Results were corrected for a control untreated with Fe(III) citrate.

TOC concentrations of HA were measured in a TOC-meter (Shimadzu Co. Model TOC-V_{CSN}), using previously filtered samples (0.22 µm). VSS and COD concentrations were determined according to *Standard Methods* [3]. Glucose and acetate concentrations were measured using a capillary electrophoresis ion analyzer (Agilent G1600A, Waldbronn, Germany) equipped with a capillary column (50 µm ID × 72 cm) under the following conditions: temperature, 15 °C; current, 45 µA; negative polarity. A buffer composed of 25 mM of 2,6-pyridinecarboxylic acid and 5 mM of hexadecy-trimethyl ammonium bromide (pH 12) was used as eluant. Samples were also filtered (0.22 µm) before processing the electrophoresis analyses. Finally, dissolved Al was measured by ICP-OES (Varian 730 series, Palo Alto, CA, USA).

6.2.6 Scanning electron microscopy (SEM)

In order to observe the interactions between NP and the anaerobic consortium studied, incubations with 2 g/L of γ-Al_2O_3 were prepared. One drop of suspension was placed on the top of a pin, and then the sample was dried at room temperature during 12 h. Finally, the sample was covered with a thin layer of gold to make their surface conductive.

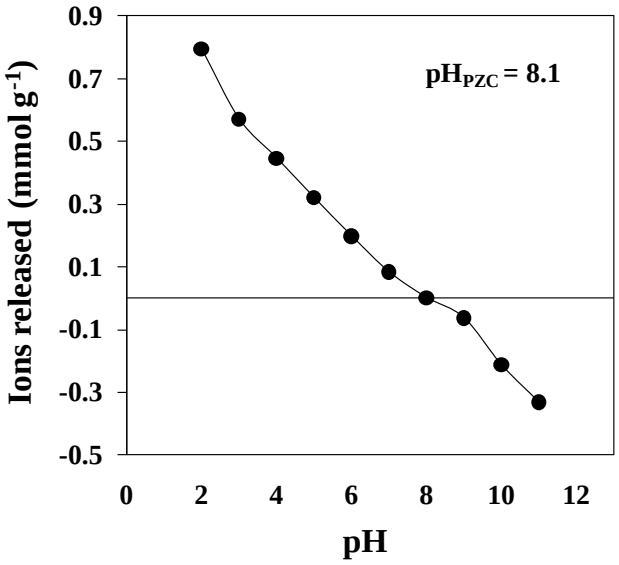

Figure 6.1 Surface charge distribution of γ-Al_2O_3 nanoparticles evaluated under different pH conditions.

6.3 Results

6.3.1 Immobilization of HA on γ-Al_2O_3 NP

Surface charge distribution of NP of γ-Al_2O_3 at different pH values is given in Figure 6.1. The pH point of zero charge (pH_{PZC}) of γ-Al_2O_3 was 8.1; this indicates that surface of γ-Al_2O_3 is positively charged below this pH value, and negatively charged at higher pH values than 8.1. According to surface charge distribution, an appropriate value for the adsorption of HA on γ-Al_2O_3 is 4 [45].

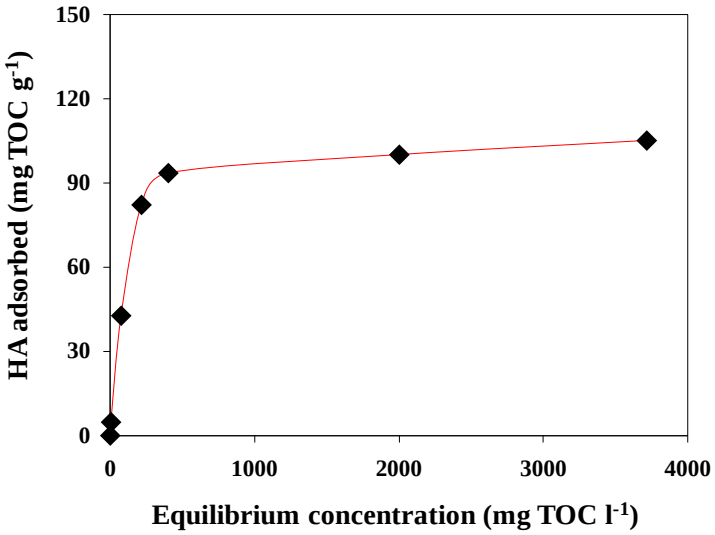

Figure 6.2 Adsorption isotherm of humic acids on γ-Al_2O_3 NP. Maximum adsorption capacity was ~93 mg TOC/g.

Adsorption isotherm indicated that the maximum adsorption capacity (Q_{max}) of HA on γ-Al_2O_3 was ~93 mg TOC/g (Figure 6.2). Q_{max} value was achieved using a concentration of HA of ~2,300 mg TOC/L, with a mass/volume ratio of 20. The isotherm showed an initial slope for the lower concentrations of HA tested, and then a plateau and the Q_{max} value were observed. The adsorption followed a typical Langmuir isotherm, also observed in other studies [20, 44-45]. Electrostatic attraction could explain the adsorption of HA by γ-Al_2O_3 NP. According to the surface charge distribution (Figure 6.1), the positive charges on

surface of γ-Al_2O_3 (at pH 4) and negative charges of HA, due to unprotonated groups (e.g. carboxyl, phenolic), promoted an electrostatic attraction [41]. Once the HA are adsorbed on γ-Al_2O_3, the surface of this NP becomes less positively charged as reported by Yang et al. [45].

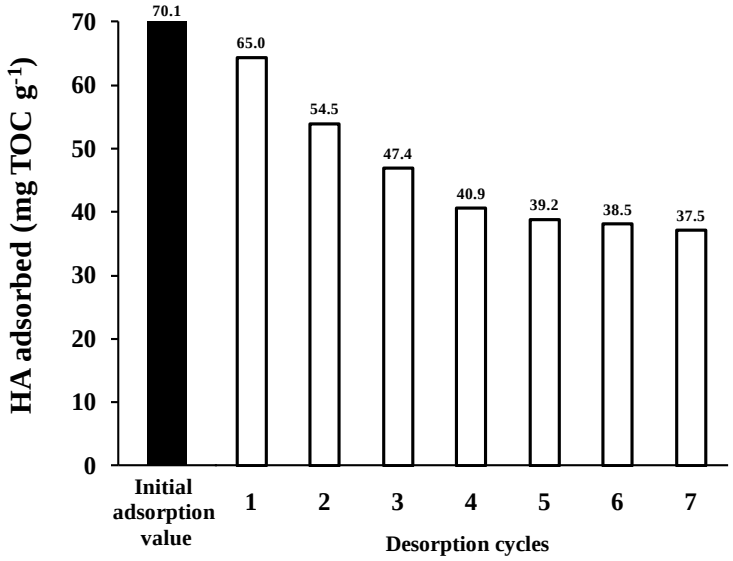

Figure 6.3 Adsorption (black) and desorption (white) of humic acids on γ-Al_2O_3. Adsorbed humic acids become stable after four desorption cycles with basal medium. This material was used during methanogenic and humus reducing incubations.

On the other hand, after the material was exposed to seven desorption cycles with basal medium, the adsorption capacity value decreased 53.5% respect to the initial value. This decrement can be explained because of the pH value (7.0) of basal medium changes the surface charge of γ-Al_2O_3 particles (Figure 6.1), which promotes a decrease of attraction forces, and consequently the desorption of HA. However, after the fourth desorption cycle, the material becomes stable (Figure 6.3). FTIR-ATR spectra confirmed that quinone moieties remained available once HA were adsorbed on γ-Al_2O_3 particles (Figure 6.4). Certainly, the spectral signal of carbonyl (C=O) groups at 1700-1630 cm^{-1} associated to quinone groups [35] appeared on the surface of γ-Al_2O_3 particles in which HA were previously immobilized. These functional groups were also detected in the spectra of HA,

but not in γ-Al_2O_3 lacking HA. In addition, EDX analysis confirmed adsorption of HA on γ-Al_2O_3 because an increment in the content of C and N was detected in the surface of HA-amended γ-Al_2O_3, compared with their counterpart lacking HA; also, a decrease in the content of Al and O occurred once HA was adsorbed on this material (data not shown).

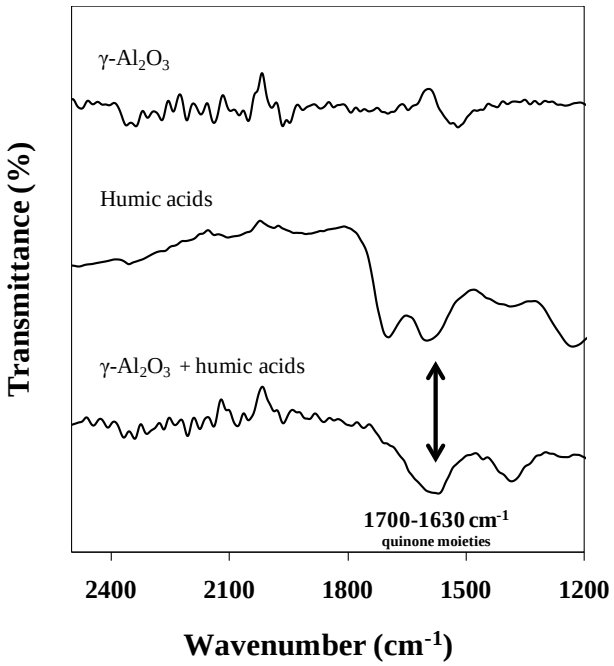

Figure 6.4 FTIR spectra of HA, γ-Al_2O_3, and γ-Al_2O_3 coated with HA. Arrows indicate the spectral signals for quinone (1700-1630 cm^{-1}) group.

6.3.2 SMA of anaerobic sludge in the presence of γ-Al_2O_3 NP

Methane production was observed under all concentrations of γ-Al_2O_3 NP and with the three substrates tested (Table 6.1 and Figure 6.5). In all cases, SMA was higher in the absence of NP, and was consistently affected with the increment of γ-Al_2O_3 concentration, decreasing 62.2% and 84.6% at 100 g/L of γ-Al_2O_3 when glucose and acetate were supplied as electron donors, respectively, compared with their corresponding controls lacking NP. Nevertheless, the SMA observed in incubations with hydrogen was less affected decreasing only 14.2% compared to those incubations lacking γ-Al_2O_3 NP. Decrease in SMA could be

associated to inhibitory effects caused by exposure of this consortium to γ-Al_2O_3 NP, but also to substrate limitation due to substrate adsorption on NP, especially in incubations with glucose and acetate. Electrophoretic analysis revealed that there was not glucose and acetate remaining in those incubations with γ-Al_2O_3 at the end of the incubation period, but the amount of produced methane (recovery ranging between 24-93%) did not agree with the total consumption of substrate, suggesting that these substrates were partly adsorbed on γ-Al_2O_3, thus limiting the availability of electron donor during SMA tests. Further experiments revealed that the adsorption capacity of acetate on γ-Al_2O_3 is 1.4 g COD/g; this phenomenon could play an important role affecting SMA, which was not evident when a gaseous substrate like hydrogen was used as electron donor.

Table 6.1 Specific methanogenic activity (SMA) by anaerobic consortia using 1 g COD/L and different concentrations of γ-Al_2O_3. Values are given mili-electron equivalents (m-Eq)/g VSS•h. The results are the mean of triplicate and in all cases standard deviation was less than 8.5%.

γ-Al_2O_3 (g/L)	**SMA**		
	Glucose	**Acetate**	**Hydrogen**
0	0.643	0.540	1.573
25	0.452	0.257	1.349
50	0.361	0.171	1.505
75	0.287	0.119	1.263
100	0.246	0.083	1.350

SMA was also conducted using 100 g/L of γ-Al_2O_3 and high concentration of acetate, in order to evaluate activity under conditions not limited by substrate. Before inoculating with the anaerobic consortium, the bottles were pre-incubated during ~24 h to achieve equilibrium of acetate by adsorption on γ-Al_2O_3 NP. During this period, concentration of

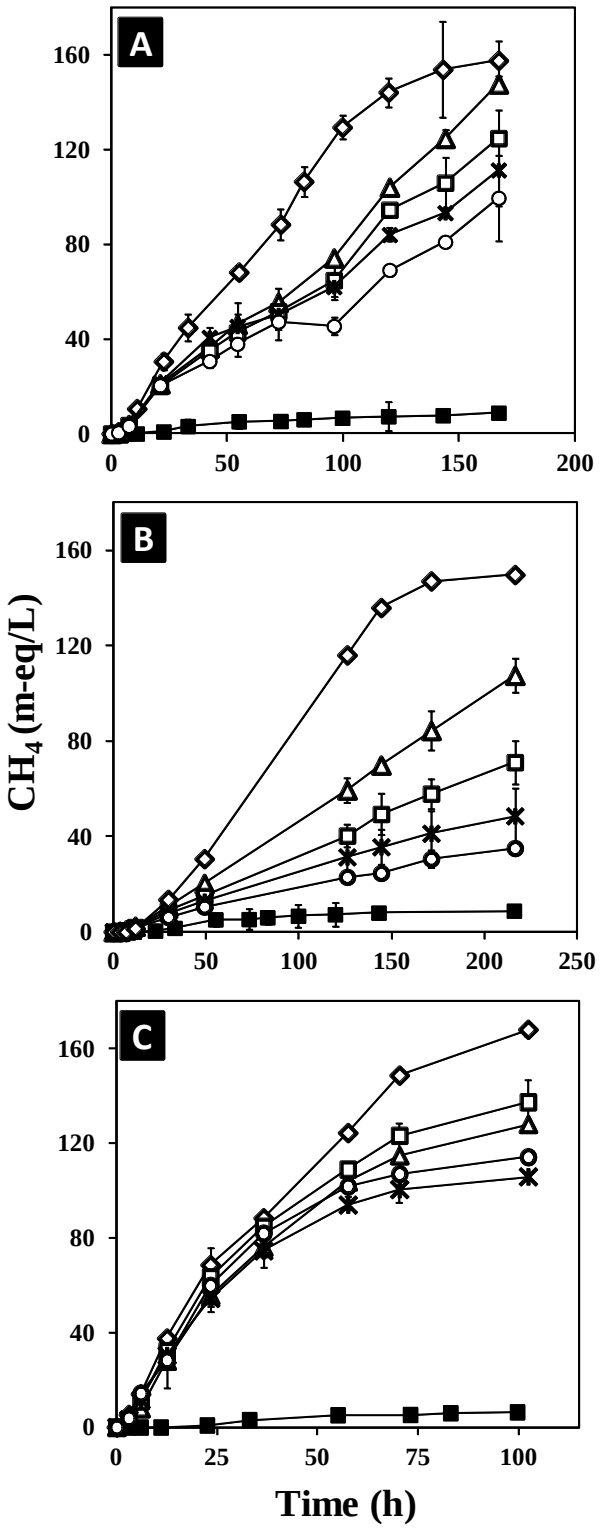

Figure 6.5 Concentration of methane produced by anaerobic consortia using 1 g COD/L of glucose (A), acetate (B), and hydrogen (C). Symbols (g of γ-Al_2O_3/L): (◊) without γ-Al_2O_3, (Δ) 25, (□) 50, (x) 75, (○) 100, and (■) endogenous control without γ-Al_2O_3.

acetate decreased from 7.03±0.08 g COD/L to 6.5±0.17 g COD/L. SMA was calculated for each phase during the incubation period; each phase represents the replacement of produced methane by saturating the headspace with a gas mixture of N_2/CO_2 (80%/20%), and then continuing with incubation. For almost 400 h, sludge incubations with γ-Al_2O_3 showed a stable methane production, but always lower than that obtained with the control lacking NP (Figure 6.6 and Table 6.2). The stable methane production in the presence of γ-Al_2O_3 was evidenced by the values obtained of SMA during the three phases of experiment, which are very closed among them (mean of 539±14 μEq/g VSS•h), this indicates that some methanogenic microorganisms were physiologically active even in the presence of γ-Al_2O_3 NP. These results clearly confirm that γ-Al_2O_3 NP had a toxicological effect on some methanogenic microorganisms.

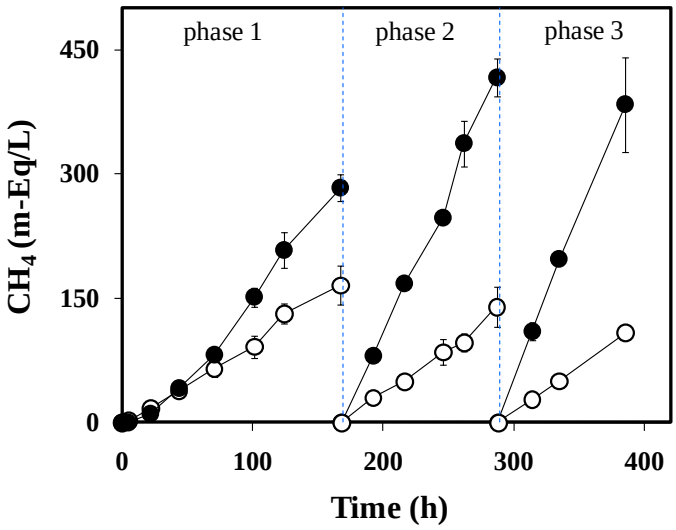

Figure 6.6 Concentration of methane produced by anaerobic consortia using acetate. Symbols: (○) Experiment with 100 g/L of γ-Al_2O_3; (●) control lacking γ-Al_2O_3.

6.3.3 SMA and HRA of anaerobic sludge in the presence of HA

SMA and HRA of the anaerobic consortium were conducted in the presence of 100 g/L of γ-Al_2O_3 NP coated with HA, representing ~3.75 g TOC/L of immobilized HA (HA_{Imm}). This concentration of HA was also provided in incubations without γ-Al_2O_3, but in

suspended form (HA_{Sus}). The established concentrations of HA and γ-Al_2O_3 NP for these incubations are very distant from what could be expected in natural ecosystems. However, they were intentionally selected for two purposes: 1) to have quantifiable levels to accurately measure the microbial reduction of HA_{Imm} and HA_{Sus}; and 2) to establish HA concentrations demanded for redox-mediating reactions in anaerobic bioreactors since HA immobilized in metal oxides NP have been proposed as solid-phase redox mediator for the anaerobic biotransformation of priority pollutants [2].

Table 6.2 Impact of γ-Al_2O_3 NP on SMA and HRA by anaerobic sludge (values are given in micro-electron equivalents (μEq)/g VSS•h)[a]

Condition	SMA		
	0-167 h	168-287 h	288-385 h
Without γ-Al_2O_3	967 ± 9.5	1754 ± 112	1965 ± 285
With γ-Al_2O_3	518 ± 66	541 ± 83	559 ± 49
	SMA		HRA
	0-96 h	97-166 h	0-166 h
HA_{Sus} without γ-Al_2O_3	1759 ± 150	2678 ± 73	6.0 ± 0.28
HA_{Imm} on γ-Al_2O_3	768 ± 26	1084 ± 34	22.3 ± 4.1

[a]Experimental conditions: acetate added, 7.03±0.07 g COD/L; acetate concentration after pre-incubation period (after adsorption on γ-Al_2O_3 NP), 6.51±0.17 g COD/L; γ-Al_2O_3 concentration, 100 g/L. The results are the mean of triplicate ± standard deviation.

After 166 h of incubation, HA reduction was 2.4-fold higher using HA_{Imm} compared with the control with HA_{Sus} at the end of incubation period (Figure 6.7A). Conversely, methane production was higher by 3.6-fold and 1.6-fold during the first and second phases respectively, when HA_{Sus} was provided as compared with incubations with HA_{Imm} (Figure 6.7B). SMA and HRA obtained in sludge incubations are given in Table 6.2. When HA_{Imm} was provided, SMA decreased 56% and 59% during the first and second phases

respectively, compared with the treatment lacking NP, but with HA_{Sus}. Nevertheless, HRA in incubation with HA_{Imm} was 73% faster than the control with HA_{Sus} (Table 6.2).

SMA values obtained in the presence of HA-coated γ-Al_2O_3 NP (e.g. HA_{Imm}) were higher than those obtained with incubations using uncoated γ-Al_2O_3 (Table 6.2). These results can be explained by the fact that adsorption of HA on the surface of γ-Al_2O_3 NP decreases their toxicological effects. NP of γ-Al_2O_3 coated with HA could enhance Al (Al^{3+}) sorption, thus decreasing also toxicological effects of this ion. Previous studies showed that association (adsorption) of HA with zero-valent iron NP dramatically mitigated their toxicological effects on bacterial cultures [13]. On the other hand, Figure 6.7 and Table 6.2 show that methanogenesis was the preferable pathway over HA reduction to oxidize acetate in both experiments with HA_{Imm} and HA_{Sus}.

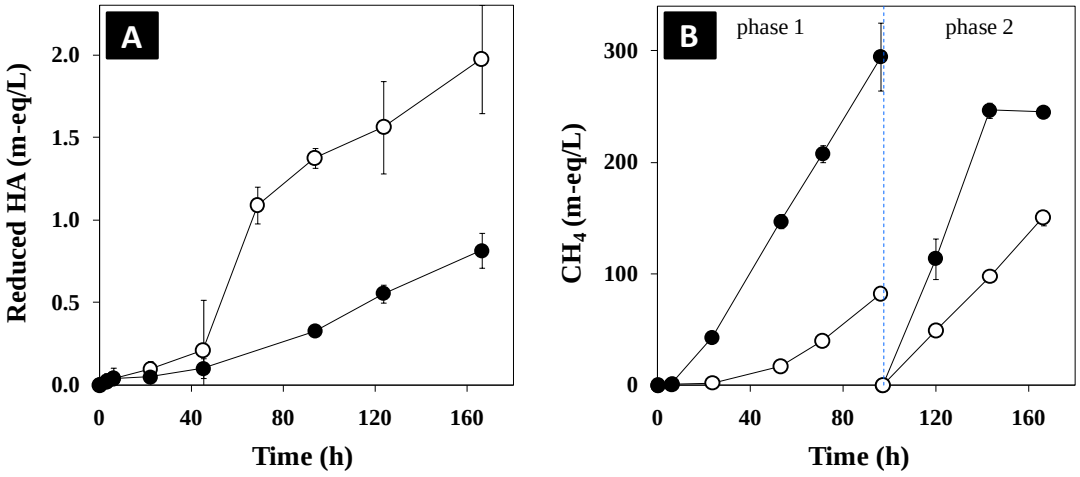

Figure 6.7 Humic acid reduction (A) and concentration of methane produced (B) by anaerobic sludge. Symbols: (○) Experiment with 100 g/L of γ-Al_2O_3 coated with HA; (●) control lacking γ-Al_2O_3 but suspended HA. In all cases, HA concentration was ~3750 mg TOC/L.

6.3.4 Interaction of γ-Al_2O_3 with anaerobic bacteria

Figure 6.8 shows interaction between γ-Al_2O_3 NP and bacteria. SEM images revealed aggregates of NP ranging 100-1000 nm, in both coated (with HA) and uncoated γ-Al_2O_3,

which could decrease their adverse impact on the anaerobic consortium evaluated. Cell membrane damage was observed in those sludge incubations exposed to uncoated γ-Al_2O_3 NP (Figure 6.8A-B). The fact that cell damage was not observed in incubations with HA-coated γ-Al_2O_3 NP (Figure 6.8C) suggests that HA mitigated the toxicological effects of γ-Al_2O_3 NP. On the other hand, interaction of NP with cell membrane could be attributable to electrostatic attraction between positive charges of γ-Al_2O_3 NP and negative charges on the membrane of bacteria. Charges are promoted because the pH of basal medium is 7.2, which is lower than the pH_{PZC} of γ-Al_2O_3 (Figure 6.1). Figure 6.8C shows HA particles adsorbed on cell membrane, which was common only in those images from incubation with HA-coated γ-Al_2O_3 NP. This phenomenon could explain why HRA was higher in the treatment with HA_{Imm} compared with sludge incubations supplied with HA_{Sus} (Figure 6.7A).

Figure 6.8 SEM images of interaction of bacteria with γ-Al_2O_3 (A-B), and γ-Al_2O_3 coated with HA (C). Images A and B: Yellow arrow indicates cell membrane damage, only appreciated in those incubations with uncoated γ-Al_2O_3. Image C: Surface of bacteria is covered with HA-coated γ-Al_2O_3 NP, only observed in these incubations.

6.4 Discussion

The aim of this study was to evaluate the impact of γ-Al_2O_3 NP in an anaerobic consortium through methanogenic and humus reducing activities. The adverse impact of γ-Al_2O_3 NP on anaerobic consortium was evidenced by a lower methane production in comparison to the control lacking γ-Al_2O_3 NP. Previously, Luna-delRisco et al. [26] and Nyber et al. [30] evaluated the effect of metal oxides (CuO and ZnO) and fullerene, respectively on methane

production by anaerobic consortia. In the case of metal-oxides, inhibition of methane production can partially be attributed to the release of toxic ions (Cu and Zn) from NP, as well as its size [26]. Nevertheless, fullerene did not show adverse effects on an anaerobic community because no changes in methane production were observed [30]. In the present study, inhibition of methane production in the anaerobic consortium studied could be associated to the size of γ-Al_2O_3 NP. Jiang et al. [19] compared the toxicity of Al_2O_3 on bacteria at micro- and nano-scale. These authors found that Al_2O_3 at nano-scale showed higher toxicity, with a mortality rate of 57% to *Bacillus subtilis*, 36% to *Escherichia coli*, and 70% to *Pseudomonas Fuorescens*, while their bulk counterpart showed no toxicity. Thus, because agglomeration of γ-Al_2O_3 (Figure 6.8A) was not controlled in the present study, their toxicity could be lower compared with individual particles, as mentioned by Simon-Deckers et al. [37]. Conversely, no toxicological effects by Al_2O_3 NP were observed on *Cupriavididus metallidurans*; which indicates that this microorganism has suitable defense mechanisms to this NP [37]. The great diversity of microorganisms that are present in anaerobic consortia [15], and especially with distinctive characteristics among them, could be responsible that SMA were not completely inhibited by γ-Al_2O_3 NP. For this reason, SMA become stable (Figure 6.6) after ~400 h of incubation, indicating that not all methanogenic microorganisms in the anaerobic consortium were affected by γ-Al_2O_3 NP. Furthermore, a concentration of 0.28±0.09 mg/L of Al was detected in incubations with 100 g/L of γ-Al_2O_3, and represents the highest level of Al measured respect all experiments. This could be another adverse mechanism causing inhibition of SMA on the anaerobic consortium evaluated. Illmer and Erlebach [18] evaluated the toxicity effect of Al (0.8-2.4 mg/L) on bacteria, and they observed a partial or complete growth inhibition according to the different concentrations tested. Al released from γ-Al_2O_3 can induce both production of intracellular reactive oxygen species, causing damage in cell membrane [37], and/or production of free radicals under dark conditions [16], which could also affect cellular viability. Figure 6.8A-B confirms that exposure of anaerobic bacteria present in the studied anaerobic sludge to γ-Al_2O_3 NP caused cell membrane damage, which was not observed in sludge incubations lacking γ-Al_2O_3 NP.

Methanogenesis was the preferable pathway over microbial HA reduction to oxidize acetate in both experiments with HA_{Imm} and HA_{Sus} (Figure 6.7, Table 6.2). These results did not

agree with previously reported by the fact that it has been demonstrated that quinones and HA inhibited methanogenesis on several methanogenic sludge samples [10, 12, 21, 27]. However, when acetate was used as electron donor, several consortia were not capable to reduce the humic model compound anthraquinone-2,6-disulfonate (AQDS), but they could use it as TEA using hydrogen as electron donor [12]. In addition, methane production was not inhibited under Fe(III)-reducing conditions when acetate was used by different methanogenic species in comparison with the use of H_2/CO_2 [42]. More recently, it has been reported that *Methanosarcina barkeri* was able to reduce ferric iron minerals with H_2/CO_2 and methanol, but not with acetate [24], which indicates that methane production in the presence of alternative electron acceptors, such as ferric iron and HA, varied with methanogenic substrate and species involved. On the other hand, HA_{Imm} was more effective to serve as TEA than HA_{Sus} by the anaerobic consortium studied (Figure 6.7). During the last years, it was suspected that HA in solid-phase were able to effectively act as TEA [17, 36]. Recently, Roden et al. [33] elucidated a new mechanism for microbial electron transfer to reduce solid-phase HS. These authors found values (mmol/L) of 3.5 and 4.0 for microbial reduction of solid-phase HS, using *Geobacter sulfurreducens* and *Shewanella putrefaciens*, respectively. These values represent until 4.5-fold higher as compared with suspended HS, which is nearby to the increment observed in this study with HA_{Imm}, with 3.7-fold higher as compared to HA_{Sus}. On the other hand, in section 6.3.4 is mentioned that only in those incubations with HA_{Imm} were observed particles adhered to bacteria cell membrane, a probable cause of the increment in ETC with respect to HA_{Sus}. This increment in ETC can be explained because of an extracellular electron transport through a conductive network composed of bacterial nanowires [47, 48], combined with dissolved RM and outer-membrane cytochromes, promoted a better electron transport. Thus, a direct contact of humus reducing microorganisms (cell membrane components) used in this study, with HA_{Imm}, could be the responsible for better ETC in those incubations using nanoparticles coated with HA, as mentioned by Hartshorne et al. [49].

The results of the present study could explain, in part, the role of released γ-Al_2O_3 NP on aquatic ecosystems. Adsorption of HA can modify size distribution, bioavailability, toxicity, fate, transport, and cell penetration and transport within the organisms of NP [14]. It is well know that HS have a significant relevance in aquatic environments because of

their role in several chemical and biological redox reactions, and in adsorption of different chemicals (ions, organic and inorganic compounds). In aquatic environments, HS adsorbed on NP could also participate in redox reactions as evidenced here. Indeed, HA adsorbed on γ-Al_2O_3 NP deposited on the surface of bacteria promoting a better interaction HA-bacteria, thus achieving a faster reduction of HA as compared to incubations performed in the absence of γ-Al_2O_3 NP. In addition, coating γ-Al_2O_3 NP with HA decrease their toxicological effects; therefore, interaction between γ-Al_2O_3 NP and HA, which are expected to occur in aquatic environments considering the increasing discharge of NP to the environment, significantly affect the mobility and toxicity of these NP [22]. Although the concentration of γ-Al_2O_3 NP and HA established in the present study are not close to those expected in aquatic environments, the collected evidence provides clear demonstration that HA immobilized in γ-Al_2O_3 NP are effective TEA for microbial respiration. Therefore, interaction of HA with metal oxides NP could enhance their role for the anaerobic oxidation of priority pollutants, which has been demonstrated with suspended HA for the anaerobic oxidation of vinyl chloride, dichloroethane [6], toluene [8], and benzene [11]. In addition, this study represents the first evidence, to best of our knowledge, that methanogenesis outcompetes humus reduction when HA were supplied both in suspended form and attached to γ-Al_2O_3 NP. This evidence is relevant for understanding microbial processes in organic rich environments.

On the other hand, results from this study provide important evidence about the potential to use immobilized HS (on NP) as a solid-phase RM. As described by Alvarez and Cervantes [1], co-immobilization of humus reducing microorganisms and NP covered with HA (as RM) during granular sludge formation could be possible. This granular sludge, with enhanced redox properties, could then be used in UASB reactors in order to eliminate the prerequisite of continuous addition of RM, making possible the treatment of wastewater containing recalcitrant contaminants susceptible to redox reactions. Previously, Alvarez et al. [2] demonstrated that the humic model compound, AQDS, immobilized on $Al(OH)_3$ NP could serve as an effective solid-phase redox mediator increasing up to 7.5 the decolorization rate of an azo model compound.

References

1. Alvarez LH, Cervantes FJ (2011) (Bio)nanotechnologies to enhance environmental quality and energy production. J Chem Technol Biot 86:1354–1363

2. Alvarez LH, Perez-Cruz MA, Rangel-Mendez JR, Cervantes FJ (2010) Immobilized redox mediator on metal-oxides nanoparticles and its catalytic effect in a reductive decolorization process. J Hazard Mater 184:268–272

3. APHA (1985) Standard methods for examination of water and wastewater. American Public Health Association, Washington, D. C.

4. Baek YW, An YJ (2011) Microbial toxicity of metal oxide nanoparticles (CuO, NiO, ZnO, and Sb_2O_3) to *Escherichia coli, Bacillus subtilis, and Streptococcus aureus*. Sci Total Environ 409:1603–1608

5. Biswas P, Wu CY (2005) Nanoparticles and the environment. J Air Waste Manage 55:708–746

6. Bradley PM, Chapelle FH, Lovley DR (1998) Humic acids as electron acceptors for anaerobic microbial oxidation of vinyl chloride and dichloroethene. Appl Environ Microbiol 64:3102-3105

7. Brunner TJ, Wick P, Manser P, Spohn P, Grass RN, Limbach LK, Bruinink A, Stark WJ (2006) In vitro cytotoxicity of oxide nanoparticles: comparison to asbestos, silica, and the effect of particle solubility. Environ Sci Technol 40:4374–4381

8. Cervantes FJ, Dijksma W, Duong-Dac T, Ivanova A, Lettinga G, Field JA (2001) Anaerobic mineralization of toluene by enriched sediments with quinones and humus as terminal electron acceptors. Appl Environ Microb 67:4471-4478

9. Cervantes FJ, Garcia-Espinosa A, Moreno-Reynosa MA, Rangel-Mendez JR (2010) Immobilized redox mediators on anion exchange resins and their role on the reductive decolorization of azo dyes. Environ Sci Technol 44:1747-1753

10. Cervantes FJ, Gutiérrez CH, López KY, Estrada-Alvarado MI, Meza-Escalante ER, Texier AC, Cuervo F, Gómez J (2008) Contribution of quinone-reducing microorganisms on the anaerobic biodegradation of organic compounds under different redox conditions. Biodegradation 19:235-246

11. Cervantes FJ, Mancilla AR, Ríos-del Toro EE, Alpuche-Solis AG, Montoya-Lorenzana L, (2011) Anaerobic benzene oxidation by enriched inocula with humic acids as terminal electron acceptors. J Hazard Mater 195:201-207

12. Cervantes FJ, van der Velde S, Lettinga G, Field JA (2000) Competition between methanogenesis and quinone respiration for ecologically important substrates in anaerobic consortia. FEMS Microbiol Ecol 34:161-171

13. Chen J, Xiu Z, Lowry GV, Alvarez PJJ (2011) Effect of natural organic matter on toxicity and reactivity of nano-scale zero-valent iron. Water Res 45:1995-2001

14. Christian P, Von der Kammer F, Baalousha M, Hofmann Th (2008) Nanoparticles: structure, properties, preparation, and behavior in environmental media. Ecotoxicology 17:326–343

15. Díaz E, Amils R, Sanz JL (2003) Molecular ecology of anaerobic granular sludge grown at different conditions. Water Sci Technol 48:57–64

16. Green M, Howman E (2005) Semiconductor quantum dots and free radical induced DNA nicking. Chem Commun 121–123

17. Heitmann T, Blodau C (2006) Oxidation and incorporation of hydrogen sulfide by dissolved organic matter. Chem Geol 235:12–20

18. Illmer P, Erlebach C (2003) Influence of Al on growth, cell size and content of intracellular water of *Arthrobacter sp*. PI/1-95. A Van Leeuw J Microb 84:239–246

19. Jiang W, Mashayekhi H, Xing B (2009) Bacterial toxicity comparison between nano- and micro-scaled oxide particles. Environ Pollut 157:619-1625

20. Kang S, Xing B (2008) Humic acid fractionation upon sequential adsorption onto goethite. Langmuir 24:2525-2531

21. Keller JK, Weisenhorn PB, Megonigal JP (2009) Humic acids as electron acceptors in wetland decomposition. Soil Biol Biochem 41:1518-1522

22. Limbach LK, Bereiter R, Muller E, Krebs R, Galli R, Stark WJ (2008) Removal of oxide nanoparticles in a model wastewater treatment plant: influence of agglomeration and surfactants on clearing efficiency. Environ Sci Technol 42:5828-5833

23. Limbach LK, Wick P, Manser P, Grass RN, Bruinink A, Stark WJ (2007) Exposure of engineered nanoparticles to human lung epithelial cells: influence of chemical composition and catalytic activity on oxidative stress. Environ Sci Technol 41:4158-4163

24. Liu D, Dong H, Bishop ME, Wang H, Agrawal A, Tritschler S, Eberl DD, Xie S (2011) Reduction of structural Fe(III) in nontronite by methanogen *Methanosarcina barkeri*. Geochim Cosmochim Ac 75:1057-1071

25. Lovley DR, Coates JD, Blunt-Harris EL, Phillips EJP, Woodward JC (1996) Humic substances as electron acceptors for microbial respiration. Nature 382:445–448

26. Luna-del Risco M, Orupõlda K, Dubourguiera HC (2011) Particle-size effect of CuO and ZnO on biogas and methane production during anaerobic digestion. J Hazard Mater 189:603-608

27. Minderlein S, Blodau C (2010) Humic-rich peat extracts inhibit sulfate reduction, methanogenesis, and anaerobic respiration but not acetogenesis in peat soils of a temperate bog. Soil Biol Biochem 42:2078-2086

28. Monroy O, Famá G, Meraz M, Montoya L, Macarie H (2000) Anaerobic digestion for wastewater treatment in Mexico: state of the technology. Water Res 34, Issue 6:1803-1816

29. Nevin KP, Lovley DR (2000) Potential for nonenzymatic reduction of Fe(III) via electron shuttling in subsurface sediments. Environ Sci Technol 34:2472-2478

30. Nyberg L, Turco RF, Nies L (2008) Assessing the impact of nanomaterials on anaerobic microbial communities. Environ Sci Technol 42:1938–1943

31. Pelletier DA, Suresh AK, Holton GA, McKeown CK, Wang W, Gu B, Mortensen NP, Allison DP, Joy DC, Allison MR, Brown SD, Phelps TJ, Doktycz MJ (2010) Effects of Engineered Cerium Oxide Nanoparticles on Bacterial Growth and Viability. Appl Environ Microb 76:7981–7989

32. Ratasuk N, Nanny MA (2007) Characterization and quantification of reversible redox sites in humic substances. Environ Sci Technol 41:7844-7850

33. Roden EE, Kappler A, Bauer I, Jiang J, Paul A, Stoesser R, Konishi H, Xu H (2010) Extracellular electron transfer through microbial reduction of solid-phase humic substances. Nat Geosci 3:417-421

34. Sadiq IM, Chowdhury B, Chandrasekaran N, Mukherjee A (2009) Antimicrobial sensitivity of *Escherichia coli* to alumina nanoparticles. Nanomed-Nanotechnol 5:282-286

35. Salavagione HJ, Arias J, Garcés P, Morallcuírron E, Barbero C, Vázquez JL (2005) Spectroelectrochemical study of the oxidation of aminophenols on platinum electrode in acid medium. J Electroanal Chem 565:375-383

36. Scott DT, McKnight DM, Blunt-Harris EL, Kolesar SE, Lovley DR (1998) Quinone moieties act as electron acceptors in the reduction of humic substances by humics reducing microorganisms. Environ Sci Technol 32:2984–2989

37. Simon-Deckers A, Loo S, Mayne-L'hermite M, Herlin-Boime N, Menguy N, Reynaud C, Gouget B, Carrire M (2009) Size-, composition- and shape-dependent toxicological impact of metal oxide nanoparticles and carbon nanotubes toward bacteria. Environ Sci Technol 43:8423-8429

38. Sinha N, Ma J, Yeow JTW (2006) Carbon nanotube-based sensors. J Nanosci Nanotechno 6:573–590

39. Tenne R (2006) Inorganic nanotubes and fullerene-like nanoparticles. Nat Nanotechnol 1:103–111

40. Theron J, Walker JA, Cloete TE (2008) Nanotechnology and water treatment: applications and emerging opportunities. Crit Rev Microbiol 34:43–69

41. Tombacz E, Libor Z, Illes E, Majzik A, Klumpp E (2004) The role of reactive surface sites and complexation by humic acids in the interaction of clay mineral and iron oxide particles. Org Geochem 35:257–267

42. van Bodegom PM, Scholten JCM, Stams AJM (2004) Direct inhibition of methanogenesis by ferric iron. FEMS Microbiol Ecol 49:261–268

43. Van der Zee FP, Cervantes FJ (2009) Impact and application of electron shuttles on the redox (bio)transformation of contaminants: A review. Biotechnol Adv 27:256–277

44. Wang K, Xing B (2005) Structural and sorption characteristics of adsorbed humic acid on clay minerals. J Environ Qual 34:342–349

45. Yang K, Lin D, Xing B (2009) Interactions of humic acid with nanosized inorganic oxides. Langmuir 25:3571-3576

46. Zhang WX, (2003) Nanoscale iron particles for environmental remediation: An overview. J Nanopart Res 5:323–332

47. Reguera G, McCarthy KD, Mehta T, Nicoll JS, Tuominen MT, Lovley DR (2005) Extracellular electron transfer via microbial nanowires. Nature 435:1098-1101

48. Gorby YA, Yanina S, McLean JS, Rosso KM, Moyles D, Dohnalkova A, Beveridge TJ, Chang IS, Kim BH, Kim KS, Culley DE, Reed SB, Romine MF, Saffarini DA, Hill EA, Shi L, Elias DA, Kennedy DW, Pinchuk G, Watanabe K, Ishii S, Logan B, Nealson KH, Fredrickson JK (2006) Electrically conductive bacterial nanowires produced by Shewanella oneidensis MR-1 and other microorganisms. Proc Natl Acad Sci USA 103:11358-11363

49. Hartshorne RS, Reardon CL, Ross D, Nuester J, Clarke TA, Gates AJ, Mills PC, Fredrickson JK, Zachara JM, Shi L, Beliaev AS, Marshall MJ, Tien M, Brantley S, Butt JN, Richardson DJ (2009) Characterization of an electron conduit between bacteria and the extracellular environment. Proc Natl Acad Sci USA 106:221069-22174

7

Final remarks and perspectives

Different electron-accepting contaminants (EAC) such as nitroaromatics, azo dyes, and polyhalogenated compounds (aliphatic and aromatic) are extensively used and consequently discharged by several industries in their wastewater [27]. Several EAC remain unaffected during convectional aerobic wastewater treatment. However, under anaerobic conditions, EAC are susceptible to reductive biotransformations using anaerobic bioreactors [8]. Nevertheless, the biotransformation of many different recalcitrant compounds proceeds very slowly due to electron transfer limitations and to toxicity effects leading to poor performance or even collapse of anaerobic bioreactors [28, 30].

During the last two decades, evidence has been accumulated indicating that humic substances (HS) and quinoid analogues can act as redox mediators (RM) during the reductive biotransformation of EAC by different anaerobic consortia [31]. Figure 7.1 illustrates the reactions involved during the reductive biotransformation of EAC by RM. The addition of RM can promote a good performance in bioreactors (e.g. UASB and EGSB), by the fact that they can accelerate reduction rates of EAC in several orders of magnitude [30] and also can attenuate their toxicological effects on anaerobic bacteria [4]. In fact, the capacity of HS and quinone moieties to accelerate several redox reactions has significant potential to develop strategies for enhancing the redox biotransformation of priority pollutants. However, one of the main limitations for applying RM in wastewater treatment systems is that continuous addition of HS should be supplied to increase

conversion rates, which is economically and environmentally unviable. For this reason, it is important to develop innovative strategies in order to immobilize RM, taking especial care in maintaining their redox properties. In addition, further studies are demanded to identify natural sources of HS with suitable electron-transferring capacity (ETC) to be applied in wastewater treatment systems for achieving the redox biotransformation of EAC. The aim of this dissertation were: 1) to identify cost-effective sources of HS with suitable ETC for bioremediation applications; 2) to evaluate the capacity of metal-oxides (MO) particles to immobilize HS and quinone model compounds; and 3) to test the capacity of immobilized RM on MO particles, as solid-phase RM, during the reductive biotransformation of contaminants.

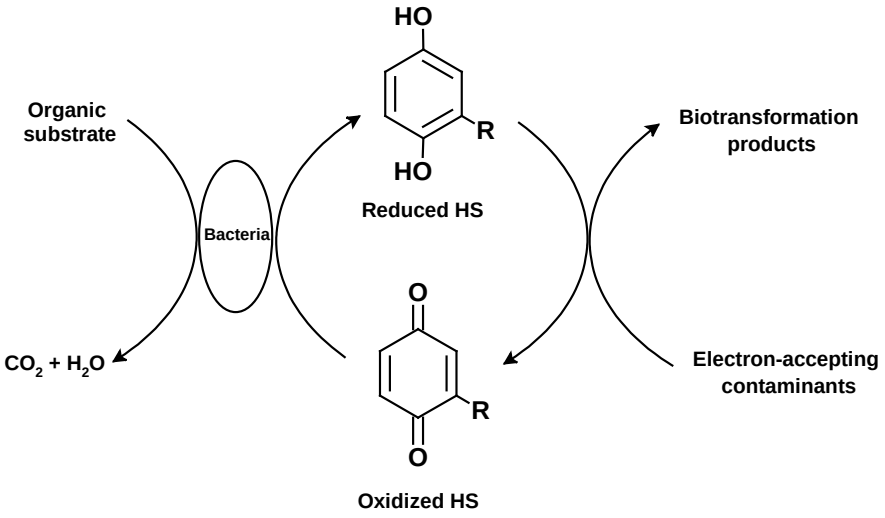

Figure 7.1 Proposed mechanism for the anaerobic biotransformation of electron-accepting contaminants in the presence of humic substances as redox mediators.

The results presented in this dissertation indicate that ETC of HS greatly varies depending on the origin of the organic bulk material, suggesting that quinone groups are the main responsible of ETC quantified; but also, those non-quinone redox functional groups in HS account for an important fraction of the ETC measured by chemical and biological methods (chapter 3). The significant ETC detected in these HS samples linked to non-quinone redox

mediating functional groups might be associated to nitrogenous and sulfurous redox mediating functional groups, such as dimethyl sulfone, 3-(methylthio)-propanoic acid, N-methyl aniline, and 1-methyl-2,5-pyrrolidinedione, as previously reported by Fimmen et al. [9]. Among the twelve samples of humic acids (HA) characterized in chapter 3, the sample with the highest ETC was that extracted from a coal mine. Nevertheless, one of the main goals of this work was to evaluate if immobilized HS could maintain their redox properties, acting as RM during reductive biotransformation processes. The results revealed that immobilized HS on MO can act as solid-phase RM for the reductive biotransformation of EAC (chapters 4 and 5).

Chapters 4 and 5 describe processes of immobilization of fulvic (FA) acids and the humic model compound, anthraquinone-2,6-disulfonate (AQDS), on MO particles at micrometric and nanometric scale, respectively; and their consequent use as solid-phase RM under anaerobic conditions. In chapter 4, it was described that the rate of carbon tetrachloride reduction to chloroform was increased up to 10.4-fold in the presence of immobilized FA, which was also reflected in a higher reduction efficiency (>90%) compared to the control lacking FA, with only 16.6% of conversion. On the other hand, in chapter 5 the immobilization of AQDS was carried out in MO nanoparticles (NP). Immobilized AQDS increased up to 7.5–fold the rate of decolorization of Reactive Red 2 as compared to the control without RM. There are some studies showing the use of different materials to immobilize RM. Among them, the most relevant materials used are ion exchange resins [2, 3], calcium alginate [11, 12], polypyrroles [16, 17], polyurethane foam [18], and carbon based materials [19-21]. A complete list with other examples can be found in Tables 2.2 and 2.3 in chapter 2.

Chapter 6 describes the impact of NP of γ-Al_2O_3 on methane production and humus reduction by an anaerobic consortium. The anaerobic consortium was exposed to coated (with HS) and uncoated γ-Al_2O_3. Uncoated γ-Al_2O_3 affected the methane production, but coated nanoparticles decreased the toxicological effects on methanogenesis. In addition, microbial HS reduction occurred 3.7-fold faster using HS immobilized on γ-Al_2O_3, compared with the control with suspended HS. Methanogenesis out-competed microbial humus reduction regardless if HS was immobilized or suspended.

7.1 Suitable sources of HS

Among the different redox active molecules reported in the literature, such as cytochromes [25], flavines [10], pyridines [15], cobalamins [34], phenazines [13], and porphyrins [14], quinones are recognized as the most appropriated RM for the reductive biotransformation of several EAC [8]. Different synthetic quinones, such as AQDS, have been used as model RM in reductive processes; nevertheless, quinones are present in HS, which are compounds naturally and abundantly occurring in biosphere. HS are the most plentiful and cheaply available organic matter source present in terrestrial and aquatic environments; their large residence time (>500 years) [29], prevents the deterioration of this material during bioremediation processes. Furthermore, humus is generally considered as a non-hazardous material and does not lead to the production of toxic byproducts [24].

As observed in the study of characterization of twelve HS described in chapter 3, the ETC values ranged between 112 to 392 μmol g^{-1}, depending on the origin of the organic bulk material. Other studies indicate that HS originated from peat, river sediments or soils showed an ETC ranging from 25 up to 538 μmol g^{-1} [26]. Then, in order to take advantage in selecting the suitable RM for biodegradation purposes, adequate sources of HS should be considered. Certainly, the principal factor limiting the application of HS in remediation technologies is their intrinsic variability in redox properties. Nevertheless, HS can be modified by incorporating quinone moieties in their structure in order to enhance their redox properties [24], which is required during the biotransformation of a large number of EAC. Modification of HS with quinones can be conducted following two different strategies. The first strategy considers oxidation of phenolic fragments associated with the humic aromatic core. In a second strategy, polycondensation of these phenolic fragments was carried out with hydroquinone and catechol. The ETC of copolymers ranged between 1 and 4 mmol g^{-1}, which were much higher than the parent material and the oxidized derivatives [24]. Modified HS with quinones had never been used as RM during biotransformation of priority pollutant, but seems to fulfill the requirements to serve as a feasible RM for remediation purposes.

On the other hand, Doong and Chiang [6] reported that mercaptoquinones, acting as RM, are more effective than either semiquinones or hydroquinones for transferring electrons to

CT. Thus, there is a great potential to use modified HS with enhanced redox properties in order to accelerate the redox biotransformation of priority pollutants.

7.2 Immobilization of HS on metal-oxides particles

The immobilization of HS on different MO particles has been conducted for several purposes, but not to be used as a solid-phase RM during biotransformation of EAC. For instance, the interaction of HA with different MONP was evaluated by Yang et al. [33]. In this study it was documented that the adsorption of HA on TiO_2, α-Al_2O_3, γ-Al_2O_3 and ZnO was limited by the surface area of NP and was pH-dependent. The highest adsorption capacity was achieved by TiO_2 and γ-Al_2O_3, with values of ~95 and ~80 mg TOC g^{-1} respectively, at pH 5. In this dissertation, similar results to those obtained by Yang et al. [33] were obtained using γ-Al_2O_3 NP during HA adsorption test, with a value of 93 mg TOC g^{-1} (chapter 6). On the other hand, Perminova et al. [23] developed a procedure to covalently immobilize HS on alumina particles by alkoxysilylation. This material was shown to efficiently remove Np(V) and Pu(V) by the sequestering properties of the immobilized HS [22].

In chapters 4, and 5-6 of this dissertation, the use of MO microparticles and NP, respectively, is described to immobilize HS. Chapter 4 presents the use of alumina microparticles of ~63 µm to immobilize HS, as a new alternative for the treatment of industrial wastewaters containing recalcitrant pollutants by serving as solid-phase RM. Two important advantages could be underlined for applying alumina for the immobilization of HS. First, the high settling capacity of alumina particles could prevent the wash-out of RM when this (hydr)oxide is used as supporting material in up flow anaerobic reactors such as UASB and EGSB systems. Second, alumina particles coated with HS could be used as nuclei for sludge granulation or biofilms growth, as has previously been shown with zeolite particles [34]. Figure 7.2 shows the redox reactions involved during the reductive biotransformation of EAC with alumina microparticles serving both as immobilizing material for HS and as a nuclei for biofilm formation.

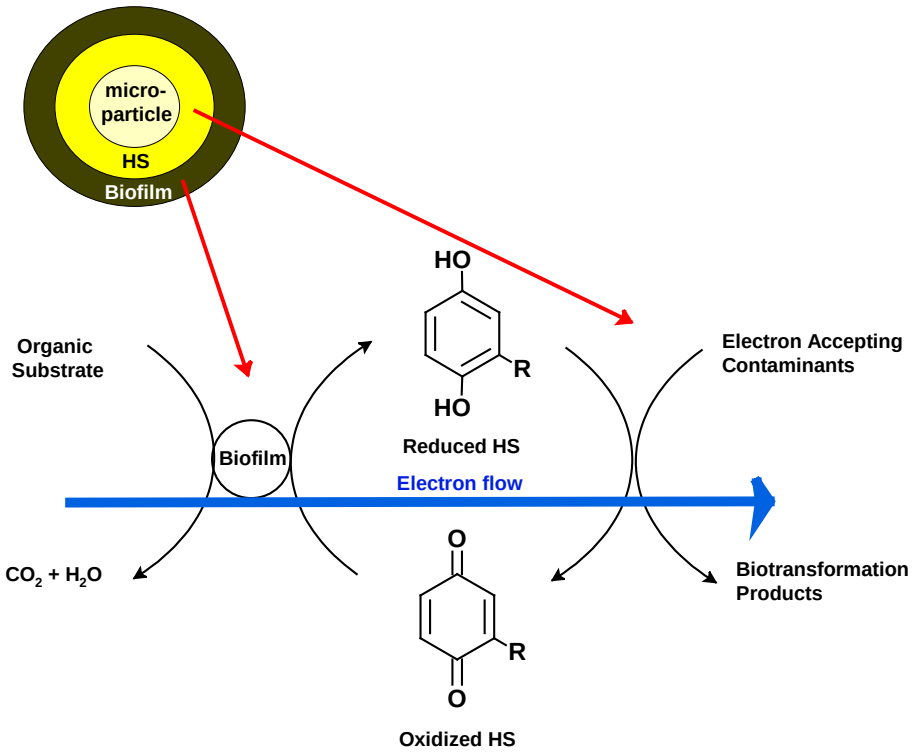

Figure 7.2 Metal-oxides microparticles coated with HS and serving as nuclei to biofilm attachment during the redox biotransformation of electron accepting contaminants. Modified from reference 5.

On the other hand, in case of using NP coated with HS to be used as solid-phase RM, as mentioned in chapters 5 and 6, it is necessary to develop a strategy to prevent their washout from the reactors above mentioned. One of the main promising strategies could be the co-immobilization of HS (adsorbed on NP) and humus reducing microorganisms by the granulation process. As mentioned in chapter 2, different factors such as microbiological, biotic and abiotic factors are involved in the process. Results from chapter 6 indicate that γ-Al_2O_3 NP, coated with HS, are suitable for the process of granulation. For instance, this novel material maintains its catalytic properties, which was evidenced during microbial respiration acting as final electron acceptor. In addition, NP covered with HS mitigates the toxicological effects on an anaerobic consortium as compared with uncoated ones. Figure 7.3 shows a scheme of granulation process simultaneously immobilizing humus reducing microorganism and HS (adsorbed on NP); which is based on the spaghetti theory proposed by Wiegant W. [32]. The model propose the use of a divalent cation such as calcium (Ca^{2+})

in order to promote a better electrostatic attraction between HS and microorganisms. Both NP covered with HS and cell membranes of microorganisms are negatively charged at circumneutral pH, thus Ca^{2+} ions could diminish the repelling forces between HS and microorganisms promoting a better formation of granules.

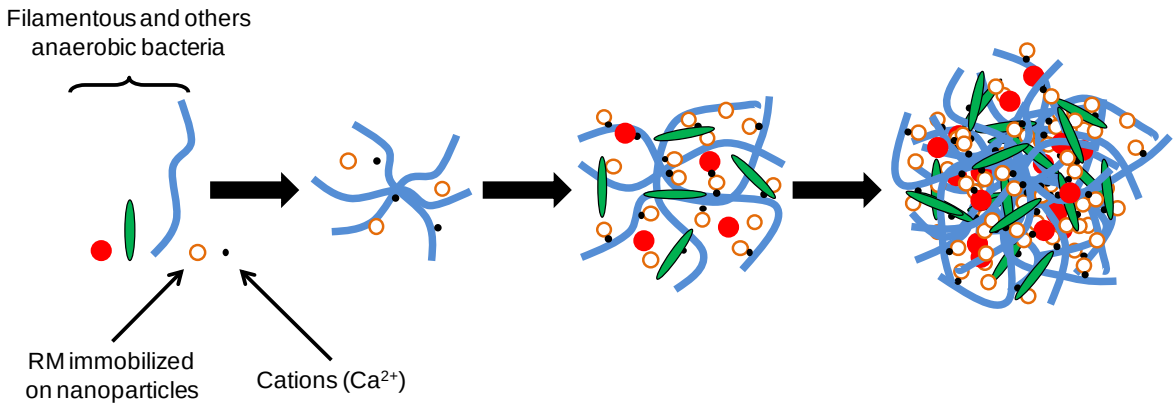

Figure 7.3 Proposed model for granulation co-immobilizing humus reducing microorganisms and nanoparticles coated with humic substances [1].

7.3 Perspectives

In spite of quinones and HS have extensively been used in redox biotransformations acting as RM, their potential to treat pollutants in groundwater and wastewaters generated by several industrial sectors has not been exploited. The different immobilization techniques could allow, in the near future, the application of RM to wastewater treatment systems to improve the biodegradation of recalcitrant EAC. Nevertheless, it is also necessary to contemplate other issues in order to use RM in proper way, between them, cost-effective sources of redox active groups, engineered HS, and overcoming limitations during catalysis involving RM [31] could be considered. In the case of immobilized RM, the following topics should be considered:

- The strength of immobilization of RM is important by the fact that a better immobilization mechanism could allow to maintain the redox capacity for a long time,

reducing operational costs. In this sense, covalent immobilization seems to be the most adequate option; nevertheless, others techniques also have proved adequate (e.g. electrostatic attraction).

- Evaluation of the catalytic properties of immobilized RM during long-term experiments with continuous reactors, not only in batch. This is related with the previous point. The utilization of continuous reactors would identify if immobilized RM maintain or not their redox mediating capacity, especially using non synthetic wastewaters.

- Elucidate the impacts of biofilm formation on immobilizing material in both the transfer of electrons from an electron donor (substrate) to reduce HS (microbial reaction), and the transfer of electrons from HS to reduce EAC (chemical reaction).

- The great diversity of EAC (azo dyes, nitroaromatics, polyhalogenated compounds, among others) used in the industry, makes necessary to test the immobilized RM under a mixture of pollutants or with real samples of wastewater.

References

1. Alvarez LH, Cervantes FJ (2011) (Bio)nanotechnologies to enhance environmental quality and energy production. *J Chem Technol Biot* 86:1354–1363.

2. Cervantes FJ, Garcia-Espinosa A, Moreno-Reynosa MA, Rangel-Mendez JR, (2010) Immobilized redox mediators on anion exchange resins and their role on the reductive decolorization of azo dyes. *Environ Sci Technol* 44:1747–1753.

3. Cervantes FJ, Gonzalez-Estrella J, Márquez A, Alvarez LH, Arriaga S, (2011) Immobilized humic substances on an anion exchange resin and their role on the redox biotransformation of contaminants. *Biores Technol* 102:2097-2100.

4. Cervantes FJ, López-Vizcarra MI, Siqueiros E, Razo-Flores E, (2008) Riboflavin prevents inhibitory effects during the reductive decolorization of Reactive Orange 14 by methanogenic sludge. *J Chem Technol Biotechnol* 83:1703-1709.

5. Cervantes FJ, Martínez CM, Gonzalez-Estrella J, Márquez A, Arriaga S, (In Press) Kinetics during the redox biotransformation of pollutants mediated by immobilized and soluble humic acids. *Appl Microbiol Biotechnol*

6. Doong RA, Chiang HC, (2005) Transformation of carbon tetrachloride by thiol reductants in the presence of quinone compounds. *Environ Sci Technol* 39(19):7460-7468.

7. Field JA, Cervantes FJ, (2005) Microbial redox reactions mediated by humus and structurally related quinones. In: Perminova IV, Hatfield K, Hertkorn N, editors. Use of humic substances to remediate polluted environments: from theory to practice, vol. 52. Dordrecht, The Netherlands: Springer, p. 343–52.

8. Field JA, Stams AJM, Kato M, Schraa G (1995) Enhanced biodegradation of aromatic pollutants in cocultures of anaerobic and aerobic bacterial consortia. *Anton Leeuw Int J G* 67:47–77.

9. Fimmen RL, Cory RM, Chin Y-P, Trouts TD, McKnight DM, (2007) Probing the oxidation –reduction properties of terrestrially and microbially derived dissolved organic matter. *Geochim Cosmochim Ac* 71, 3003-3015.

10. Guerrero-Barajas C, Field JA, (2005) Riboflavin- and cobalamin-mediated biodegradation of chloroform in a methanogenic consortium. *Biotechnol Bioeng* 89:539–50.

11. Guo J, Kang L, Lian J, Yang J, Yan B, Li Z, Liu C, Yue L, (2010) The accelerating effect and mechanism of a newly functional bio-carrier modified by redox mediators for the azo dyes decolorization. *Biodegradation* 21:1049-1056.

12. Guo J, Kang L, Yang J, Wang X, Lian J, Li H, Guo Y, Wang Y, (2010) Study on a novel non-dissolved redox mediator catalyzing biological denitrification (RMBDN) technology. *Bioresour Technol* 101:4238-4241.

13. Hernandez ME, Kappler A, Newman DK, (2004) Phenazines and other redox-active antibiotics promote microbial mineral reduction. *Appl Environ Microbiol* 70:921–8.

14. Koons BW, Baeseman JL, Novak PJ, (2001) Investigation of cell exudates active in carbon tetrachloride and chloroform degradation. *Biotechnol Bioeng* 74:12–17.

15. Lee CH, Lewis TA, Paszczynski A, Crawford RL, (1999) Identification of an extracellular catalyst of carbon tetrachloride dehalogenation from Pseudomonas stutzeri strain KC as pyridine-2,6-bis(thiocarboxylate). *Biochem Biophys Res Commun* 261:562–566.

16. Li L, Zhou J, Wang J, Yang F, Jin C, Zhang G, (2009) Anaerobic biotransformation of azo dye using polypyrrole/anthraquinonedisulphonate modified active carbon felt as a novel immobilized redox mediator. *Sep Purif Technol* 66:375-382.

17. Li L,Wang J, Zhou J, Yang F, Jin C, Qu Y, (2008) Enhancement of nitroaromatic compounds anaerobic biotransformation using a novel immobilized redox mediator prepared by electropolymerization. *Biores Technol* 99:6908–6916.

18. Lu H, Zhou J, Wang J, Si W, Teng H, Liu G, (2010) Enhanced biodecolorization of azo dyes by anthraquinone-2-sulfonate immobilized covalently in polyurethane foam. *Bioresour Technol* 101:7185–7188.

19. Mezohegyi G, Fabregat A, Font J, Bengoa C, Stuber F, Fortuny A, (2009) Advanced bioreduction of commercially important azo dyes: modeling and correlation with electrochemical characteristics. *Ind Eng Chem Res* 48:7054-7059.

20. Mezohegyi G, Goncalves F, Órfão JJM, Fabregat A, Fortuny A, Font J, Bengoa C, Stuber F, (2010) Tailored activated carbons as catalysts in biodegradation of textile azo dyes. *Appl Catal B: Environ* 94:179–185.

21. Mezohegyi G, Kolodkin A, Castro UI, Bengoa C, Stuber F, Font J, Fabregat A, (2007) Effective anaerobic decolorization of azo dye acid orange 7 in continuous upflow packed bed reactor using biological activated carbon system. *Ind Eng Chem Res* 46:6788–6792.

22. Perminova I, Karpiouk L, Shcherbina N, Ponomarenko S, Kalmykov S, Hatfield K, (2007) Preparation and use of humic coatings covalently bound to silica gel for Np(V) and Pu(V) sequestration. *J Alloy Compd* 444-445:512-517.

23. Perminova I, Ponomarenko S, Karpiouk L, Hatfield K, (2006) PCT application RU2006/000102, Humic derivatives, methods of preparation and use, Filed on March 7.

24. Perminova IV, Kovalenko AN, Schmitt-Kopplin P, Hatfield K, Hertkorn N, Belyaeva EY, et al. (2005) Design of quinonoid-enriched humic materials with enhanced redox properties. *Environ Sci Technol* 39:8518–24.

25. Picardal FW, Arnold RG, Couch H, Little AM, Smith ME, (1993) Involvement of cytochromes in the anaerobic biotransformation of tetrachloromethane by Shewanella putrefaciens 200. *Appl Environ Microbiol* 59:3763–70.

26. Ratasuk N, Nanny MA, (2007) Characterization and quantification of reversible redox sites in humic substances. *Environ Sci Technol* 41:7844–50.

27. Razo-Flores E, Macarie H, Morier F, (2006) Application of biological treatment systems for chemical and petrochemical wastewaters. In: Cervantes F.J., Pavlostathis S.G., Van Haandel A.C., editors. Advanced biological treatment processes for

industrial wastewaters: principles & applications. London, UK: IWA Publishing; p. 267–297.

28. Rodgers JD, Bunce NJ, (2001) Treatment methods for the remediation of nitroaromatic explosives. *Water Res* 35:2101–11.

29. Stevenson FJ (1994) Humus chemistry: genesis, composition, reactions. New York: John Wiley and Sons, Inc.

30. Van der Zee FP, Bouwman RHM, Strik DPBTB, Lettinga G, Field JA, (2001) Application of redox mediators to accelerate the transformation of reactive azo dyes in anaerobic bioreactors. *Biotechnol Bioeng* 75:691–701.

31. Van der Zee FP, Cervantes FJ, (2009) Impact and application of electron shuttles on the redox (bio)transformation of contaminants: A review. *Biotechnol Adv* 27:256–277.

32. Wiegant WM, (1987) The spaghetti theory on anaerobic sludge formation, or the inevitability of granulation, in *Granular anaerobic sludge: Microbiology and technology*, ed by Lettinga G, Zehnder AJB, Grotenhuis JTC and Hulshoff Pol LW. The Netherlands: Pudoc. Wageningen.

33. Yang K, Lin D, Xing B, (2009) Interactions of humic acid with nanosized inorganic oxides *Langmuir*. 25:3571-3576.

34. Yoda M, Kitagawa M, Miyaji Y, (1989). Granular sludge formation in the anaerobic expanded micro carrier process. *Wat Sci Technol* 21:109-122.

35. Zou S, Stensel HD, Ferguson JF, (2000) Carbon tetrachloride degradation: effect of microbial growth substrate and vitamin B12 content. *Environ Sci Technol* 34:1751–1757.

The Author

Luis H. Alvarez Valencia was born in Ciudad Obregon Sonora, Mexico, on December 7th 1979. After accomplished his service as a full time missionary (LDS Church) in Oaxaca, Mexico during two consecutive years, Luis got married with Faby Castro on April 6th 2004, two months before he obtained his Bachelor degree in Biotechnology Engineering at Instituto Tecnológico de Sonora (ITSON). His Master Science degree in Natural Resources was accomplished in 2006 at ITSON, under supervision of Dr. Francisco J. Cervantes. The topic of his thesis was the removal of perchlorate using biofilters, and was developed in the laboratories of Department of Chemical and Environmental Engineering at The University of Arizona, under supervision of Dr. Jim Field and Dr. Reyes Sierra. The author started (January, 2009) his Doctoral studies in Environmental Sciences at Instituto Potosino de Investigación Científica y Tecnológica, under direction of Dr. Cervantes. His project was on immobilization of humic substances on metal-oxides (nano)particles and their use as a solid-phase redox mediators during the biotransformation of priority pollutants.

List of publications

1. **Alvarez LH**, Cervantes FJ (**2012**) Assessing the impact of alumina nanoparticles in an anaerobic consortium: methanogenic and humus reducing activity. *Applied Microbiology and Biotechnology* (DOI 10.1007/s00253-011-3759-4)

2. **Alvarez LH**, Jimenez L, Hernandez-Montoya V, Cervantes FJ (**2012**) Enhanced dechlorination of carbon tetrachloride by immobilized fulvic acids on alumina particles. *Water Air and Soil Pollution* 223:1911-1920

3. Hernández V, **Alvarez LH**, Montes-Moran MA, Cervantes FJ (**2012**) Reduction of quinone and non-quinone redox functional groups in different humic acid samples by *Geobacter sulfurreducens*. *Geoderma* 183–184:25–31

4. Martinez CM, **Alvarez LH**, Cervantes FJ (**2012**) Simultaneous biodegradation of phenol and carbon tetrachloride mediated by humic substances. *Biodegradation* (DOI 10.1007/s10532-012-9539-8)

5. **Alvarez LH**, Cervantes FJ (**2011**) (Bio)Nanotechnologies to enhance environmental quality and energy production. *Journal of Chemical Technology and Biotechnology* 86:1354-1363

6. Cervantes FJ, Gonzalez-Estrella J, Marquez A, **Alvarez LH**, Arriaga S (**2011**) Immobilized humic substances on an anion exchange resin and their role on the redox biotransformation of contaminants. *Bioresource Technology* 102:2097-2100

7. **Alvarez LH**, Perez-Cruz MA, Rangel-Mendez JR, Cervantes FJ (**2010**) Immobilized redox mediator on metal-oxides nanoparticles and its catalytic effect in a reductive decolorization process. *Journal of Hazardous Materials* 184:268-272

8. **Alvarez LH**, Martinez CM, Cervantes FJ Advances on the application of redox mediators during the (bio)transformation of pollutants. (In Preparation)

Attendance at Conferences

1. **Alvarez LH**, Cervantes FJ **(2011**) Biotransformation of contaminants mediated by solid-phase (immobilized) humic substances. *Wetland Pollutant Dynamics and Control Symposium*. Prague, Chezc Republic. July 3-8

2. **Alvarez LH**, Martínez CM, Cervantes FJ **(2011)** Methanogenic and humus reducing activities of anaerobic sludge in presence of γ-A_{l2O3} nanoparticles. *XIV Congreso Nacional de Biotecnología y Bioingeniería*. Querétaro, México. June 19-24

3. **Alvarez LH**, Perez-Cruz MA, Cervantes FJ **(2010)** Catalytic effect of immobilized redox mediators on nanoparticles during the reductive decolorization of reactive red 2. *2nd México Young Water Professionals*. Juriquilla, Querétaro, Mexico, April 12-14

4. **Alvarez LH**, Jiménez L, Hernandez-Montoya V, Cervantes FJ **(2010)** The role of immobilized fulvic acids on alumina particles during the reductive dechlorination of carbon tetrachloride. *12th World Congress on Anaerobic Digestion*, Guadalajara, Jalisco, México, October 31-November 4